DETERMINISTIC CULTURING OF SINGLE CELLS IN 3D

by

Rohil Jain

A Dissertation

Submitted to the Faculty of Purdue University

In Partial Fulfillment of the Requirements for the degree of

Doctor of Philosophy

School of Mechanical Engineering

West Lafayette, Indiana

May 2021

THE PURDUE UNIVERSITY GRADUATE SCHOOL
STATEMENT OF COMMITTEE APPROVAL

Dr. Cagri Savran, Chair

School of Mechanical Engineering with courtesy in Biomedical Engineering

Dr. Chun-Li Chang

School of Mechanical Engineering

Dr. Sophie Lelievre

Department of Basic Medical Sciences

Dr. Bumsoo Han

School of Mechanical Engineering with courtesy in Biomedical Engineering

Dr. Babak Ziaie

School of Electrical and Computer Engineering

Approved by:

Dr. Nicole L. Key

Dedicated to my parents- Mrs. Bhawna Jain & Mr. Sanjay Jain, family & friends who supported me in this journey.

I would also like to thank the countless number of spirited scientists and frontline workers who fought Covid-19 and continue to motivate me to make an impact through science.

ACKNOWLEDGEMENTS

I would like to thank my advisor, Professor Cagri Savran, for his guidance and support throughout my Ph.D. studies. His thoughtful and motivational approach to mentorship encouraged me to explore novel ideas in the field of cancer. Without his confidence in my abilities, I would not have been able to explore this field of single-cell culture and complete this project. In the same breath I would like to thank Professor Chun-Li Chang for patiently working with me in the lab and teaching me the importance of organization and discipline in not just my work, but also my thinking. By way of his calm demeanor, he also taught me to be polite and courteous. Without their inspiration and encouragement, it would have been hard to work on this challenging project. I will always be deeply grateful to them and will look up to them for a lifetime of mentorship.

I am also grateful to Professor Sophie A. Lelièvre and her postdoctoral trainee Dr. Shirisha Chittiboyina for working with me over the years- teaching me many concepts and techniques in biology as well as giving their invaluable suggestions throughout my Ph.D. project.

Next, I would like to thank my academic advisory committee members, Professor Babak Ziaie, and Professor Bumsoo Han for their invaluable advice and suggestions which have broadened my vision of research.

Then, I would like to thank my colleagues and friends, Yuan Zhong, Dr. Onur Gur, Dr. Wanfeng Huang, Dr. Bin-Da Chan, Dr. Norman Brault, and Maulee Seth for their help and the ideas they contributed to my research, and the friendship and support they provided through the years.

Finally, I would like to acknowledge the support of my many great friends over the years in Asha for Education-Purdue Chapter who helped me develop personally as well as professionally; other Purdue friends: Viplove, Vibhav, Ashutosh, Akash, Vaibhav, Harsha, Bipin, Shayak, Rohit, for bearing with me through the ups and downs of past few years. Charu and Kanika, for their motivational support and professional allyship. Special thanks to two wonderful friends in Surabhi and Rachana for having my back and giving me the courage to face challenges these past years.

Last but not least, I would like to thank my family- parents, Mrs. Bhawna Jain and Mr. Sanjay Jain, who supported me during my Ph.D. even though it was very hard for them to send me to another country; my aunts Mrs. Sunita and Mrs. Meeta, my uncles Mr. Sunil and Mr. Manjul, and my sister Kriti and brother Rohak for their endless love and support.

TABLE OF CONTENTS

LIST OF TABLES 7
LIST OF FIGURES 8
ABSTRACT 11
1. INTRODUCTION 12
1.1 *In vitro* models for cancer 12
1.2 3D cell culture based *in vitro* modelling 15
1.2.1 Types of 3D Cell Culturing Approaches 16
1.2.2 Matrix based 3D cell culture in diseases and drug discovery 18
1.3 Single cell analysis and heterogeneity 18
1.4 Techniques for Single Cell Culture 19
1.5 Current Protocol 24
2. METHODS 26
2.1 Cell line, culture medium, and treatment 26
2.2 Extracellular Matrix 26
2.3 Cell picking device 26
2.4 Single cell culture seeding and maintenance 27
2.5 Hoechst staining and microscopy 28
2.6 Retrieval of tumors 28
2.7 Re-culturing of single cells from a tumor 29
2.8 Statistical Analyses 29
3. RESULTS & DISCUSSION 31
3.1 Development phase 31
3.2 Current version 33
3.3 Morphological observations 34
3.4 Drug toxicity-based heterogeneity analysis 45
3.5 Intratumor heterogeneity analysis 48
3.6 Tumor transfer and re-culture as single cells 53
4. CONCLUSIONS 56
5. FUTURE WORK 59

5.1 Future applications of the protocol 59
5.2 Automation for future high-throughput assay 60
5.3 Co-culture with other cell types 61
5.4 Other types of cell lines, stem cells, and rare cells 62
LIST OF REFERENCES 65

LIST OF TABLES

Table 3.1. Cell survival and proliferation efficiency: percentage of the total number of islands. 34

Table 3.2. Pearson correlations between all other parameters for the six tumors in Figure 2.11. 52

LIST OF FIGURES

Figure 1.1. Advantages and disadvantages of 2D cell culture models 15

Figure 1.2. Commonly used techniques for 3D cell culture (Adopted from Gupta et. al.[15])..... 17

Figure 1.3. Representative images of the micro-raft array platform for single cell culture (a) multiple cells may go into a single well due to stochastic distribution of cells (b) wells are broken and transferred to 96 well plate with the intestinal enteroid (Adapted from Gracz et al.[36])..... 22

Figure 1.4. Representative images from the gel-island chip platform (a) Image of a fabricated device. (b) Schematic of the fabricated device showing cell culture chambers and main channel for exchange of fluids (c) Graph showing stochastic distribution of cells in the device (Adopted from Zhang et al.[37])..... 23

Figure 1.5. (a) Steps followed in the single cell culturing protocol: In a small Petri-dish, make spots of collagen matrix and seed them with single cells while the spots are partially submerged in culture media. After cell adhesion, fill the Petri dish with culture media to completely submerge the spots with cells. In 9-10 days, observe the spheroids that have developed from single cells that are available for further analysis. (b) Culture dish with 40-50 spots (c) Micromanipulator based micro-pipetting setup. 25

Figure 2.1. Cell picking setup parts with magnified images..... 30

Figure 3.1. Single cell culturing characteristics of 3 cell lines from 3 different types of cancer on 2D surface of a 96 well plate. Columns are of 3 types: cells without beads, cells conjugated with beads with the help of antibodies and cells spiked in blood and captured using antibody-magnetic bead separation method. Each column has three subtypes for single cells, 2 cells in a well and a control with hundreds of cells in a single well. 32

Figure 3.2. Island tracking over time reveals variable increases in tumor size. Single MCF7 cells were cultured on collagen I islands, as described in Figure 1 and resulting tumors were manually outlined (as shown in red) to measure their areas with Image J. a, Bright-field images of three tumors (Islands 1,2,3) over time. Grape-like features on the tumor top and at the periphery are indicated by white arrows. b, Temporal evolution of tumor area over 10 days for three biological replicates. Each solid dot represents the average area of 26 (in black), 48 (in red) and 47 (in blue) tumors with standard deviation. Inset shows the increasing trend in ratio of standard deviation to the average of tumor area for each experiment over time. c, Images of tumors from another experiment that were maintained in culture for 21 days. 36

Figure 3.3. Observation of necrotic core in long-term cultures: Single MCF7 cells were cultured on collagen islands for 24 to 26 days. a, Images of four tumors after 24 days of culture (with tumors delineated in red) b, Images of two tumors from another experiment after 26 days of culture that display darker central regions, as recorded with bright-field microscopy. Propidium Iodide (orange diffuse staining) images of necrosis are shown for the two tumors. Such darker central areas are observed in less than 8% of tumors that are cultured for long periods of time (more than 21 Days). 38

Figure 3.4. Tumors formed by single MCF7. Individual MCF7 cells were cultured on collagen I islands of 3320 Pa stiffness, as described before, and resulting tumors at day 10 of culture were outlined in red to visualize their size and shape. a: i to xv, Bright-field images of MCF-7 tumors; short 'arm-like' structures are indicated by white arrows in iii and viii. Secondary tumor formation possibly linked to cell migration is visible on image #xii as shown by blue arrows. b-d, Quantitative assessment of morphometry (area, circularity, aspect ratio) in three replicates (Exp. #1, 2 and 3) of MCF7 single cell cultures that gave rise to 26 to 47 tumors. Inset in all graphs represents the box plot for each experiment. 40

Figure 3.5. Morphological characteristics (area, aspect ratio and circularity) for MCF-7 tumors in 2020 Pa Collagen I stiffness. Comparison with 3320 Pa stiffness shows no significant difference as indicated by the high p-values for all three parameters studied. 42

Figure 3.6. Tumors formed by single Caco-2 cells. Individual Caco-2 cells were cultured on collagen I islands of 3320 Pa stiffness, as described before, and resulting tumors at day 10 of culture were outlined in red to visualize their size and shape. a: 1 to 7, Bright-field and Hoechst images of Caco-2 tumors; short 'arm-like' structures are indicated by white arrows in 1, 4, and 5. Secondary tumor formation possibly linked to cell migration is visible on image 2 as shown by blue arrows. b, Quantitative assessment of morphometry (area, circularity, aspect ratio) in a single replicate of Caco-2 single cell cultures. Inset in all graphs represents the box plot for each experiment..... 43

Figure 3.7. MDA-MB-231 cell behavior on collagen I islands: Single MDA-MB-231 cells were cultured on collagen islands for 10 days. In four representative islands some of the individual cells resulting from proliferation are indicated by an asterisk (rounded cells are either still, dying or undergoing mitosis). Some of the cells display a pseudopodia-like extension that may indicate migratory activity (see white arrows), which gives a possible explanation for the distance observed between cells on an island, and other cells display spindle-like shape (black arrow) characteristic of aggressive breast carcinomas that contain a mesenchymal type of cells. Cell division may lead to daughter cells of uneven size (red arrows). 44

Figure 3.8. Z-stack images of a tumor using Confocal imaging show tumors exist in many layers. 45

Figure 3.9. Treatment of MCF7 tumors with paclitaxel: Single MCF7 cells were cultured on collagen islands for 13 days before treatment with paclitaxel or vehicle DMSO (Control) for 24 hours. a: i & ii, Bright-field and confocal fluorescence (Hoechst) images of a tumor after treatment with 5 nM of paclitaxel. iii Zoomed portion of image ii showing nuclei (in blue) with one apoptotic (smaller and brighter) nucleus (white arrow). Scale bar: 100 µm. b, Bar graph of the percentage of apoptotic cells. Black dots represent individual tumors and black vertical lines represent standard deviations. Two-tailed heteroscedastic t-test based P-values for each of the six pairs of treatment are as follows: DMSO with 5 nM-0.972, DMSO with 20 nM-0.291, DMSO with 100 nM-0.004, 5 nM with 20 nM-0.297, 5 nM with 100 nM-0.004, 20 nM with 100 nM-0.477. 47

Figure 3.10. Morphometry analysis reveals a positive correlation between tumor area and high average as well as heterogeneity in nuclear area: Single MCF7 cells were cultured on collagen I islands, as described before. At day 14 of culture, area and circularity of tumors and areas of nuclei were analyzed with ImageJ. Trendline and associated R-square for the fit are shown with high positive Pearson correlation ($r \geq 0.70$, $n=6$) between nuclear area and tumor area (a) and between

tumor area and standard deviation [S.D.] in nuclear area (used as a measure of heterogeneity) (b). c & d, violin plots of nuclear area and circularity for each of the six tumors where fifty to 75 nuclei were analyzed per tumor. 49

Figure 3.11. Images and tumor area for the six tumors used for heterogeneity analysis: Single MCF7 cells were cultured on collagen islands for 14 days. a, Area and circularity for each tumor in the group. b, Merged images of six tumors (S1 to S6) recorded using bright-field and fluorescence imaging (fluorescence microscope, Nikon ECLIPSE 8i) following Hoechst staining that were used to obtain tumor morphology information. This information combined with nuclear morphometry information obtained with the confocal microscope were used for the analysis of the potential link between parameters of tumor morphometry and nuclear morphometry. 51

Figure 3.12. A tumor on top of the collagen I island can be easily extracted. **Top:** Successive images of a tumor being extracted from a collagen island, after 20-30 minute treatment with collagenase, using a glass tip of ~150 μm diameter; **Bottom:** Successive images of the same tumor being released at an alternate location (e.g., for applications such as dissociation and re-seeding of selected single cells from the tumor). The red outline delineates the visible portion of the tumor during different steps of the process. 54

Figure 3.13. Re-cultured cells forming tumors: Day 10 bright field images of tumors (marked in red) obtained by re-culturing of single cells after breaking an initial tumor into single cells as described in the methods section. 55

Figure 5.1. Possible future applications of the single cell culturing protocol..... 59

Figure 5.2. Schematic for automation of the different aspects of the protocol..... 61

Figure 5.3. Co-culture with other cell types 62

Figure 5.4. An example of a future application involving an automated high-throughput machine to study heterogeneity in primary cells from patient biopsy. 63

Figure 5.5. Schematic showing a proposed approach for personalized modeling and drug testing for cancer patients using liquid biopsies followed by deterministic single cell culturing in 3D. . 64

ABSTRACT

Models using 3D cell culture techniques are increasingly accepted as the most biofidelic *in vitro* representations of tissues for research. These models are generated using biomatrices and bulk populations of cells derived from tissues or cell lines. This thesis study focuses on an alternate method to culture individually selected cells in relative isolation from the rest of the population under physiologically relevant matrix conditions. Matrix gel islands are spotted on a cell culture dish to act as support for receiving and culturing individual single cells; a glass capillary-based microfluidic setup is used to extract each desired single cell from a population and seed it on top of an island. Using examples of breast and colorectal cancers, we show that individual cells evolve into tumors or aspects of tumors displaying different characteristics of the initial cancer type and aggressiveness. By implementing a morphometry assay with luminal A breast cancer, we demonstrate the potential of the proposed approach to studying phenotypic heterogeneity. Results reveal that intertumor heterogeneity increases with time in culture and that varying degrees of intratumor heterogeneity may originate from individually seeded cells. Moreover, we observe a positive correlation between fast-growing tumors and the size and heterogeneity of their nuclei.

1. INTRODUCTION

1.1 *In vitro* models for cancer

It is estimated that around 1.8 million new cases of cancer will be diagnosed in the year 2020 in the United States and roughly 600,000 will die from this disease[1]. The number of deaths from all forms of cancer is reported to be roughly 9.6 million worldwide (2018 estimate)[2]. This makes cancer the second leading cause of death worldwide (the first being heart disease), with one in every six people dying from cancer. There is a lot of focus, hence, on the development of drugs to manage this deadly disease. However, the process of drug development is slow and costly. One study estimates that it takes between $157.3 million to $1950.8 million (median $648 million) and 5.8 to 15.2 years (median 7.3 years) to bring a single viable cancer drug candidate to market [3].

One of the most important pieces of the drug development pipeline in cancer is the *in vitro* models that are used to study the safety and efficacy of drug candidates. *In vitro* cell culture models are used as surrogates for real tissue for cancer research and drug testing. *In vitro* models for cancer typically consist of immortalized cell lines that are derived from biopsies of cancer patients and mimic aspects of the original tumor such as cellular morphology, proliferation, and protein expression profile. The immortalized cell lines from solid tumors such as breast cancer, lung cancer, prostate cancer, etc. are typically cultured on 2D plastic surfaces which may be modified for cell attachment and supplied with a medium that consists of nutrients essential for growth and proliferation. These models are an important part of the drug discovery process since they are used to predict response to treatments.

2D cell culture has been used for decades to model the behavior of *in vivo* physiological conditions. It is still the most widely used form of studying *in vivo* responses due to the following reasons:

1. Ease of generating models:

Many types of cells that represent different physiological components of the human body have been isolated from patients and have been conferred immortality under laboratory conditions. The culture conditions have been studied and perfected over several decades and this technology is now available for many different types of cells. Other things that are needed for maintaining 2D cultures such as culture flasks, pipettes, bio-hoods, culture medium containing appropriate

nutrients are also available for cheap from multiple commercial vendors across the world. Moreover, many researchers and workers in biological sciences are trained regularly in 2D cell culture protocols. Thus, it is very easy for academic labs as well as commercial enterprises to acquire the resources to generate 2D models of the physiological components they are interested in studying.

2. Inexpensive:

Since 2D culture is the most widely used form of modeling *in vivo* conditions, it has led to economies of scale bringing down the cost of all the related material. Although the cost of the materials may vary depending on the exact type of model, model generation by 2D methods typically takes a small fraction of the total cost of a project.

3. Availability of suitable analysis platforms:

Many different types of analysis modalities such as imaging microscopes, microfluidic manipulation setups, and molecular probes have been developed and optimized for use with cells cultured using 2D cell culture techniques. These analysis modalities allow investigations of intracellular as well as intercellular properties of cells as well as effects of external perturbations at a very high resolution.

4. Reproducibility:

2D cell cultures have been maintained and cross-validated across many labs by multiple generations of researchers. While important gaps still exist in the requirements of reproducibility, cells cultured via 2D methods are still the most reproducible when compared to other types of models.

While there are several advantages of using 2D cell culture techniques, they also suffer from some major disadvantages for recapitulating aspects of the physiological tissues. Some of them are as follows:

1. 3D architecture of the *in vivo* tissue

Inside the body, all the solid tissue exists in a 3-dimensional space. 2D models fail to account for this 3D architecture, as the cells proliferate on a flat surface. *In vivo*, the cells interact with a matrix that allows propagation in 3-dimensional space. This has some important consequences for how these cells interact with their immediate microenvironmental components such as other cells of the same type or different types, fluids containing nutrients essential for their survival, growth, and

proliferation, or drugs. More specifically, cells cultured using 2D methods are exposed to a uniform concentration of molecules in the culture medium, as opposed to *in vivo* where a gradient of the concentrations exists due to multiple layers of cells between the medium and inside of tissue.

2. Absence of matrix

In vivo tissue consists of cells embedded in a biomatrix. This biomatrix provides the following in addition to 3-dimensional support:

a. Sites of attachment via formation of biochemical bonds
b. Mechanical stimulus by increasing or decreasing the density of fibers and/or crosslinking of fibers leading to increased or decreased microenvironmental stiffness.
c. A porous structure for the exchange of nutrients and other chemicals in the cellular microenvironment

All these factors have been shown to affect cellular state and function and are important to accurately capture physiological responses. This is difficult to achieve using 2D methods which mostly use plastic containers with modified surfaces for cell attachment.

The advantages and disadvantages of using 2D cell culture methods are also shown in figure 1.1 below.

The disadvantages discussed above have been a major deterrent in the fast and inexpensive development of new drugs for diseases such as cancer. It is often observed that drugs that pass the preliminary stage of efficacy testing using 2D models fail during animal testing or human trials due to reduced efficacy. The factors mentioned above are considered the major contributing factors for the high cost of development of drugs and failure in human trials. Thus, there is a need for improved *in vitro* models that can capture physiological conditions more accurately.

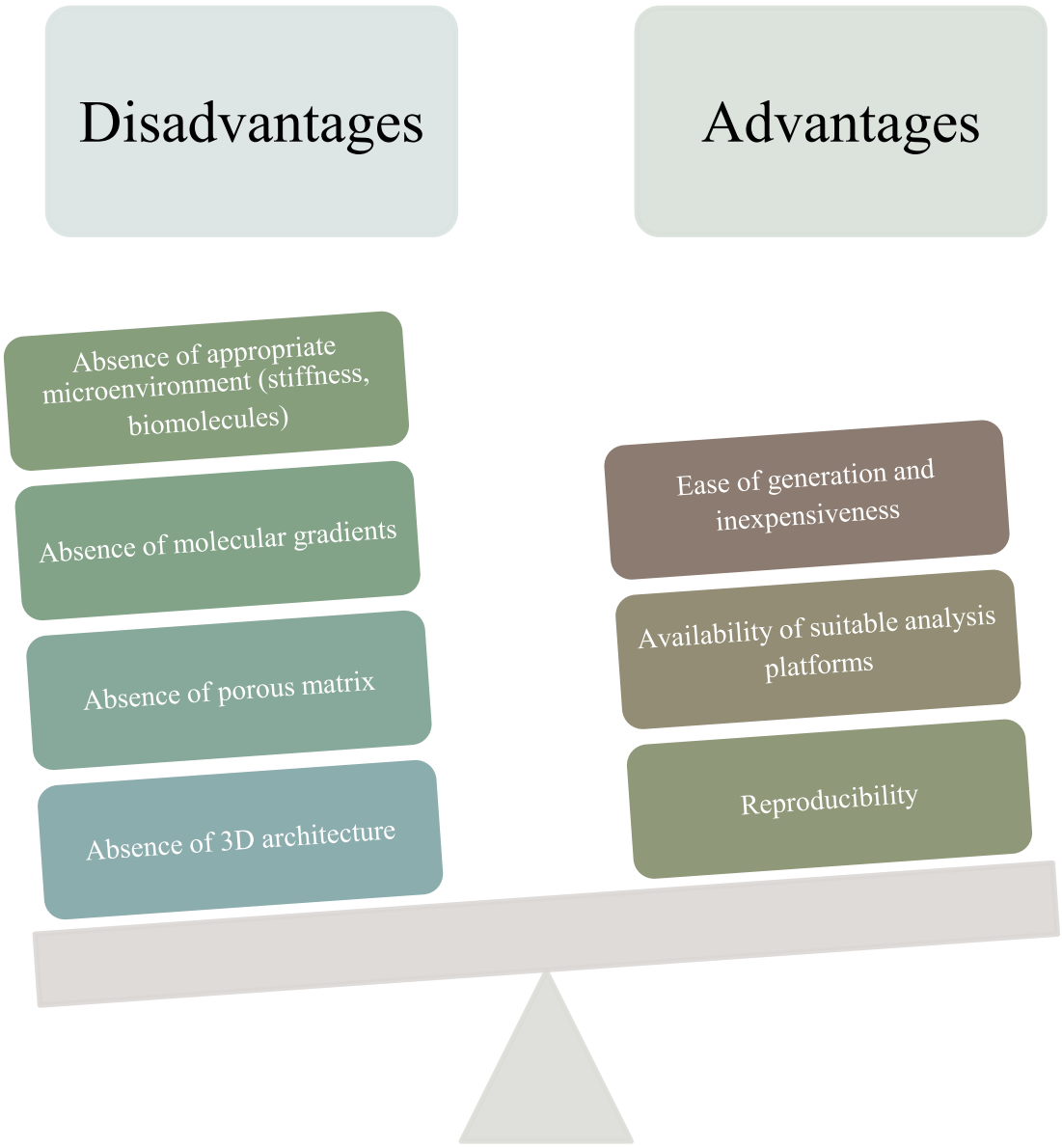

Figure 1.1. Advantages and disadvantages of 2D cell culture models

1.2 3D cell culture-based *in vitro* modeling

In the past few decades, advances in the development of biomaterials, imaging techniques, and the evolution of interdisciplinary approaches in biology have revolutionized the way cells are cultured for modeling tumors. Three-dimensional (3D) cell culture methods are increasingly used to generate complex tissue models. Multicellular structures created by 3D cell culture mimic aspects of *in vivo* microenvironments and generate organized cell assemblies that are biologically, histologically, and molecularly more similar to *in vivo* conditions than standard 2D cultures [4]. Such

models developed with cancer cells also constitute an ideal platform for *in vitro* testing of therapeutic drugs[4,5]. Cell lines and primary cells from patients' cancerous tissues have been successfully used in 3D cell cultures[6] to produce tumors (which we define as abnormal growths of tissue).

1.2.1 Types of 3D Cell Culturing Approaches

Traditional approaches for forming 3D entities to represent solid tumors can be adherent or non-adherent depending on whether they use extra-cellular matrices. Methods that employ non-adherent conditions including the hanging drop method[7], rotating bioreactor[8,9], magnetic levitation[10], or microfabricated modalities in various forms[11,12] have been reported. In a simple hanging drop method, hundreds of cells are encapsulated in a droplet of the culture medium, which hangs from the ceiling of a dish. These cells aggregate under the influence of gravity and attach with the nearby cells, giving rise to a 3-dimensional lump of cells that may mimic the porosity and concentration gradients of *in vivo* tumors. One or more cell types may be incorporated in this model and is more physiologically relevant than 2D cultures[13]. It is a fast and relatively inexpensive method of generating a 3D model of cancer. As opposed to the hanging drop method where gravity is used as an advantage, a rotating bioreactor offsets the effect of gravity by keeping the cells in a constant freefall inside the culture chamber. The combination of drag force of the fluid and gravity keeps the cells in a state of suspension. It was observed that rotating bioreactors lead to an increase in cell proliferation compared to 2D cultures with optimized conditions such as the velocity of rotation and seeding density of cells[14].

Yet another form of 3D culture is magnetic levitation schemes which achieve a similar state of suspension with the use of magnetic beads attached to cells and a constant magnetic field that keeps them suspended. The key to improved growth in both these schemes appears to be the increase in interaction between the cells and medium because of more surface area per cell being exposed in suspension. Finally, fluidic techniques such as microfluidic devices with non-adherent surfaces and non-adherent U-bottom plates have also been employed for 3D cell culture. These devices force the cells into self-aggregation by not allowing them to attach to the surface. These methods were summarized very accurately in a figure as shown below by Gupta et. al.[15]

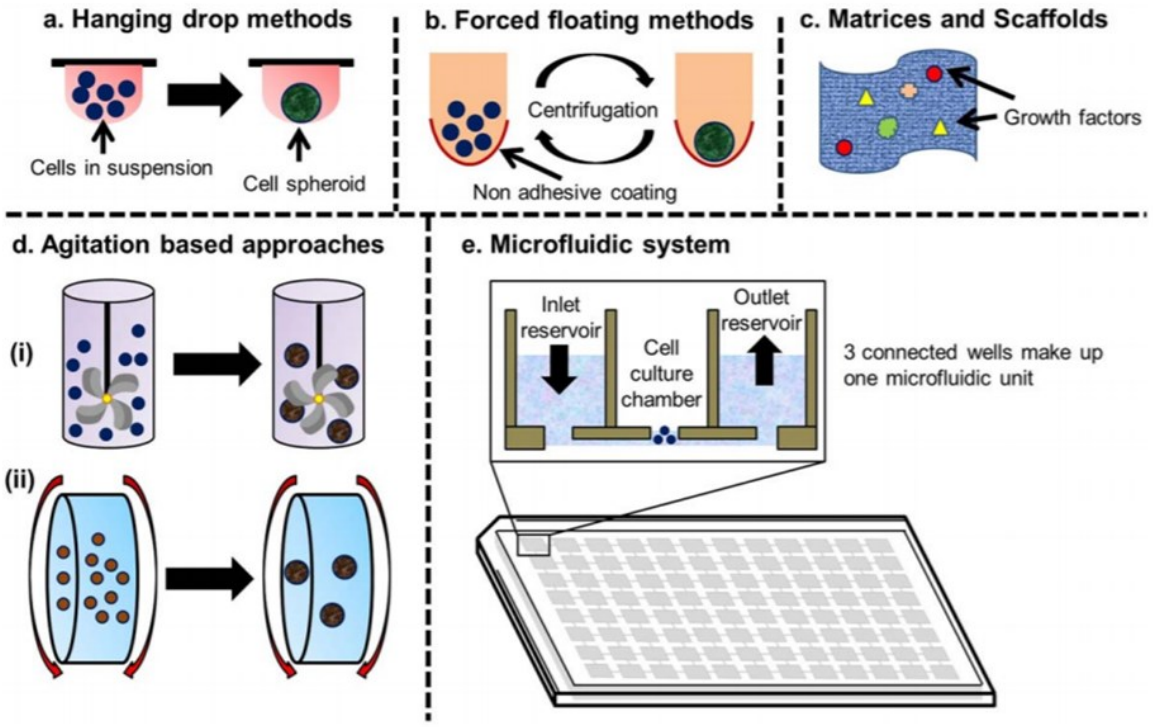

Figure 1.2. Commonly used techniques for 3D cell culture (Adapted from Gupta et. al.[15])

Some of these most widely used non-adherent techniques do not represent a true 3D cell culture that mimics tumor formation *in vivo*. When tens-of-thousands cells are aggregated into a spheroid (i.e., a mass with the spherical shape) such as in a hanging drop, reactor, or U-bottom plates, an extensive central necrotic core forms over a few hours due to the lack of nutrient and oxygen penetration beyond a 200 μm depth. Extended central necrosis is a rare phenomenon in real cancers.

This nonphysiologically-relevant cancer representation is exacerbated by the lack of progressive tumor development via cell division and the lack of interaction with an appropriate extracellular matrix (ECM). Under adherent conditions, in the presence of a matrix, 3D cell culture can be achieved in simple culture vessels or within microfluidic devices that permit a controlled supply of growth factors, drugs, and other stimulants[16,17]. Adherent 3D cell cultures may use specially designed matrices that mimic the porosity, stiffness, and adhesion strength of the original tissue[18].

1.2.2 Matrix-based 3D cell culture in diseases and drug discovery

When using 3D matrices, cells can either be embedded inside the matrix or on top of the matrix. Under such micro-physiologically appropriate conditions, cells do not only replicate morphological aspects of original tumors but also molecular aspects such as gene expression profiles, oxygen concentrations, and drug sensitivity[19]. Thus, 3D cultures are better predictors of drug sensitivity and have started replacing 2D *in vitro* models at various stages of drug discovery. Fang and Eglen describe how different 3D cell culturing techniques that use various sources of cells such as cancer cell lines, stem cells, or primary cells from patients are used at various points of the drug discovery process [5]. This study breaks down the drug discovery process into 5 stages: target identification (ID) stage, high throughput screen (HTS) stage, lead optimization and selection stage, preclinical stage, and finally clinical trials. It is suggested that other 3D culturing methods such as spheroid models and/or organ-on-a-chip models are used at the early stages. These are replaced with more complex models such patients derived spheroids and body-on-a-chip models for preclinical evaluation.

1.3 Single-cell analysis and heterogeneity

Most 3D cell culture models that generate tumors, start with a large bulk of cells that is used to "seed" the culture vessel. The techniques discussed above use either non-adherent conditions or adherent conditions and at least hundreds of cells to generate 3D multicellular structures. Although cells in the seed may originate from the same population, they can still be phenotypically different from each other at the single-cell level. Phenotypic variability exists *in vivo* where it creates hurdles in designing effective therapies (e.g. for cancer), requiring a better understanding of cellular heterogeneity[20–22]. The combination of subtle genetic variations and epigenetic traits arising from different sources of origin or microenvironmental conditions underlies phenotypic heterogeneity since it leads to different protein expression patterns. To better understand cell-to-cell variations, tumor cells have been isolated from tumor tissue or bodily fluids and analyzed[23,24]. Advances in sequencing techniques have helped tremendously the study of cell heterogeneity from a genomic perspective[25–27].

These techniques have various applications in developmental biology, disease modeling, and drug discovery. The advancement of these techniques has come due to the improvement in our

understanding of physical principles at the micro and nano-scale. This understanding has allowed the fabrication of devices that can work with the length scales of individual cells. This has further led to biological insights by observations of single cells as opposed to ensemble measurements of bulk populations of cells. Phenotypic heterogeneity occurring due to genetic and epigenetic differences between single cells has been studied in detail by various single-cell analysis approaches. A recent focus in this area has been on the integrated approaches that can yield multi-dimensional information about cell states including genetic information such as gene expression, DNA methylation, RNA profile and, spatial information such as location, clustering of same cell types, and morphology of cells in tissue[28]. Such multifaceted information has led to a better understanding of temporal and spatial heterogeneity between different tissues of the same type (inter-tissue) or within a single tissue (intra-tissue).

To further facilitate the study of cell heterogeneity from a functional perspective, it is highly desirable to generate tumor models that generate a tumor from one cell. Such studies can elucidate heterogeneity within a tumor generated by the proliferation of one given cell, as well as the heterogeneity among tumors obtained from different single cells. Such models can enable quantitative measurement and delineation of phenotypic variability caused by the microenvironment as opposed to the variability that is intrinsic to a given population of cells. This information can help uncover the underlying mechanisms and the role played by microenvironmental parameters that lead to heterogeneity.

Capturing the heterogeneity and the molecular mechanisms that lead to heterogeneity will help design therapies that better target the different phenotypes of cells within tumors and other tissues. It may also lead to more personalized treatment of diseases by the use of patient-specific phenotypes. Technologies such as this will be very useful in the future that relies on the principles of precision as well as personalized medicine[29].

1.4 Techniques for Single Cell Culture

Novel devices and protocols have been developed to generate 3D spheroids from single cells. These methods allow multivariate tracking of single-cell properties. To further facilitate the study of cell heterogeneity from a functional perspective, it is highly desirable to generate tumor models that each originates from one cell. Such studies can reveal heterogeneity within a tumor generated

by the proliferation of one given cell, as well as the heterogeneity among tumors obtained from different single cells. It allows quantitative measurement of phenotypic variability by making it easy to study Spatio-temporal development of heterogeneity using conventional assays. Single-cell culturing also enables quantification of the effects of microenvironmental variables by providing individualized control of cell culture conditions for each cell in the culture.

Automated technologies to separate a large number of cells into single cells of interest, such as Fluorescence-Activated Cell Sorting (FACS), have been employed to dispense single cells into microwells for culture[30]. This is a fast and high throughput method of obtaining cells of interest by first tagging them with the desired antibody-dye combination, and then using fluorescent sorting to put them into individual wells. However, FACS technique needs the introduction of at least 1000 cells at the inlet to fill all wells of a 96 well plate with single cells, indicating that the cell loss during sorting is quite high. Additionally, some wells invariably end up with more than 1 cell or no cells at all in a well. This is undesirable for single-cell analysis.

A limiting dilution method corresponding to the serial dilution of a suspension of cells has also been used to statistically (but not deterministically) contain one cell in a unit volume. This limiting dilution suspension is either mixed with an appropriate ECM or overlaid on top of it for cell culture[31–33]. This is a very fast and inexpensive approach for culturing single cells. However, there is considerable cell loss during the mixing and transfer process with this approach. While this approach works great to obtain single cells from a large population of cells, it is impractical when the cell population is small. These drawbacks make it less desirable for single-cell analysis especially when the cells of interest are rare.

Microfluidic platforms have been developed to address the unique problem of single-cell culture in 3D[34–38]. Among the examples, a micro-raft array was used to generate intestinal enteroids and organoids by exposing a group of cells to the culture platform until each cell in the group randomly occupied a micro-raft[37]. Then, all micro-rafts were covered with a gel matrix (MATRIGEL). Culture medium is supplied after the layer of Matrigel and can easily be exchanged from the top. Cells grow into the Matrigel and completely occupy the raft after sufficient days in culture. The micro-raft array provides individualization of the cells by separating them in the micro-rafts. Thus, each individualized compartment can be followed over several days and the fate of cell/cells in

each raft is determinable at any point during the assay. It is also amenable to automatic imaging because each raft has an indexed location that can be accessed via a translation stage. It can be used to perform co-cultures as discussed in the study, albeit by a stochastic distribution of different cell populations. Furthermore, a unique feature of this array is that each of the more than roughly 5000 rafts of the array can be separated from the rest of the rafts using a magnetic separation mechanism and the sample that is contained within it can be used for genetic analysis. This allows for doing multivariate functional analysis on the single-cell clonal population including cellular morphological analysis, studying effects of co-culture of different number and type of cells on the target cells, and gene expression profiles. It is a simple method of analyzing single clonal cell cultures that can easily be made completely automatic. It also has some important limitations. Since the cells are introduced into micro-rafts by limiting dilution, there is no control over the number and type of cells going into each well. Thus, the number of cells in each well follows a stochastic distribution, more specifically the Poisson distribution. This limits the ability to get single-cell information and gives less control over the co-culturing of different species of cells. Another important disadvantage is that it does not allow for long-term clonal cultures due to the limited volume of a single raft. When the generated spheroids indeed expand to the size of the raft, they are subjected to mechanical stresses due to confinement which may lead to mechano-transduction effects. Representative images from the platform are shown in the figure below.

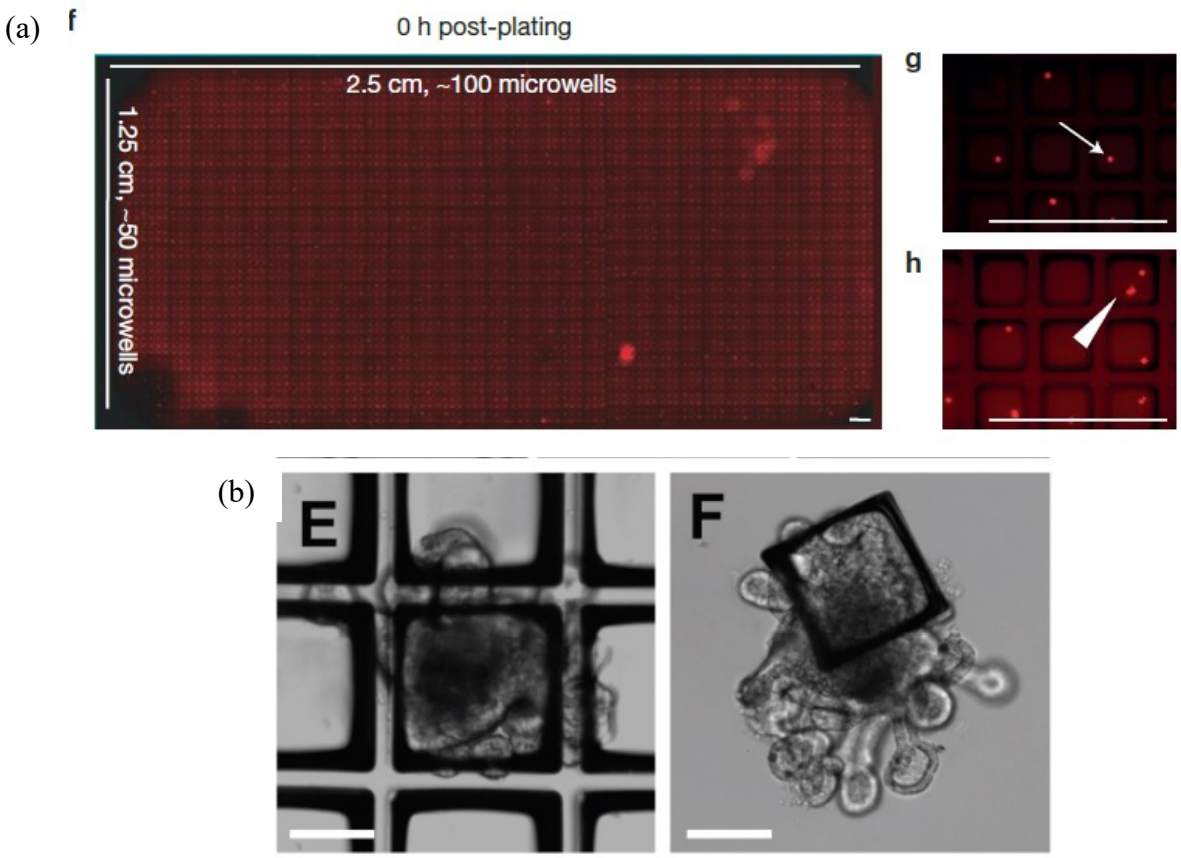

Figure 1.3. Representative images of the micro-raft array platform for single-cell culture (a) multiple cells may go into a single well due to stochastic distribution of cells (b) wells are broken and transferred to 96 well plate with the intestinal enteroid (Adapted from Gracz et al.[37])

A gel-island chip was also used for the formation and the analysis of tumors that originate from single cancer stem-like cells[38]. In this method, a liquid suspension of cells embedded in a collagen matrix flowed through the chip. The gel-encapsulated cells randomly occupied the islands, 34% of which end up with a single cell. This method of loading cells is like the limiting dilution method as discussed above and leads to a stochastic distribution of cells according to Poisson distribution. An additional drawback of this loading technique is the potential cell loss during loading. This is undesirable when the population of cells of interest is low. Then, the culture medium and growth factors were supplied through a channel to which all the islands were connected. The images of this device and the cell loading curve from the study are shown below.

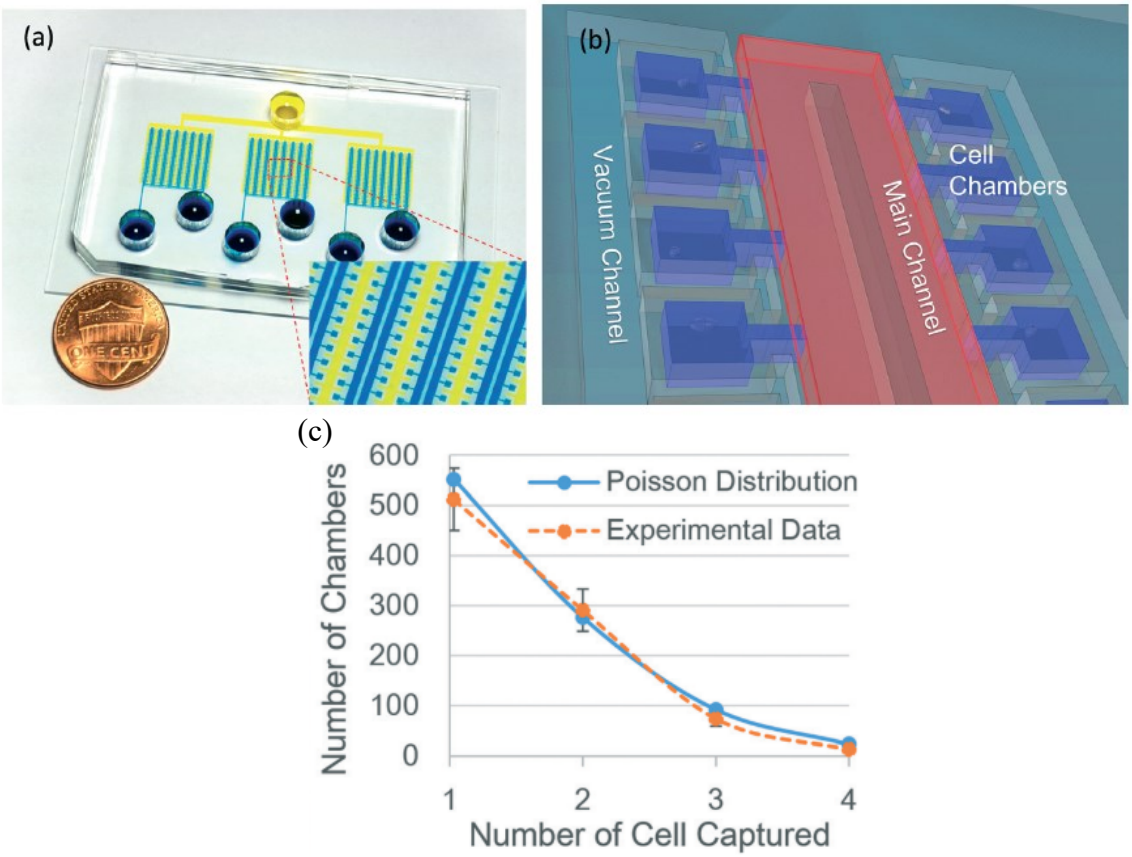

Figure 1.4. Representative images from the gel-island chip platform (a) Image of a fabricated device. (b) Schematic of the fabricated device showing cell culture chambers and main channel for exchange of fluids (c) Graph showing stochastic distribution of cells in the device (Adapted from Zhang et al.[38])

A common trait of these approaches for single-cell culture is they start with a suspension containing a large number of cells that are 'individualized' by random confinement in microstructures. As a result, all cells in the original suspension are eventually cultured without discrimination. Even in cases that involve heterogeneous mixtures of cells, where one may be interested in culturing and analyzing only a subset, all cells in the original mixtures need to be cultured and possibly analyzed. Both these approaches require fabricating many microstructures or wells so that each cell in the original suspension is accommodated. It also requires imaging of all microstructures to not miss the tumors originating from specific single cells, the proliferation of which is of interest. Moreover, the stochastic distribution of cells into the microstructures/wells introduces the possibility of multiple cells occupying a single well, which prevents developing a tumor from a single-cell.

Another commonality of the above schemes is the confinement of single cells within a microstructure that introduces the possibility of altering the cell phenotype by mechanical restriction[39,40], as well as difficulties to extract individual tumors after the culture is completed. Especially in applications that involve rare cells[41], such as circulating tumor cells (CTCs)[42–44], metastasis initiating cells (MICs)[45–47], or fetal cells[48,49], where the targeted cells are only a few and sometimes only one, a deterministic method that enables growing a tumor or another tissue only from a single targeted seed cell, as well as facile extraction of the resulting tissue for downstream analysis, would be highly advantageous.

1.5 Current Protocol

Here we describe a method (Fig. 1.5a-c) that uses a deterministically targeted single cell as the seed. Only the chosen single cells are individualized on top of collagen islands. Our approach combines the flexibility to choose single cells of interest through micromanipulation with the benefits of 3D culturing in physiological conditions and explores the evolution of single cell-derived tumors. It makes use of standard Petri dishes and micro-manipulating pipettes commonly used in embryological studies thus avoiding the need for specialized and costly equipment. We demonstrate the growth of individually selected single breast cancer (MCF-7 & MDA-MB-231) and colon cancer (Caco-2) cells on collagen support that mimics cancer tissue. The single cells are cultured for anywhere between 7 and 20 days depending on the application. The tumor size varies considerably and may get as big as 1 mm in diameter after 20+ days. The smaller tumors can be easily extracted from their culture location and transferred elsewhere for long-term culture or subsequent downstream analyses. Using morphometric parameters as an example, we demonstrate the method's potential for the study of inter- and intra-tumor heterogeneity and show preliminary information regarding a potential relationship between tumor architecture and the organization of cell nuclei as it relates to cancer aggressiveness. We also provide proof of concept experiments for the protocol's potential use in drug screening. We expect this method to be highly amenable to a wide range of applications, including culturing of rare circulating tumor cells or fetal cells.

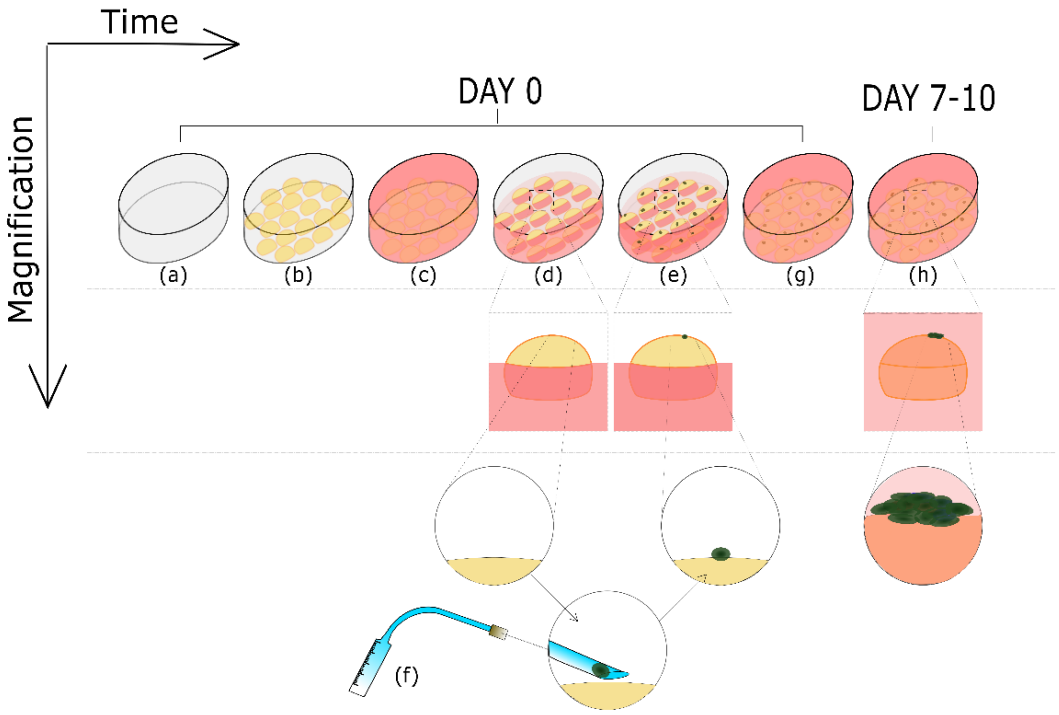

(a)

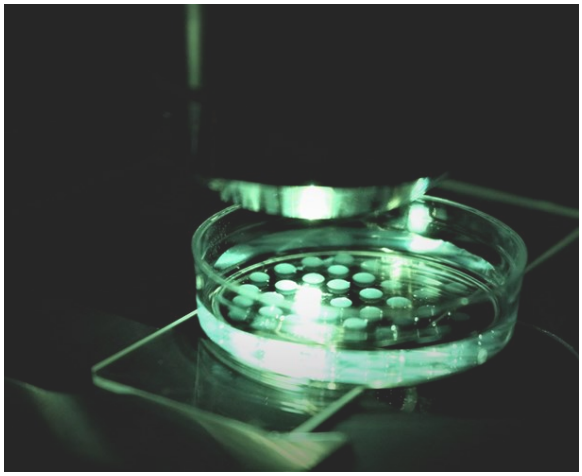

(b)

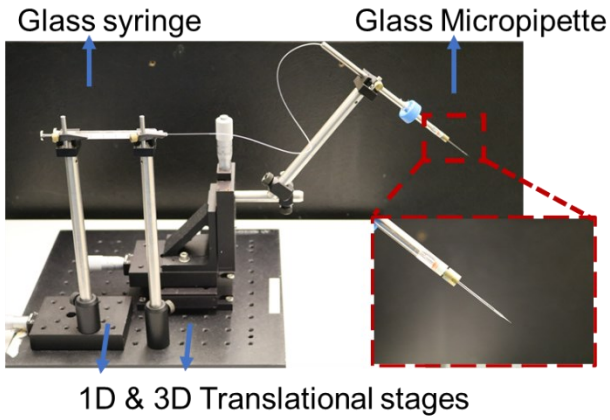

(c)

Figure 1.5. (a) Steps followed in the single-cell culturing protocol: In a small Petri-dish, make spots of collagen matrix and seed them with single cells while the spots are partially submerged in culture media. After cell adhesion, fill the Petri dish with culture media to completely submerge the spots with cells. In 9-10 days, observe the spheroids that have developed from single cells that are available for further analysis. (b) Culture dish with 40-50 spots (c) Micromanipulator based micro-pipetting setup.

2. METHODS

2.1 Cell line, culture medium, and treatment

MCF-7 cells (American Type Cell Culture, Manassas, VA) were cultured in RPMI 1640 medium (ATCC) with 10% Fetal Bovine Serum (ATCC). Caco-2 cells (a kind gift from Dr. Mohit Verma) were cultured with DMEM medium (ATCC) with 20% Fetal Bovine Serum and other additives (Final concentrations: 4.5 g/L Glucose, 10 mM HEPES, 44 mM Sodium Bicarbonate, 1 mM Sodium Pyruvate, 100 µM non-essential amino acids, 50 mg/L Gentamycin Sulfate, 100 U/L Penicillin, 100 U/L Streptomycin, 2 mM Glutamine, pH 7.2). MDA-MB-231 cells (ATTC) were also cultured in RPMI 1640 medium (ATCC) with 10% Fetal Bovine Serum. Paclitaxel (Selleck Chemicals, Houston, TX) prepared in DMSO (ATCC) was used to treat some of the tumors formed by single cells seeded on collagen I islands.

2.2 Extracellular Matrix

We used the PHOTOCOL UV (Advanced BioMatrix, San Diego, CA) that is a Methacrylated Type I collagen. Depending on the desired volume, and stiffness of 3320 Pa, the lyophilized and Methacrylated Type I collagen was mixed with an appropriate amount of 20 mM acetic acid solution and a neutralization solution, as per the manufacturer's protocol. The mixture was kept on ice to maintain the final solution in the liquid state. Drops (5 µl) of collagen were printed on a culture dish and used for single-cell culture as described below. The thermosetting nature of PHOTOCOL helped keep the gel islands fixed onto the culture dish once they were deposited, and the dish was placed in a temperature-controlled incubator.

2.3 Cell picking device

A cell picking device was assembled using a glass capillary micropipette tip (Clunbury Scientific LLC, Bloomfield Hills, MI) a 3-axis translational stage for accurate movement of the pipette tip (Thorlabs Inc., Newton, NJ) and 250 µl airtight SGE glass syringe with Luer Lock (Fig. 2.1). A hollow glass capillary of 50 µm diameter worked as a micropipette. It was attached to an adapter, which in turn was attached to a syringe via Polytetrafluoroethylene (PTFE) tubing. The syringe was also fitted with a unidirectional translation stage for precise control of flow (subsystems

extensively imaged and presented in Fig. 2.1). Alternatively, the syringe can also be operated with a syringe pump. The system was optimized to manually pick up and dispense nanoliter volumes of liquid and work with an efficiency of one to two cells/min while transferring a single cell from a dish to a matrix island.

2.4 Single-cell culture seeding and maintenance

For single-cell culturing, approximately 5000 cells from the flask were obtained by dilution and placed in a dish for picking. The cells that ended up on each island were picked from among these 5000 cells. The same culture medium mixed with 1% v/v GIBCO Penicillin-Streptomycin (10,000 U/ml) antibiotic (Life Technologies, Carlsbad, CA) was used to culture single cells. The antibiotic was added to avoid bacterial contamination that can occur when transferring cells onto the matrix island in nonsterile conditions. Five µl liquid drops of collagen matrix were deposited at the desired number of spots (up to 50) on a sterile 35 mm polystyrene culture dish (CORNING 430558). The matrix was allowed to solidify for 30-45 minutes in the same incubator that is used for cell culture (maintained at 37° C temperature, 5% CO_2 concentration, and 95% Relative Humidity). After stiffening of the matrix, 2 ml of RPMI 1640 culture medium premixed with 10% v/v fetal bovine serum and 1% v/v GIBCO Penicillin-Streptomycin (10,000 U/ml) antibiotic, pre-heated to 37 °C was introduced in the dish. This was done slowly by placing the pipette tip against the side of the dish to avoid air bubbles and dislocation of the islands. Then the dish was placed into the incubator until cells were ready for seeding. Addition of the cell culture medium allowed for the matrix to remain solid without drying out. When it was time to seed the cells, 1.8 ml of culture medium was removed from a side of the dish, which exposed the top of each island while keeping the islands partially immersed to avoid drying.

The cell-picking setup was used to pick and place single cells from another dish to the top of Collagen I islands one at a time, using a microscope. After all the cells were transferred, the dish was covered and placed in the cell culture incubator for 20-30 minutes to allow the cells to stick to the matrix. During this period the surrounding liquid medium at the bottom of the dish provided enough moisture to avoid drying. At the end of this period, 1.8 ml of culture medium with 1% v/v antibiotic was replenished gently, and the culture dish was returned to the incubator.

The culture medium was changed every 5-7 days initially with single cells and when the tumors were small, and more frequently (every 2-3 days) as tumors became larger. Removing and adding medium was performed from the side of the culture dish to avoid turbulence.

2.5 Hoechst staining and microscopy

Cells were washed in PBS and fixed in 4% paraformaldehyde before staining with 1:1000 PBS diluted solution of 20 mM Hoechst 33342 (Thermo Fischer Scientific, Waltham, MA) for 10 minutes. After washing once with PBS, tumors were imaged with a ZEISS LSM 800 confocal microscope with an excitation laser of 401 nm wavelength and with a 10X magnification lens (EC Plan-Neofluar 10X/0.30 M27). Bright-field and fluorescence images obtained using NIKON ECLIPSE 80i upright fluorescence microscope were used to analyze the morphology of the tumors with ImageJ. Z-stacks were obtained for each tumor at a Z-step size equal to half of the depth of field which was 14.5 µm (using objective: EC Plan-Neofluar 10x/0.30 M27). For each tumor, dead and live nuclei at every alternate plane of the z-stack were manually counted using Fiji. Each alternate plane of the Z-stack was skipped to account for the overlap in signal due to the depth of field being twice that of Z-step size. This approach allowed for better resolution images and prevented any double-counting of cells. A similar approach was used for the assessment of nuclear morphometry after manual segmentation with Fiji.

2.6 Retrieval of tumors

The 3D cultures were treated with collagenase for 20-30 minutes to partially digest the surface of the collagen islands and help detach tumors from the top of the island. A pipette tip of ~150 µm diameter was used for retrieval of tumors of 0.1-0.2 mm^2 in size on average, under a microscope. The diameter of the tip was chosen so that it is significantly smaller than the island but similar in size to the tumor to retrieve the tumor without accidentally aspirating an entire collagen island, as shown in Figure 3.12. A larger diameter of the tip may be used depending on the size of the tumors. Manual control of the picking process permitted more precision for the retrieval of tumors, without breaking them apart.

2.7 Re-culturing of single cells from a tumor

The desired tumor was extracted as described before. Then, 10 µl of Trypsin-EDTA solution was placed in the cap of a small RNA-free tube. The extracted tumor was introduced into the trypsin solution for 5 minutes. The rest of the tube was filled with 100 µl of culture medium with 10% FBS and the tube was centrifuged gently (600 g for 5 seconds) to mix the Trypsin with the culture medium and stop Trypsin activity. The liquid was moved up and down rapidly with a 5 µl pipette to break down the tumor into smaller clusters. All of the liquid was removed and placed in the center of a 35 mm culture dish. Another 500 µl of culture medium was added gently and single cells were picked up as described before.

2.8 Statistical Analyses

To analyze the variation in nuclear area and nuclear circularity for heterogeneity analysis, the sample standard deviation formula in MS-EXCEL was used. Pearson Correlation coefficient function of MS EXCEL was used to study the correlation between every two of the following six parameters: Tumor area, tumor circularity, Average Nuclear Area, Average Nuclear Circularity, Standard Deviation of Nuclear Area, Standard Deviation of Nuclear Circularity. Violin plots for the nuclear area and nuclear circularity were created using the ORIGIN(Academic), Version 2019b, OriginLab Corporation, Northampton, MA.

A two-tailed heteroscedastic (unequal variance) T-test was used to compare the percentages of cell death between tumors treated with different concentrations of Paclitaxel (Comparisons were made between 0 nM & 5 nM; 5 nM & 20 nM; 20 nM & 100 nM). A similar test was used to check the statistical difference between the three replicates for comparing tumor morphologies.

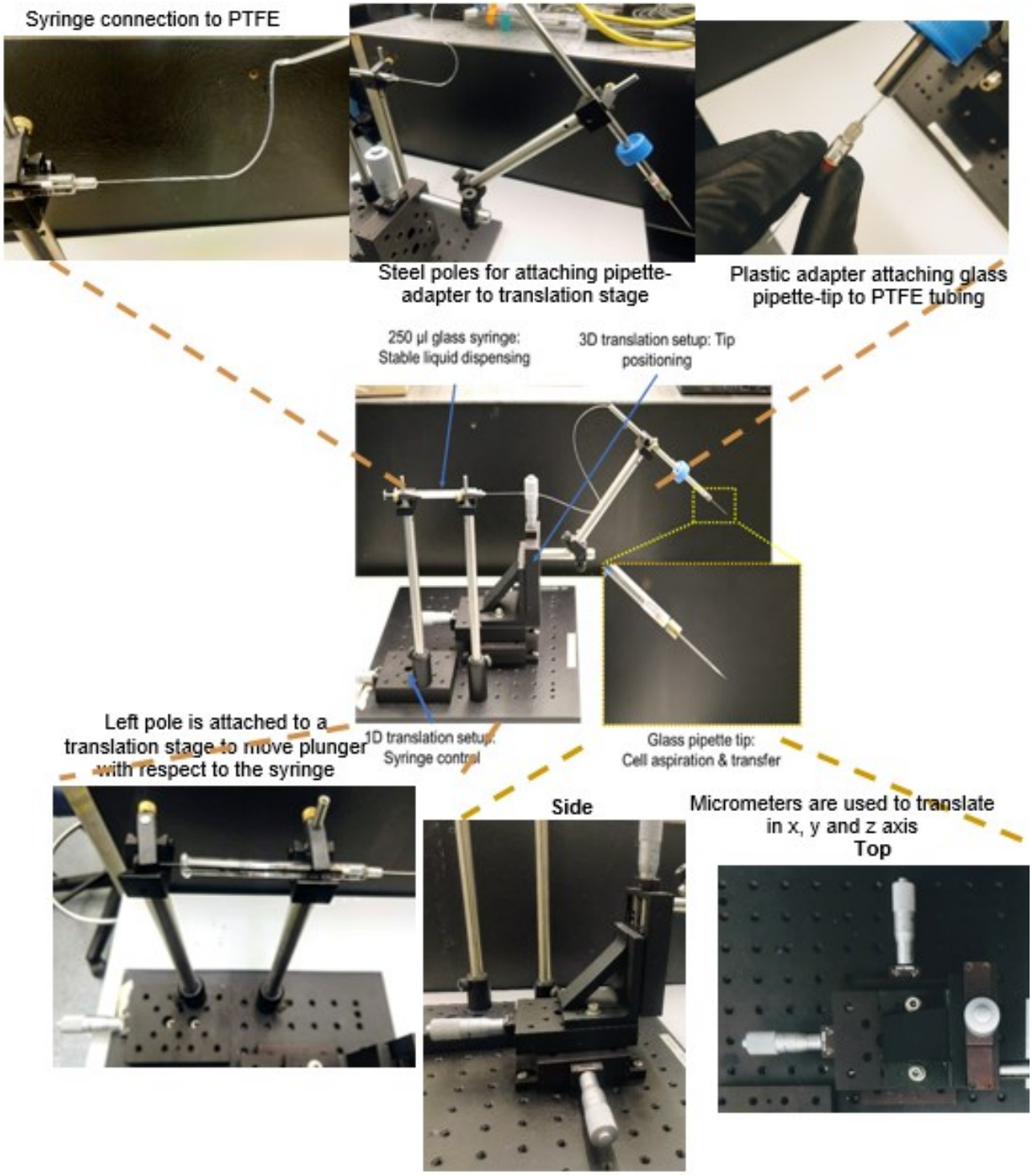

Figure 2.1. Cell picking setup components with magnified images.

3. RESULTS & DISCUSSION

The key results of the following work were published in July 2020 in Nature Scientific Reports. (Citation: Jain, R., Chittiboyina, S., Chang, CL., Lelièvre SA., Savran CA. Deterministic culturing of single cells in 3D. *Sci Rep* **10,** 10805 (2020).

https://doi.org/10.1038/s41598-020-67674-3

3.1 Development phase

To begin with, we performed characterization experiments to understand single cell culturing characteristics of single isolated cells. 10-20 wells of a 96 well plate were supplied with 1 cell from breast, lung, and pancreatic cancer epithelial cell lines and supplied with culture media according to ATCC specifications and 10% added fetal bovine serum. 100+ cells were seeded in a single well of the 96 well-plate from the same population of cells as control. It was observed that at least 50% of the wells with single cells observed after 7-8 days were alive for all three cell lines. Additionally, to mimic CTCs captured by immunomagnetic separation, all three cell lines were also cultured when conjugated with magnetic beads. There was no significant change in survival rate in comparison to cells without beads. Results are summarized in Figure 3.1. The MCF-7 cell line was selected to pursue the development of the single-cell 3D culture method in light of their high survival rate (95%). These cells are classified as luminal A type of breast cancer cells (estrogen receptor and progesterone receptor positive). This subtype of breast cancer is mostly non-aggressive, and in 3D cell culture, MCF7 cells typically form tumors that rarely present invasive extensions or migratory patterns.

Collagen I was used as the ECM for 3D cell culture because it is the most abundant fibrous molecule surrounding tumors of epithelial origin like carcinomas, and it can be tuned to the desired stiffness to mimic that of cancerous tissues. Conventional matrix-based 3D cultures in standard well plates use a large amount of collagen spread over the area of each well. For standard 3D cell culture applications that use a large number of seed cells per unit volume of the collagen, it is possible to easily identify and image cells or clusters of cells of interest. However, when seeding a small number of single cells, it is challenging to find and image one particular cell that is almost transparent against a large pool of collagen matrix. This challenge is further exacerbated if the

seeding location is not referenced, or the cell in question migrates and/or if it is embedded inside the matrix. Microplates, such as 384 and 1056 well plates have smaller wells, which reduces the amount of collagen needed. However, this setting also reduces the amount of culture medium, i.e. nutrients that need to be supplied to the growing tissue. The necessary frequent changes of the culture medium are greatly impeded by the narrow space in these wells, which prevent the user from easily maneuvering a micro pipettor. Therefore, we sought to design a method that has an optimal balance of collagen matrix and volume of medium to sustain the growth of tumors from single cells initially deposited in registered locations and enables easy observation of the growth process.

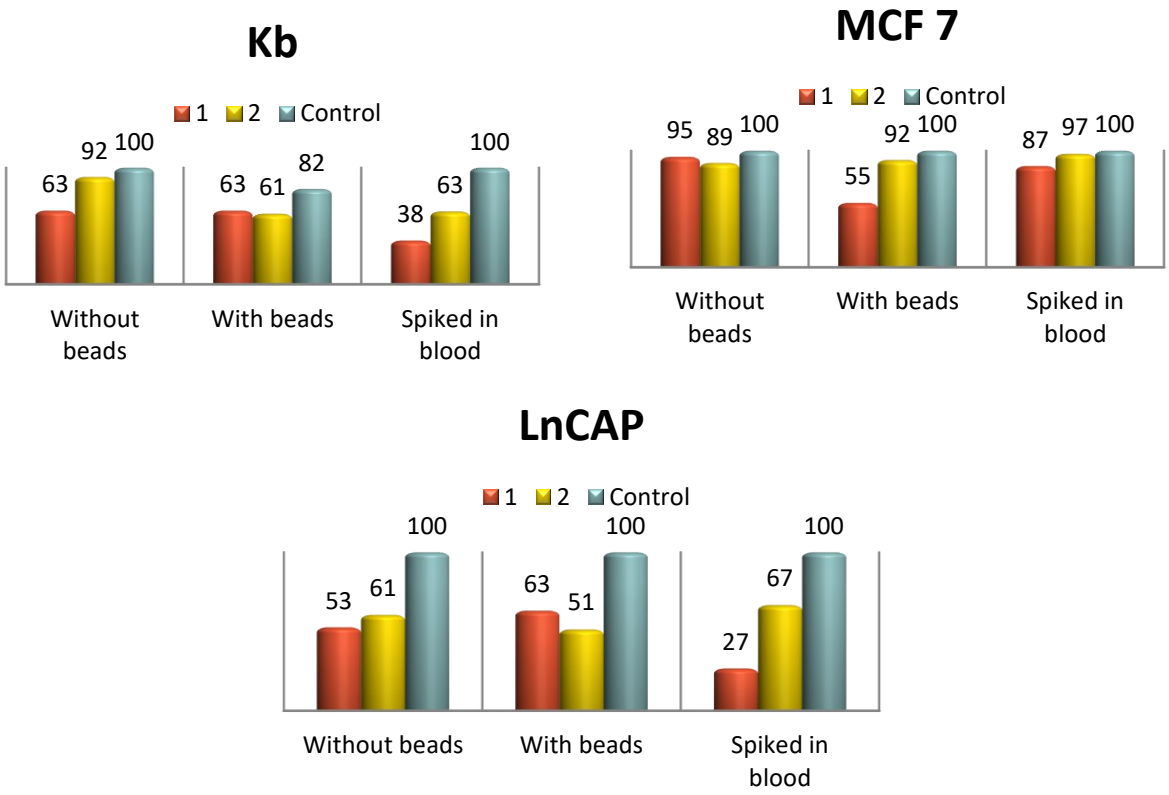

Figure 3.1. Single-cell culturing characteristics of 3 cell lines from 3 different types of cancer on the 2D surface of a 96 well plate. Columns are of 3 types: cells without beads, cells conjugated with beads with the help of antibodies, and cells spiked in blood and captured using an antibody-magnetic bead separation method. Each column has three subtypes for single cells, 2 cells in a well, and control with hundreds of cells in a single well.

3.2 Current version

In the current version of the protocol (Figure 1.5), small drops of 5 µl of collagen are made in a 35 mm Petri dish. 40-50 drops of the matrix can stick as hemispherical spots on a single polystyrene dish (Figure 1.5b). The resulting spot has a diameter of about 3 mm. Single cells are seeded on the spots using a custom-made micro-manipulating micropipette (Figure 1.5c). Each dish is incubated for 9-10 days at 37°C, 5% CO_2 and 95% RH. Methacrylated Type 1 collagen (referred to as collagen from here on) is used as the 3D matrix to mimic breast tissue. This type of gel is easy to handle and manipulate and can provide a range of stiffnesses. The matrix stiffnesses for the current demonstration: 3320 Pa and 2020 Pa; are higher than the normal breast tissue and more closely resemble the malignant breast tissue[50]. Single cells were seeded on the islands using a cell picking set-up developed in house. Culturing the cells on relatively small, fixed spots referred to as 'islands,' allowed simple tracing of a particular cell by recording still images at various intervals, without continuous time-resolved microscopy that would otherwise be necessary if multiple cells were used (since cells can often migrate over small distances on the surface of collagen).

Once a cell is seeded on top of a collagen matrix island, there are two possible immediate outcomes; the cell may successfully bind to the collagen gel or it may not bind and float away. If the cell binds to collagen, it may or may not survive, and if it survives, it may (epi)genetically be predisposed to proliferate or find the culture conditions unsuitable for proliferation. To study the reproducibility of these outcomes, three biological replicates of the cultures (i.e., using three different batches of MCF7 cells) were performed for each Collagen 1 stiffness. Collagen matrix islands were spotted on 35 mm dishes with the number of islands in each dish varying between 25 and 50. Each island was seeded with exactly one MCF-7 cell on Day 0 and observed on Day 1 to 2 to check for cell attachment and again on Day 9 to 10 to check for sustained attachment and proliferation under an upright microscope in brightfield mode. Hoechst staining was used to visualize cells in the tumor using fluorescence microscopy. As shown in Table 3.1, a great majority of the islands (83% to 98%) successfully retained a single MCF7 cell (the first column is the total number of islands in each dish that were seeded with a single MCF-7 cell on Day 0; the second column shows the percentage of islands each having a single cell successfully attached after one to two days). As illustrated in the third column of Table 3.1, the percentage of islands with visible cells nine to 10 days after seeding was lower than at day 1; it might be due to cell death in the first

few days of culture or detachment of the cells. The cell clusters that were visible on the islands at the end of the observation period varied in size. In summary, over the three biological replicates, 81-94% of the islands had visible cells (nonproliferating or organized into tumors; column 3 of Table 3.1) and 66-87% of the islands harbored tumors larger than 0.005 mm^2 (column 4 of Table 3.1), indicating that the cells that seeded these tumors had a strong proliferation potential. From this first set of observations, it could also be concluded that individual cells that came from the same nominal (MCF7) population displayed different potentials to survive and proliferate to form tumors. A detailed description of the protocol is discussed in the methods section.

Table 3.1. Cell survival and proliferation efficiency: percentage of the total number of islands

3320 Pa	Total number of islands seeded (100%)	Islands with a cell on Day 1 to 2	Islands with visible cells on Day 9 to 10	Islands with tumors of area >0.005 mm^2 on Day 9 to 10
Exp 1	26	96%	92%	77%
Exp 2	48	98%	94%	81%
Exp 3	47	83%	81%	66%
2020 Pa				
Exp 1	36	97%	94%	86%
Exp 2	45	96%	89%	87%
Exp 3	44	86%	84%	77%

3.3 Morphological observations

Single cell-derived tumors are reminiscent of the cancer type and reproduce intertumor heterogeneity.

An advantage of the current scheme is the inherent efficacy in tracking the behavior of a single cell at the beginning of the culture period. Locating and recognizing the cell on the collagen island is a rapid process, even if the cell migrates over small distances. Similarly, changes in the appearance of multicellular clusters and tumors can be made using bright-field upright microscopy. Hence, the cells can be observed by a sequence of still images, (as opposed to monitoring multiple cells using continuous time-resolved microscopy) as shown by multiple examples of a single MCF-

7 cell evolving into a tumor (Fig. 3.2 a-c). Islands 1 and 3 for instance, show grape-like features on the tumor top and at the periphery, while for the tumor on island 2 the top surface appears regular or smooth (Fig. 3.2a). All experiments show an increase in tumor size based on the duration of culture, but with increasing disparity among tumors (Fig. 3.2b). In cultures kept for 20 to 25 days, some tumors continue to grow and cover most of the collagen island's top surface, with a diameter above 500 μm (Fig. 3.2c). Very few tumors (on average two out of 30) display a dark central region. When observed under fluorescence, these regions are faintly colored in red after treatment with Propidium Iodide, confirming necrosis (Fig. 3.3)[51]. Thus, cultures should be stopped before tumors reach 400 μm in size since the maximum penetration depth of nutrients and oxygen is ~200 μm. All analyses for the rest of the experiments were performed with 10-14 days old 3D cultures and tumors below 400 μm.

These cultures can be sustained for about 20-25 days when they completely cover the spot and need to be transferred to a bigger well with more matrix. In Figure 3.3, images from another experiment show spheroids that were cultured in a Petri dish for 24 to 26 Days. The four spheroids that are shown in Figure 3.3a are all greater than 500 μm in diameter.

Heterogeneity in morphological characteristics of tumors within an experiment where micro-environmental conditions do not change reflects the heterogeneity in the initial cell that seeded those tumors. This heterogeneity for MCF-7 tumors has been depicted in Figure 3.4 where part a. shows a qualitative representation of tumor features and parts b-d show quantitative heterogeneity based on area, circularity, and aspect ratio. To analyze the extent of contribution that the Collagen 1 matrix makes to the evolution of tumors, another comparative experiment was designed where MCF-7 were seeded in a matrix of slightly different stiffness: 2020 Pa. It was observed that there was no significant difference between any of the three parameters that were studied for Collagen 1 matrix of stiffness 2020 Pa versus Collagen 1 matrix of stiffness 3320 Pa as shown in Figure 3.5.

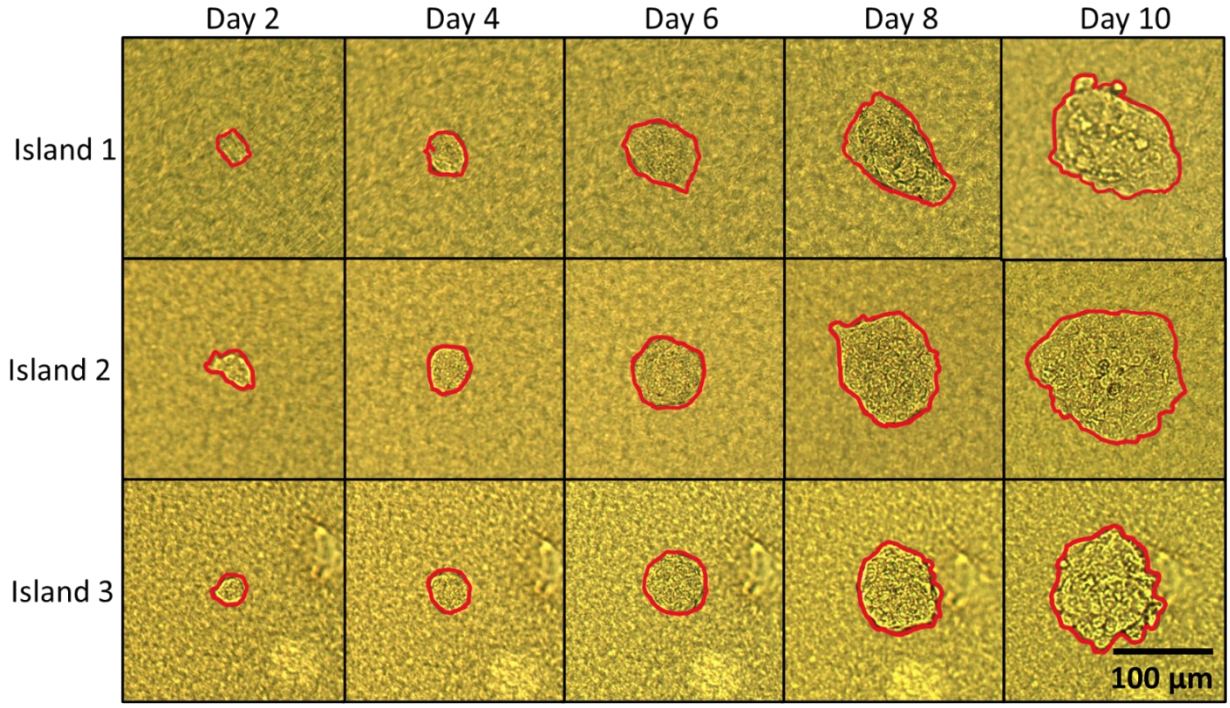

(a)

Figure 3.2. Island tracking over time reveals variable increases in tumor size. Single MCF7 cells were cultured on collagen I islands, as described in Figure 1, and resulting tumors were manually outlined (as shown in red) to measure their areas with Image J. a, Bright-field images of three tumors (Islands 1,2,3) over time. Grape-like features on the tumor top and at the periphery are indicated by white arrows. b, Temporal evolution of tumor area over 10 days for three biological replicates. Each solid dot represents the average area of 26 (in black), 48 (in red), and 47 (in blue) tumors with the standard deviation. Inset shows the increasing trend in the ratio of the standard deviation to the average tumor area for each experiment over time. c, Images of tumors from another experiment that were maintained in culture for 21 days.

Figure 3.2. (cont…)

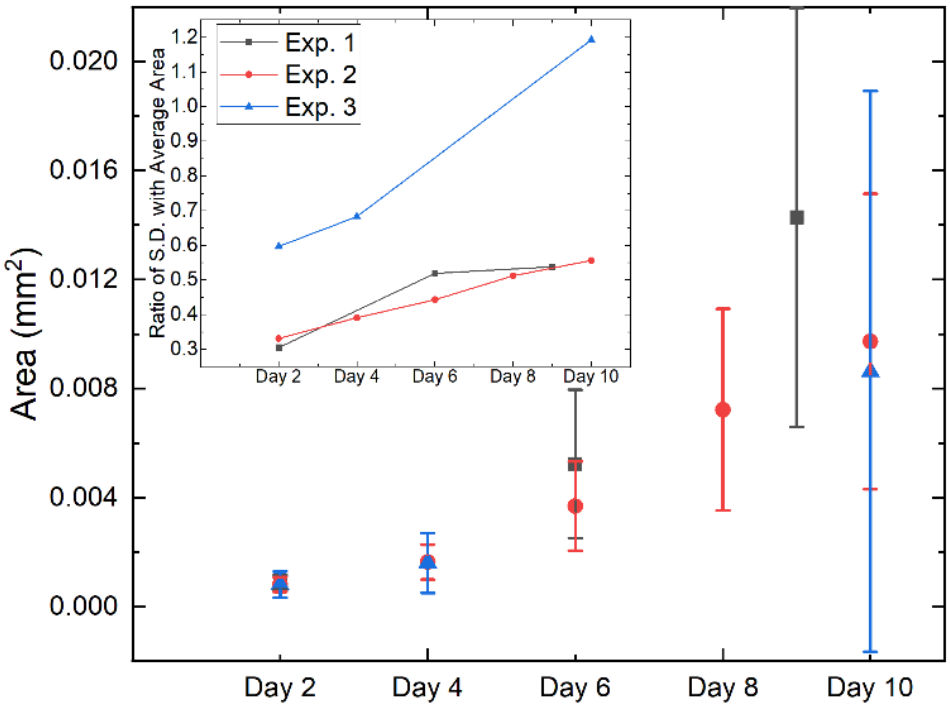

(b)

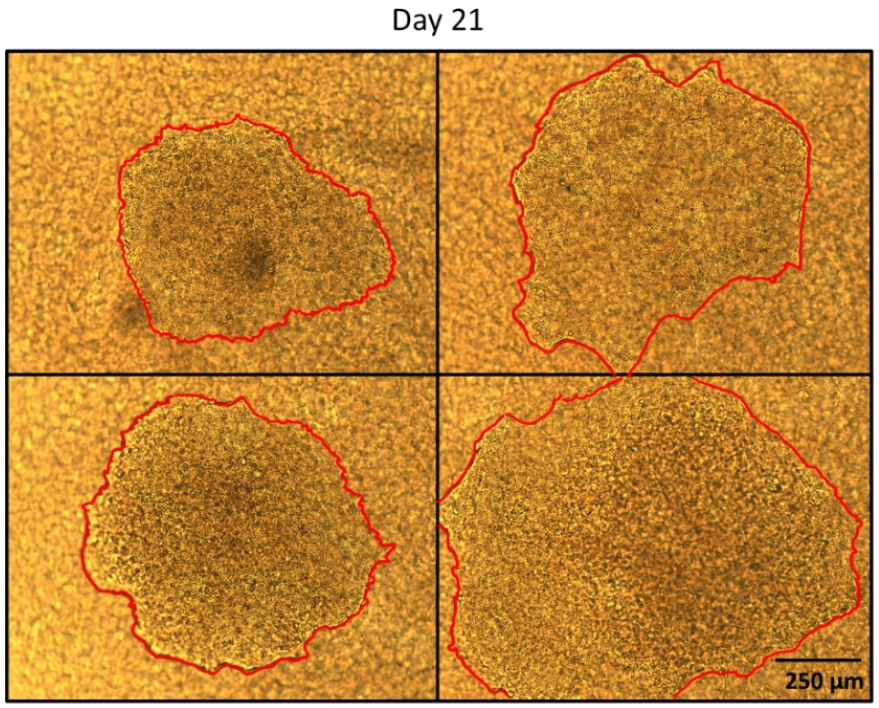

(c)

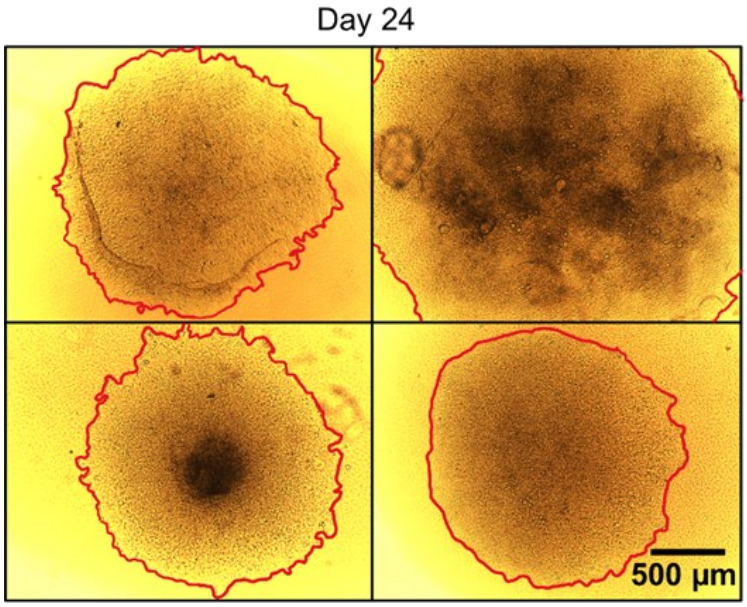

(a)

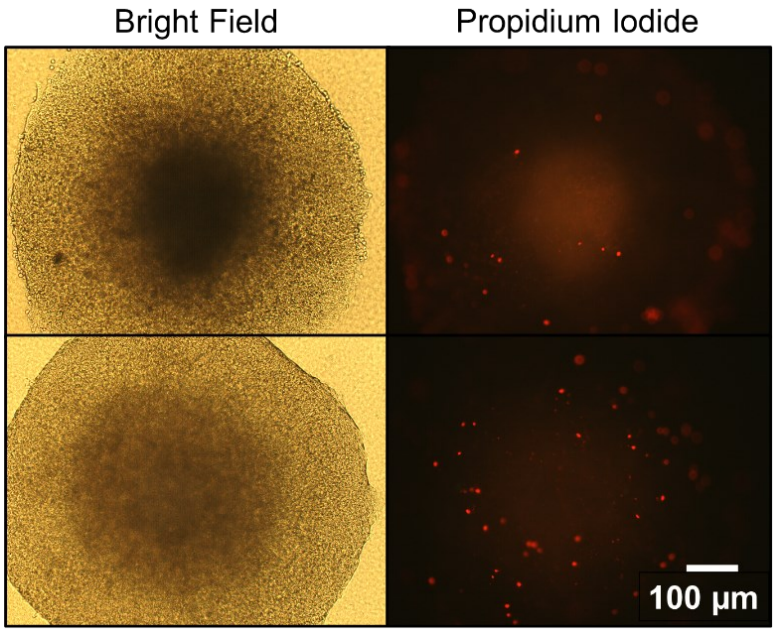

(b)

Figure 3.3. Observation of necrotic core in long-term cultures: Single MCF7 cells were cultured on collagen islands for 24 to 26 days. a, Images of four tumors after 24 days of culture (with tumors delineated in red) b, Images of two tumors from another experiment after 26 days of culturing that display darker central regions, as recorded with bright-field microscopy. Propidium Iodide (orange diffuse staining) images of necrosis are shown for the two tumors. Such darker central areas are observed in less than 8% of tumors that are cultured for long periods (more than 21 Days).

Further, to determine the extent of the single-cell culture on collagen I-island approach to recapitulate the characteristics of different types of cancer, we also tested the method with Caco-2 cells that represent a poorly aggressive colorectal carcinoma. Bright-field images obtained on day 10 of culture show that only 30% of the single cells led to tumor formation. Moreover, the rate of tumor growth seemed slower in comparison to the MCF-7 cells for the same ECM conditions, as illustrated by the smaller area of the tumors (Fig. 3.6); although it is noteworthy that these cultures were not done in parallel with those of MCF7 cells. Importantly, for both MCF7 and Caco-2 cells, the sizes and shapes of tumors varied considerably. Arm-like extensions often reveal the invasive nature of tumors[52,53]. These features were very rarely observed, but one tumor (out of 15 for MCF7 cells and out of six for Caco-2 cells) for each cancer type appeared fragmented (i.e., as if one or more cells migrated away from the main tumor to create a secondary tumor; see island xii in Fig. 3.4a & island 2 in Fig. 3.6a). Tumors produced by individual Caco-2 cells looked different from tumors produced by individual MCF7 cells. For most Caco-2 tumors, remarkable features included more angular shapes and hollow structures (islands 1, 2, 6, 7) reminiscent of glandular-like adenocarcinoma seen *in vivo*[54] (Fig. 3.6a). Interestingly, highly aggressive MDA-MB-231 cells that represent triple-negative breast cancer subtype, did not form tumors (i.e., an actual growth into a mass). Instead, the cells proliferated but moved away from each other while remaining attached to the matrix island (Fig. 3.7). The aggressive nature of these cells was expressed via their migratory behavior and spindle-like shape revealing a mesenchymal phenotype).

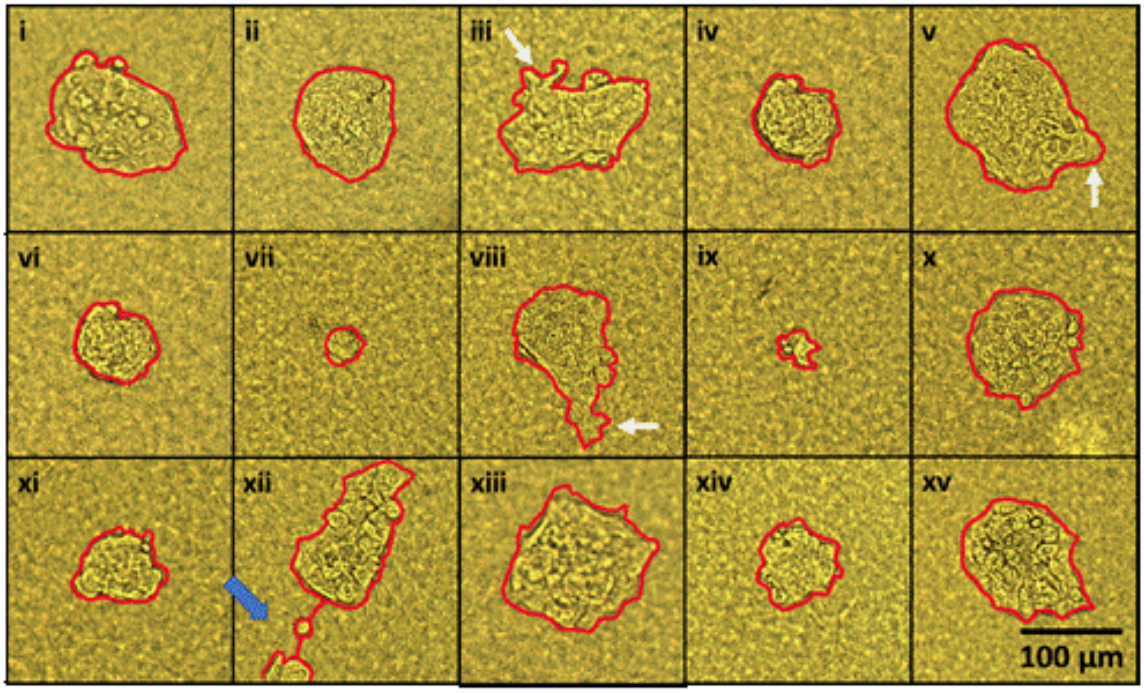

(a)

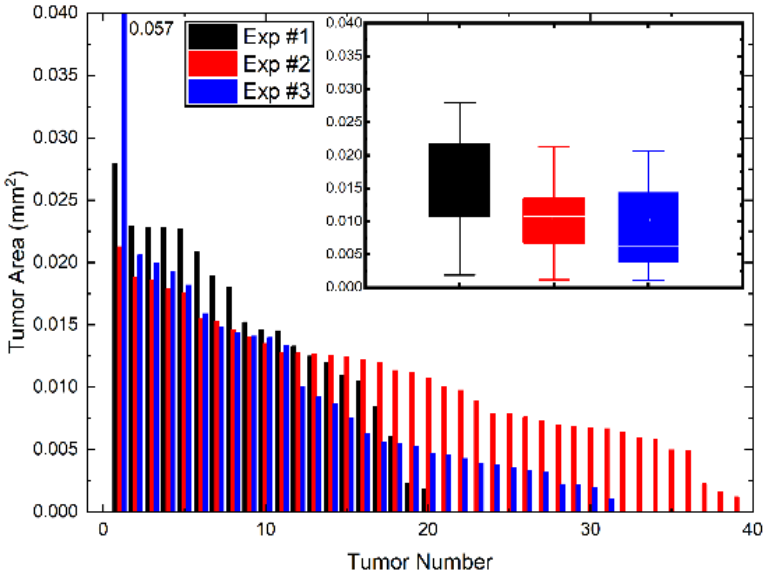

(b)

Figure 3.4. Tumors formed by a single MCF7 cell. Individual MCF7 cells were cultured on collagen I islands of 3320 Pa stiffness, as described before, and resulting tumors at day 10 of culture were outlined in red to visualize their size and shape. a: i to xv, Bright-field images of MCF-7 tumors; short 'arm-like' structures are indicated by white arrows in iii and viii. Secondary tumor formation possibly linked to cell migration is visible on image #xii as shown by blue arrows. b-d, Quantitative assessment of morphometry (area, circularity, aspect ratio) in three replicates (Exp. #1, 2, and 3) of MCF7 single-cell cultures that gave rise to 26 to 47 tumors. Inset in all graphs represents the box plot for each experiment.

Figure 3.4. (cont…)

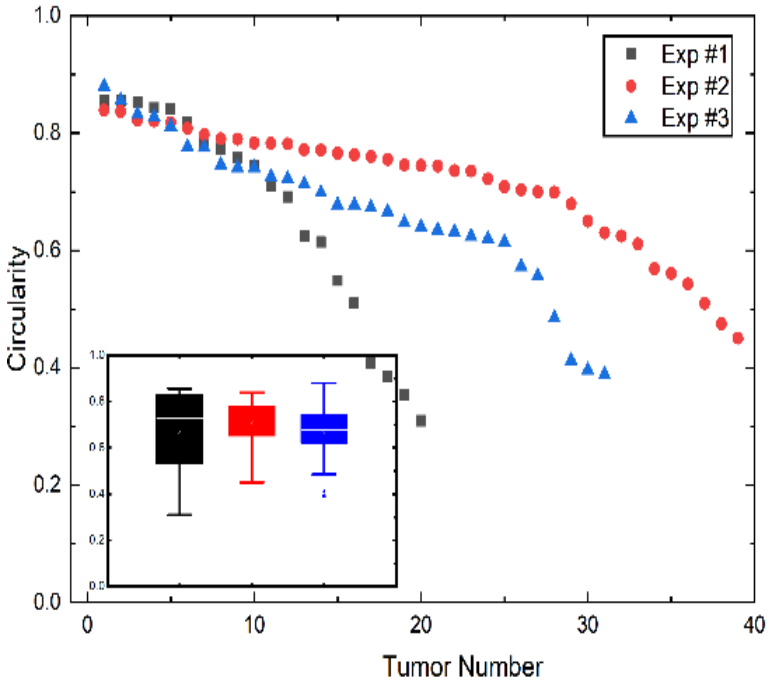

(c)

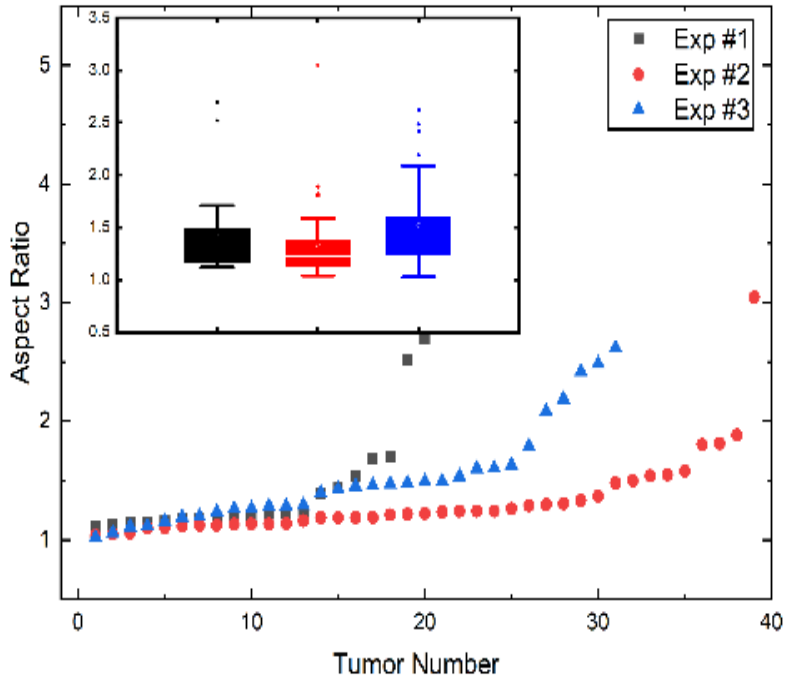

(d)

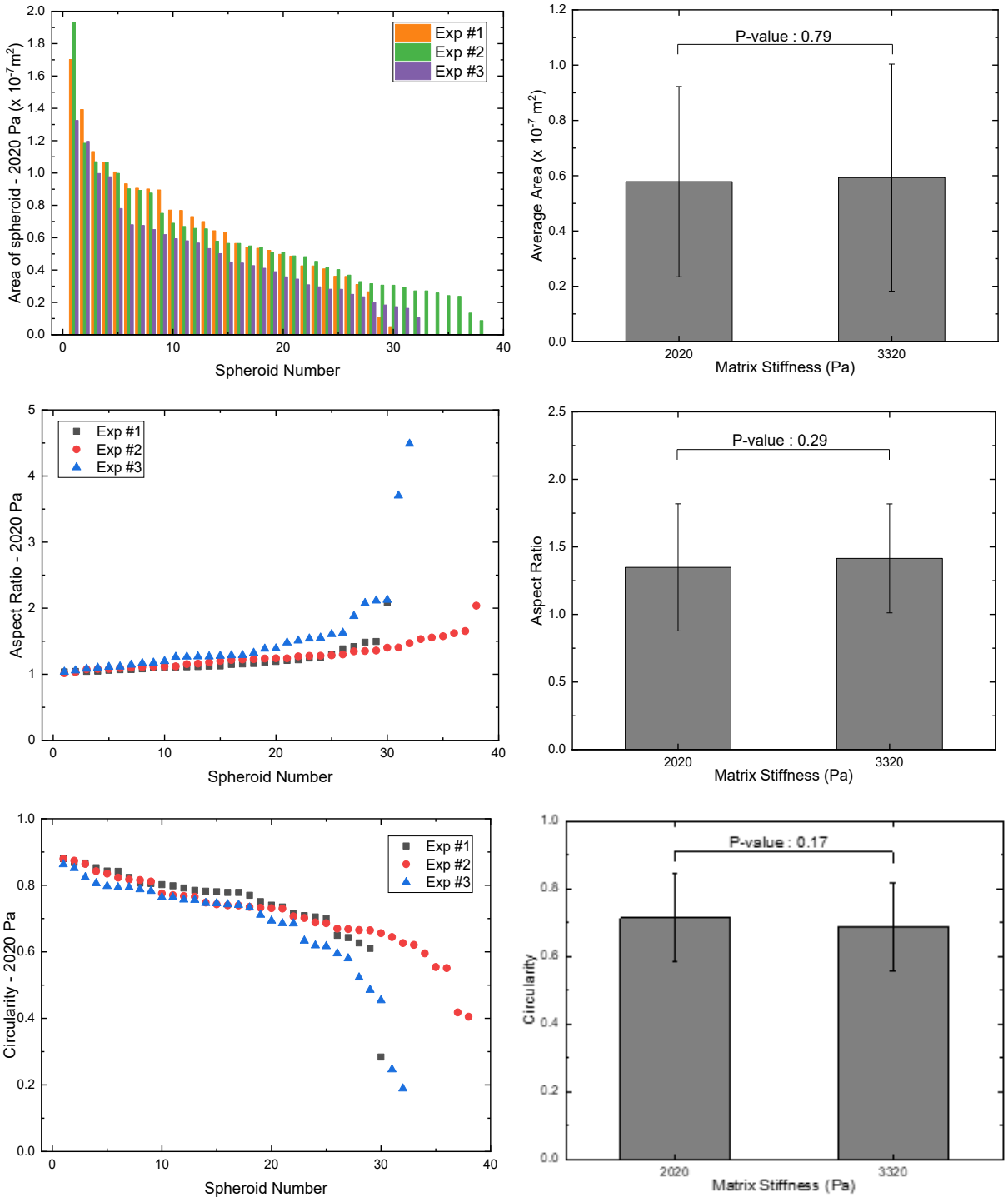

Figure 3.5. Morphological characteristics (area, aspect ratio, and circularity) for MCF-7 tumors in 2020 Pa Collagen I stiffness. Comparison with 3320 Pa stiffness shows no significant difference as indicated by the high p-values for all three parameters studied.

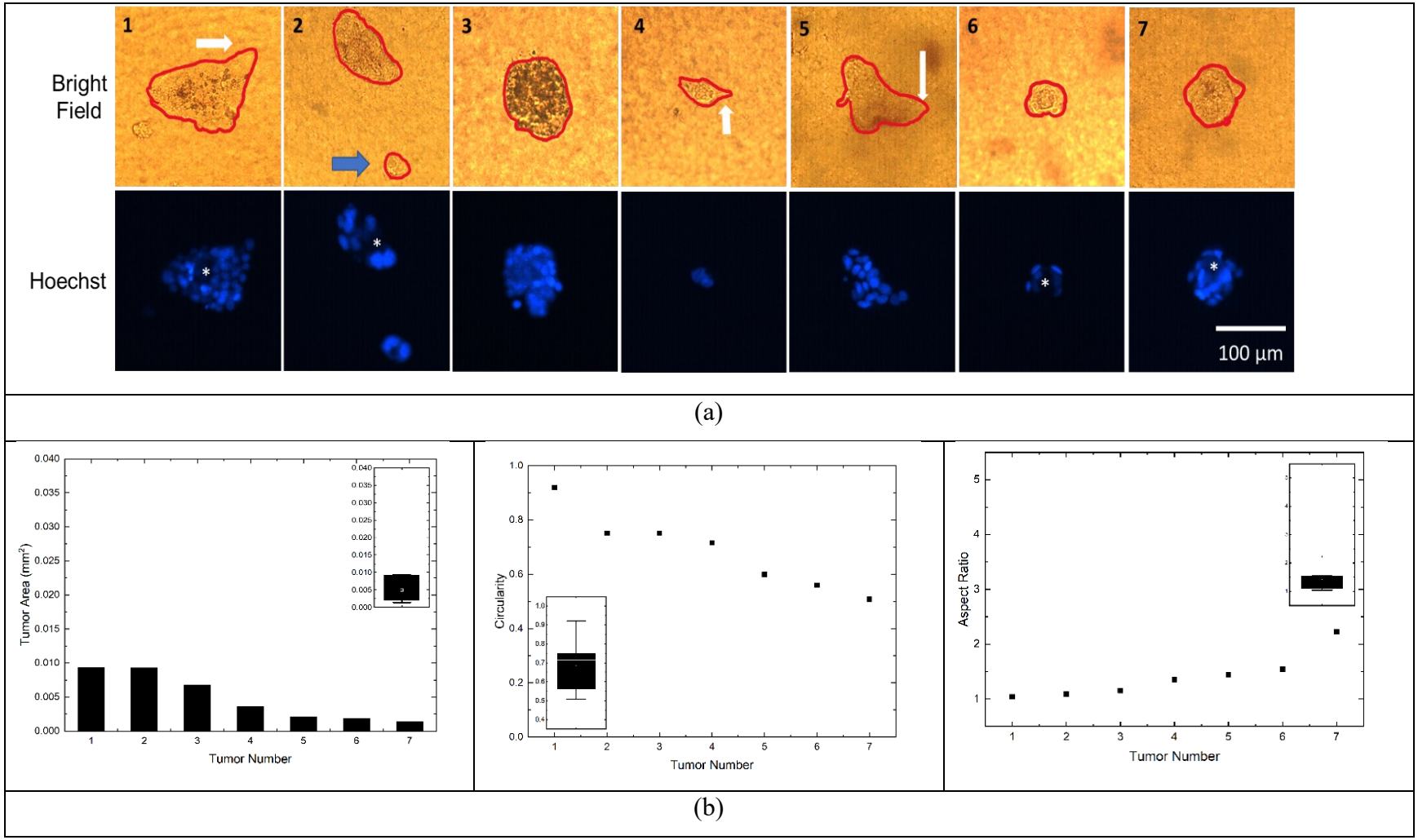

Figure 3.6. Tumors formed by single Caco-2 cells. Individual Caco-2 cells were cultured on collagen I islands of 3320 Pa stiffness, as described before, and resulting tumors at day 10 of culture were outlined in red to visualize their size and shape. a: 1 to 7, Bright-field and Hoechst images of Caco-2 tumors; short 'arm-like' structures are indicated by white arrows in 1, 4, and 5. Secondary tumor formation possibly linked to cell migration is visible in image 2 as shown by blue arrows. b, Quantitative assessment of morphometry (area, circularity, aspect ratio) in a single replicate of Caco-2 single-cell cultures. Inset in all graphs represents the box plot for each experiment.

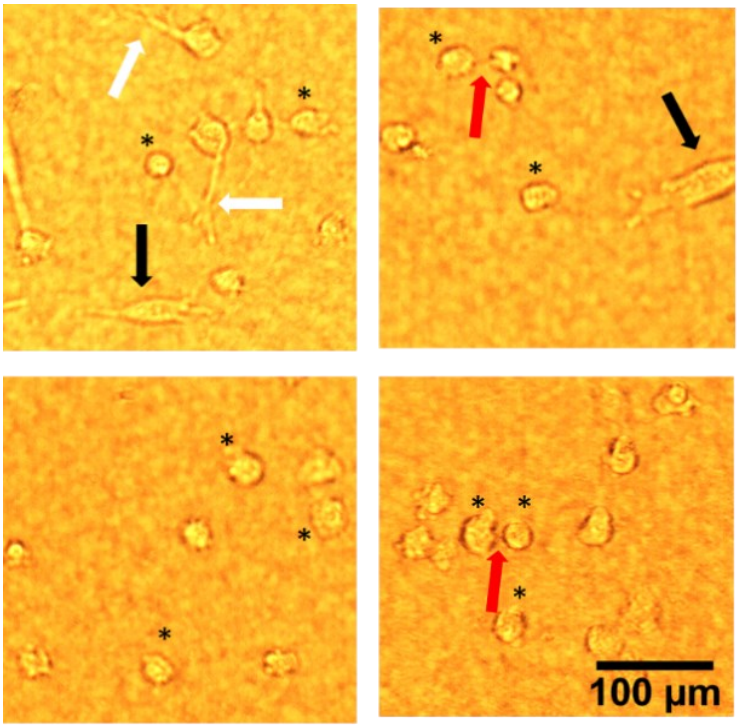

Figure 3.7. MDA-MB-231 cell behavior on collagen I islands: Single MDA-MB-231 cells were cultured on collagen islands for 10 days. In four representative islands, some of the individual cells resulting from proliferation are indicated by an asterisk (rounded cells are either still, dying, or undergoing mitosis). Some of the cells display a pseudopodia-like extension that may indicate migratory activity (see white arrows), which gives a possible explanation for the distance observed between cells on an island, and other cells display spindle-like shape (black arrow) characteristic of aggressive breast carcinomas that contain a mesenchymal type of cells. Cell division may lead to daughter cells of uneven size (red arrows).

The morphometric parameters, namely area, circularity (ratio of area to the square of the perimeter scaled by a factor of 4π) and aspect ratio (ratio of the major axis to the minor axis), were analyzed with Image J[55]. The standard deviation in the parameters was relatively high in all experiments as shown for three replicates of MCF-7 cells. Even when tumors were generated from single cells coming from the same batch and passage of the cell line, and cultured under the same microenvironmental conditions, they differed strikingly from one another in terms of morphometry, revealing intertumor heterogeneity (Fig. 3.4b-d). Similar results were observed with Caco-2 cells (Fig. 3.6b). Only moderately negative (Circularity vs. Aspect Ratio: Pearson Correlation Coefficient: -0.66) or no correlation (Pearson Correlation Coefficient: -0.14 and 0.016 for Tumor Area vs. Aspect Ratio and Tumor Area vs. Circularity, respectively) was observed between any two of the three parameters in MCF7 tumors.

Moreover, the depth of tumors was measured by using confocal imaging-based analysis. Two planes of focus, one at the top of the tumor and another at the bottom of the tumor were identified and their z-axis measurement was noted. The difference between the two measurements provided the depth of tumors as discussed in detail in the methods section. The depth of MCF-7 tumors measured after 14 Days in culture using confocal microscopy, was on average 75 μm in the z-dimension with a standard deviation of 19.7 μm, suggesting that there is significant variation in the number of layers of cells (a cell is on average ~15 μm in size) for the structures produced on the islands of collagen I.

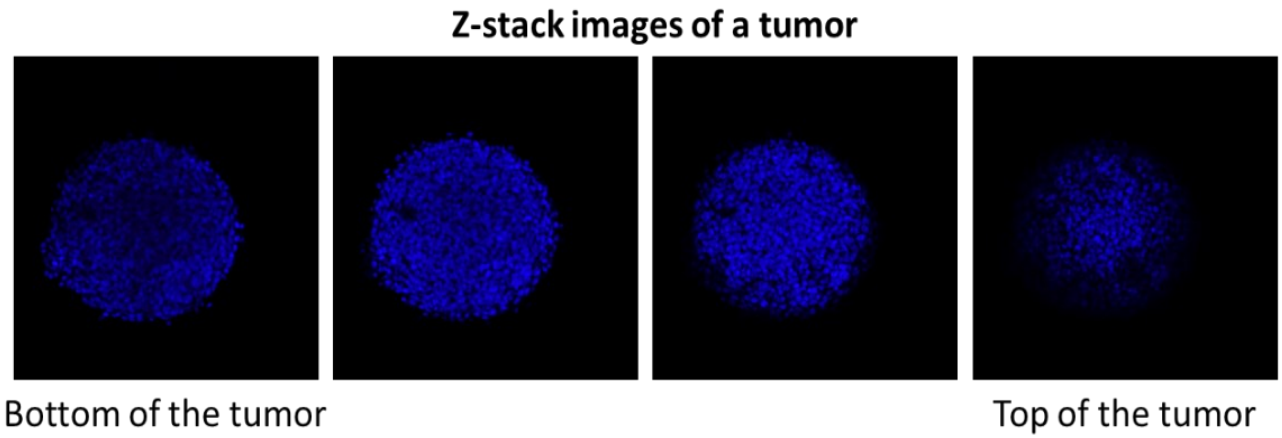

Figure 3.8. Z-stack images of a tumor using Confocal imaging show tumors exist in many layers.

3.4 Drug toxicity-based heterogeneity analysis

The degree of heterogeneity in MCF7 tumor sizes was paralleled by heterogeneity in response to Paclitaxel, a commonly used cytotoxic drug for the treatment of breast invasive ductal carcinoma, for which luminal A breast cancers may show different levels of sensitivity depending on the tumor phenotype[56]. Thirteen-day-old tumors were treated with three different concentrations of Paclitaxel (5 nM, 20 nM, and 100 nM) for 24 hours. The control was a separate dish containing islands seeded with single cells from the same population as the treated dishes and cultured with the same preparation of medium, to which 0.01% DMSO was added to match the maximum concentration of vehicle used in drug-treated samples. It is widely known that cells undergoing apoptosis exhibit a distinctive nuclear morphology as compared to healthy and necrotic cells[57]. Hence, tumors were treated with Hoechst 33342 nuclear dye to calculate the percentage of cells undergoing apoptosis based on nuclear morphology. Since each island comprises a relatively small amount of collagen

(e.g. as opposed to an entire well of a 96-well plate), the excess dye that inadvertently diffuses into the collagen can be washed easily to reduce any background fluorescence signal. Live and dead cells (the latter indicated by smaller or fragmented nuclei with intense staining due to DNA condensation) from individual planes of z-stack confocal images of each tumor were manually counted according to a procedure described by Crowley et. al.[57]. As expected, the average cell death increased with drug concentration, starting with cell death at 2.9% for the control sample (Fig. 3.9). Interestingly, there was a significant variation in the response of individual tumors for each drug concentration, confirming intertumor heterogeneity. In conclusion, although tumors from the cell population display some of the main characteristics of the type of cancer from which they originated, there are significant phenotypic variations among tumors produced by cells that are individually picked from this population.

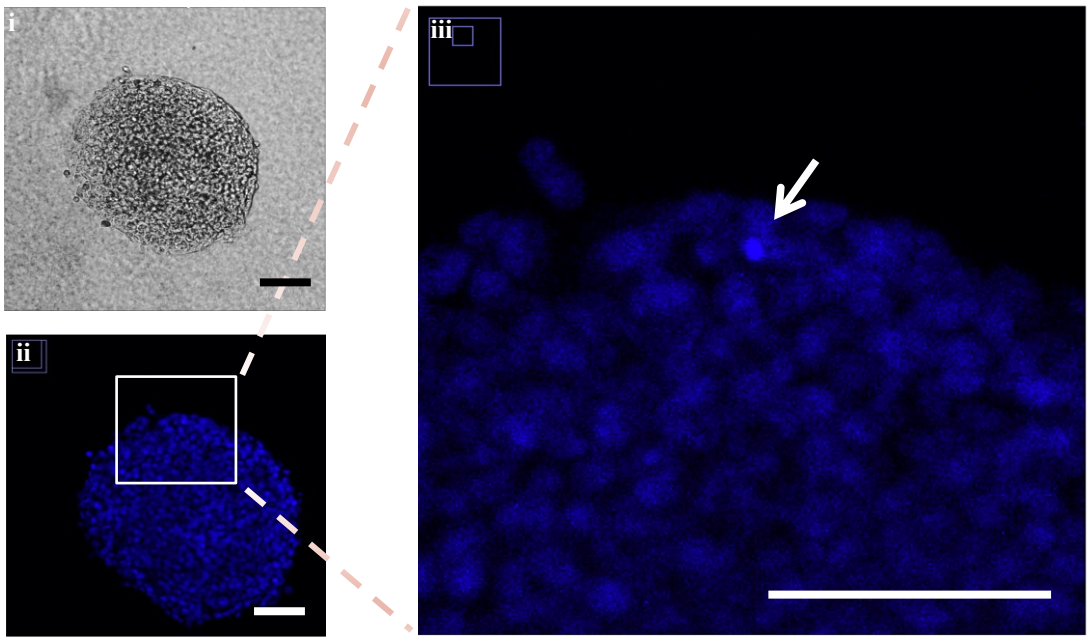

(a)

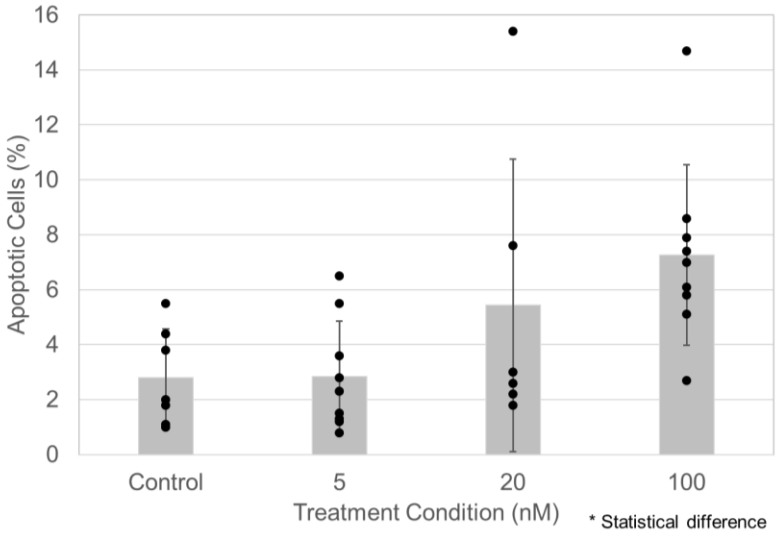

(b)

Figure 3.9. Treatment of MCF7 tumors with paclitaxel: Single MCF7 cells were cultured on collagen islands for 13 days before treatment with paclitaxel or vehicle DMSO (Control) for 24 hours. a: i & ii, Bright-field and confocal fluorescence (Hoechst) images of a tumor after treatment with 5 nM of paclitaxel. iii Zoomed portion of image ii showing nuclei (in blue) with one apoptotic (smaller and brighter) nucleus (white arrow). Scale bar: 100 µm. b, A bar graph of the percentage of apoptotic cells. Black dots represent individual tumors and black vertical lines represent standard deviations. Two-tailed heteroscedastic t-test based P-values for each of the six pairs of treatment are as follows: DMSO with 5 nM-0.972, DMSO with 20 nM-0.291, DMSO with 100 nM-0.004, 5 nM with 20 nM-0.297, 5 nM with 100 nM-0.004, 20 nM with 100 nM-0.477.

3.5 Intratumor heterogeneity analysis

Tumor size positively correlates with intratumor heterogeneity and nuclear size in luminal A type of breast cancer

Results related to tumor size and shape presented above deserved particular attention in terms of possible new biological information. We investigated whether the variation in tumor size and shape formed by individual cells from the same initial population might be an indication of phenotypic heterogeneity. Pathologists have relied on simple nuclear morphometric features such as size (or area) and shape (or circularity) for decades to determine tumor aggressiveness. We have also applied this method to assess tumor progression in 3D cell culture of preinvasive breast cancer cells[58]. The nuclei from six MCF-7 tumors at day 14 of culture, from the same biological replicate (i.e., seeding cells were from the same cell culture flask), were stained with Hoechst and imaged by confocal microscopy (Fig. 3.11a). The analysis was performed with Fiji[59] for nuclear area and circularity and was compared to the area and circularity of the corresponding tumors. Based on 50-75 randomly selected nuclei for each tumor, there was a significantly positive correlation (Pearson's coefficient correlation $r \geq 0.70$) between tumor area and the average nuclear area (i.e., the bigger the tumor, the bigger the nuclei on average in that tumor) (Fig. 3.10a). We also compared the same morphometric parameters (circularity and area) for each tumor with the standard deviation of the circularity and area of their nuclei, since intratumor heterogeneity has been associated with changes in phenotype[60]. There was a significant positive correlation (Pearson's correlation coefficient, $r \geq 0.70$) between tumor area and the degree of heterogeneity in the nuclear area (Fig. 3.10b). There was no significant correlation between any other two parameters (i.e., Pearson's coefficient < 0.7) (Table 3.1). The trends in nuclear area and circularity for each tumor are observed in more detail in violin plots (Fig. 3.10c-d). The two tumors with the highest variation in the nuclear area (tumors 2 and 4) have a narrow tail, indicating that a small number of all the nuclei have a significantly larger nuclear area. As can be noted from Fig. 3.11b, these particular tumors also have the largest area (0.4 and 0.35 mm^2). Hence, this small population of cells might indeed have a causal relationship with the large tumor area and maybe the chief driver of tumor aggression. Heterogeneity in the nuclear area does not always correspond to heterogeneity in nuclear circularity. Higher heterogeneity for nuclear circularity exists in tumors 1, 2, and 6. Especially in tumors 2 and 6, we observe the wider distribution of nuclear circularity around the mean of the violin plots indicating amplified heterogeneity. It is possible that the

observed differences in intratumor heterogeneity influence the variation in tumor area as seen in Fig. 2.4.

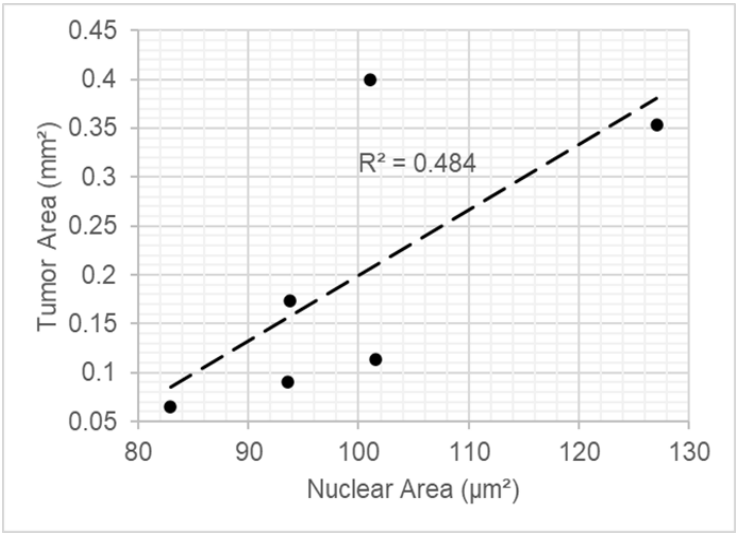

(a)

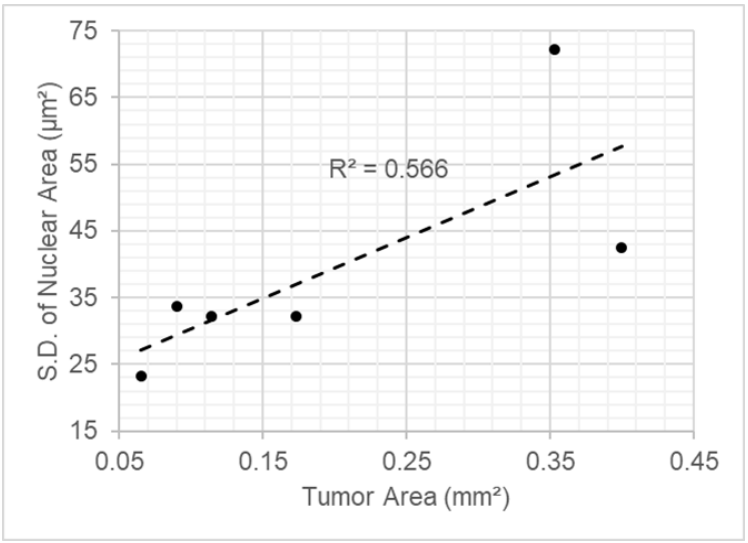

(b)

Figure 3.10. Morphometry analysis reveals a positive correlation between tumor area and high average as well as heterogeneity in the nuclear area: Single MCF7 cells were cultured on collagen I islands, as described before. On day 14 of culture, the area and circularity of tumors and areas of nuclei were analyzed with ImageJ. Trendline and associated R-square for the fit are shown with a high positive Pearson correlation ($r \geq 0.70$, $n=6$) between nuclear area and tumor area (a) and between tumor area and standard deviation [S.D.] in the nuclear area (used as a measure of heterogeneity) (b). c & d, violin plots of nuclear area and circularity for each of the six tumors where fifty to 75 nuclei were analyzed per tumor.

Figure 3.10. (cont…)

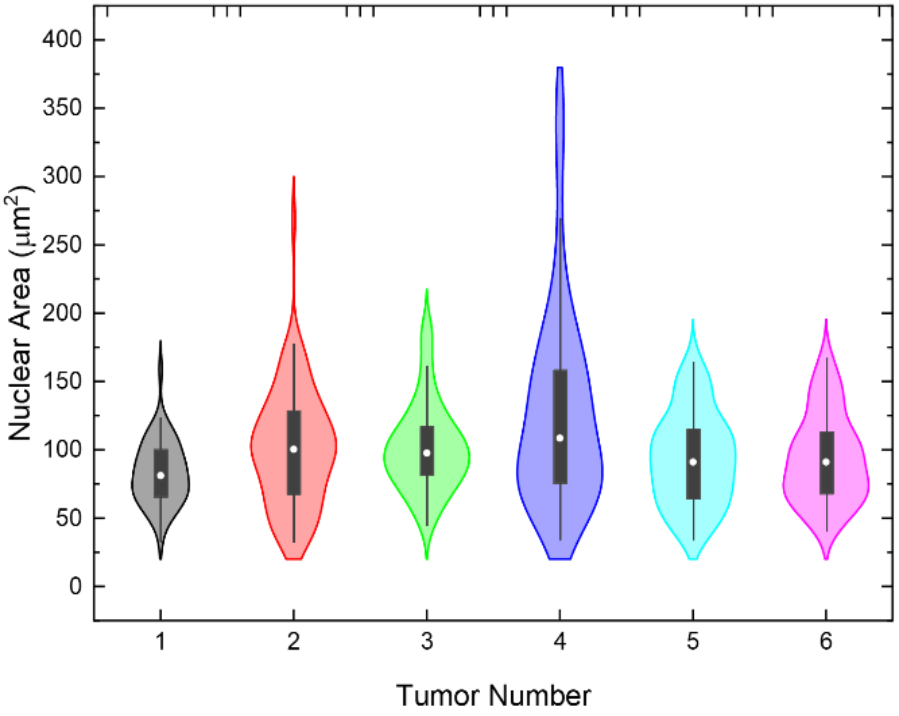

(c)

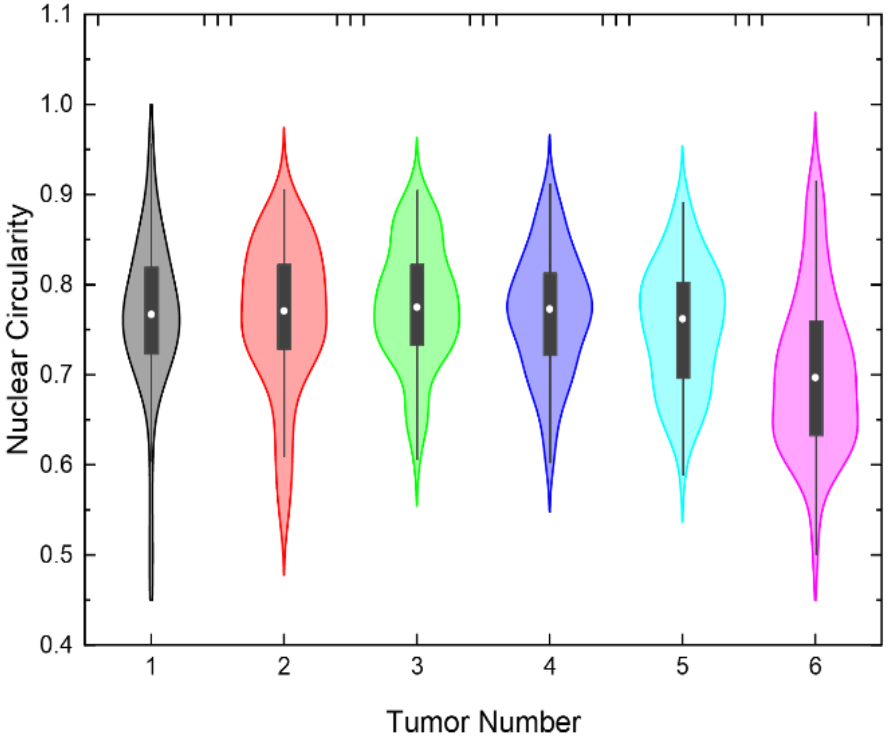

(d)

Tumor number	1	2	3	4	5	6
Area (mm^2)	0.065	0.40	0.114	0.353	0.091	0.173
Circularity	0.547	0.233	0.81	0.636	0.767	0.75

(a)

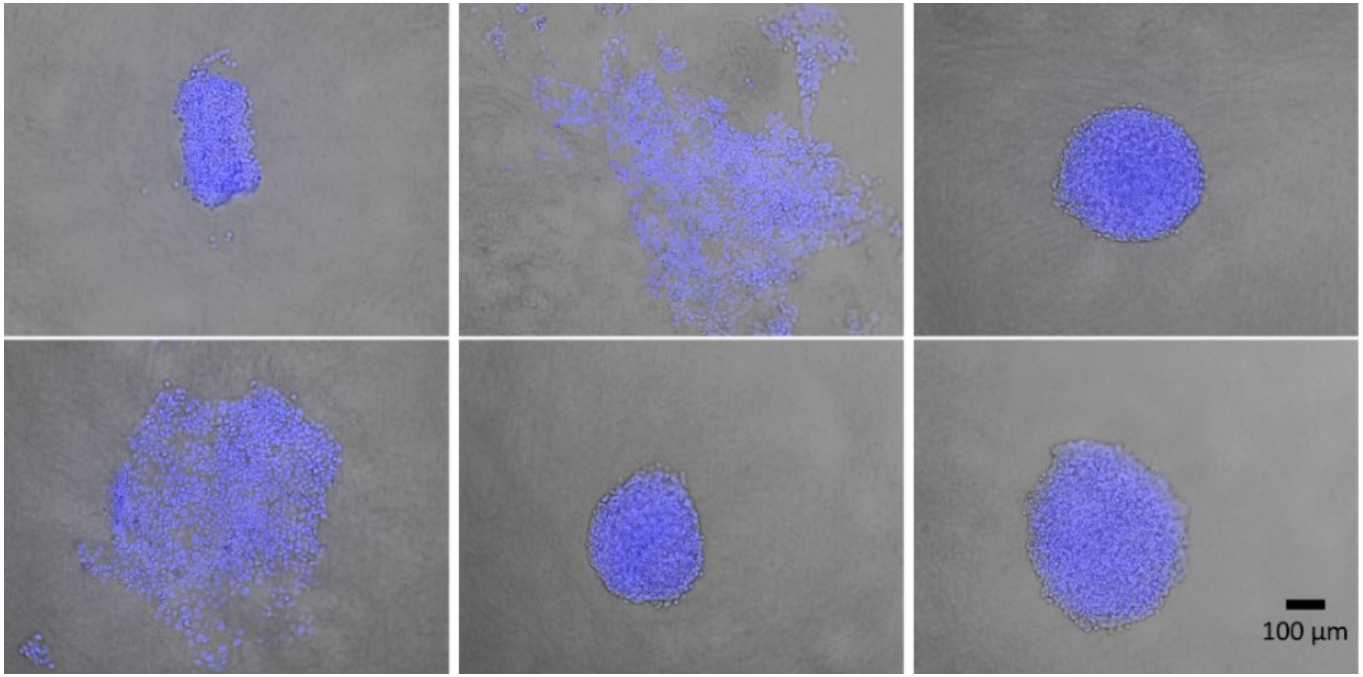

(b)

Figure 3.11. Images and tumor area for the six tumors used for heterogeneity analysis: Single MCF7 cells were cultured on collagen islands for 14 days. a, Area and circularity for each tumor in the group. b, Merged images of six tumors (S1 to S6) recorded using bright-field and fluorescence imaging (fluorescence microscope, Nikon ECLIPSE 8i) following Hoechst staining that were used to obtain tumor morphology information. This information combined with nuclear morphometry information obtained with the confocal microscope were used for the analysis of the potential link between parameters of tumor morphometry and nuclear morphometry.

Table 3.2. Pearson correlations between all other parameters for the six tumors in Figure 2.11.

	Average Nuclear Circularity	Average Nuclear Area	Tumor Circularity	Tumor Area	S.D. Nuclear Circularity	S.D. Nuclear Area
Average Nuclear Circularity	1					
Average Nuclear Area	0.29	1				
Tumor Circularity	-0.26	-0.01	1			
Tumor Area	0.13	**0.70**	-0.66	1		
S.D. Nuclear Circularity	-0.58	-0.62	-0.39	-0.06	1	
S.D. Nuclear Area	0.23	0.97	-0.14	**0.75**	-0.50	1

3.6 Tumor transfer and re-culture as single cells

An additional advantage of culturing tumors on top of collagen islands (instead of inside) is the simplicity of tumor retrieval for further analysis (Fig. 3.12). To determine whether intratumor heterogeneity revealed by nuclear morphometry analysis corresponds to the presence of different cell phenotypes, a 14-day tumor formed by one MCF7 cell was released from the matrix using collagenase and cell/tumor picking setup for transfer. After separation with Trypsin-EDTA, 32 single cells were picked and seeded on new collagen islands. On day 10 of culture, 24 of the islands displayed cells. Measurement of heterogeneity based on size and shape of these second-generation tumors showed high variability in three morphometric parameters (average area: 0.03 mm^2 with standard deviation (S.D.) 0.023 mm^2, average circularity: 0.49 with S.D. 0.18, and average aspect ratio: 1.75 with S.D. 0.72). Thus, intratumor heterogeneity in the first-generation tumor was associated with the formation of second-generation tumors with varied sizes and shapes (Fig. 3.13).

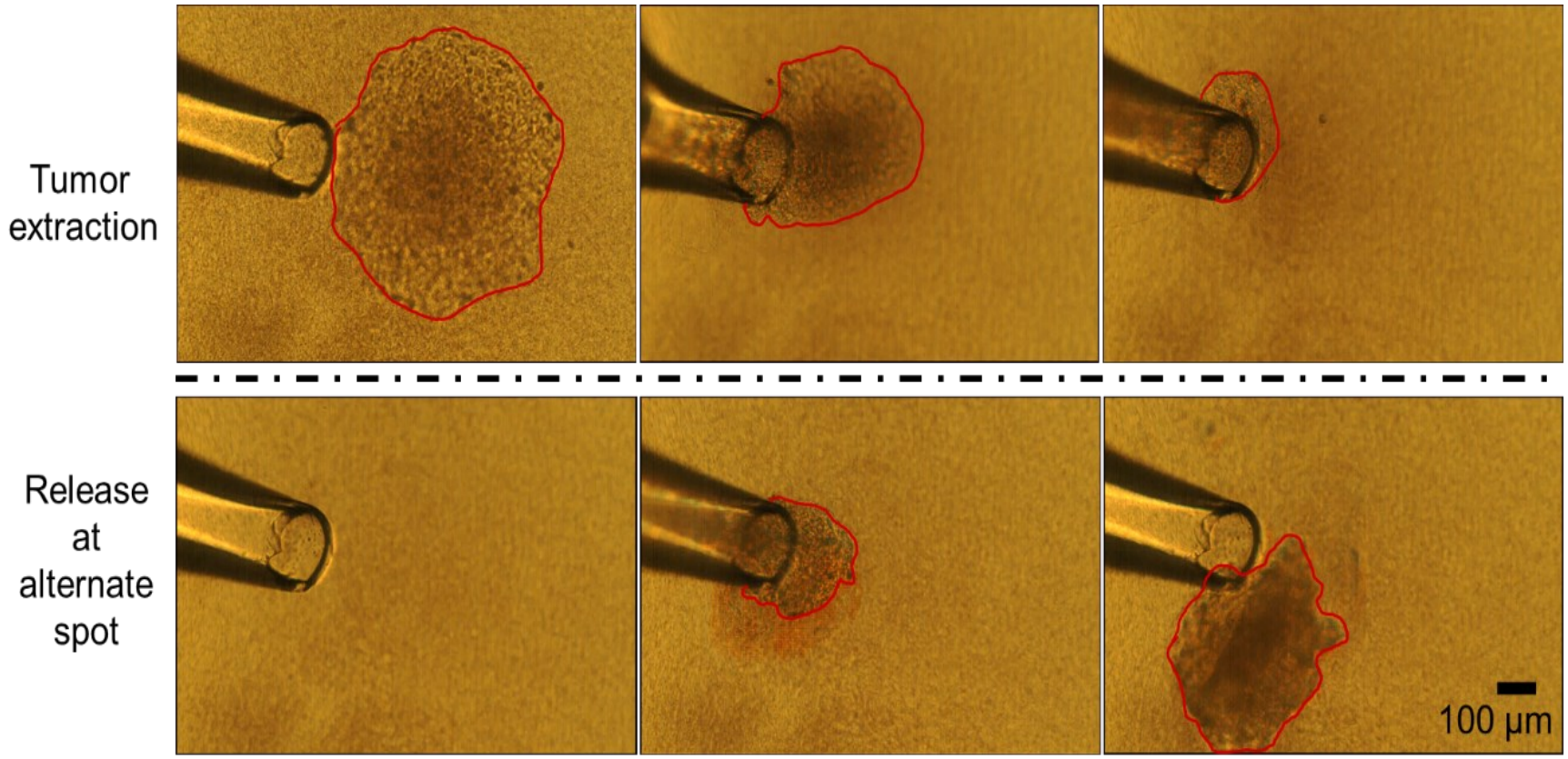

Figure 3.12. A tumor on top of the collagen I island can be easily extracted. **Top:** Successive images of a tumor being extracted from a collagen island, after 20-30 minute treatment with collagenase, using a glass tip of ~150 µm diameter; **Bottom:** Successive images of the same tumor being released at an alternate location (e.g., for applications such as dissociation and re-seeding of selected single cells from the tumor). The red outline delineates the visible portion of the tumor during different steps of the process.

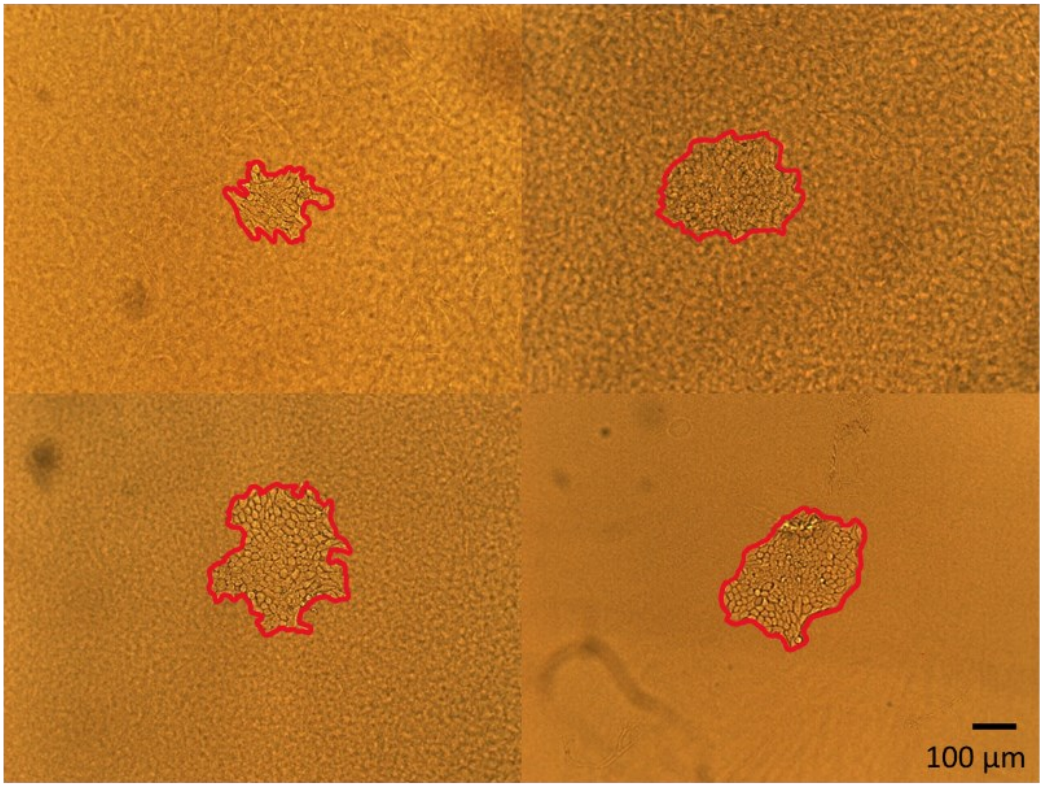

Figure 3.13. Re-cultured cells forming tumors: Day 10 bright field images of tumors (marked in red) obtained by re-culturing of single cells after breaking an initial tumor into single cells as described in the methods section.

4. CONCLUSIONS

We have developed a highly efficient and effective method to generate tumors from isolated, individually targeted single cells. Our protocol achieves this goal in a deterministic manner by physically relocating each individual cell from its source to the top of a matrix island. Morphometric analysis of the tumors produced by single cancer cells revealed both intertumor and intratumor heterogeneity. Notably, a comparison of morphometric parameters between tumors and their nuclei demonstrated a positive link between tumor size in luminal A breast cancers and the size of the nucleus (based on its average and its variability).

For a preliminary demonstration of the utility of the approach, we cultured single cells from MCF-7 (poorly aggressive luminal A) and MDA-MB-231 (highly aggressive, triple-negative) breast cancers and Caco-2 (poorly aggressive) colorectal cancer. Both breast and colorectal poorly aggressive lines gave rise to tumors with morphologies reminiscent of their cancer subtypes, without striking signs of invasion or migration for the great majority of tumors. The success of tumor formation was lower with Caco-2 cells compared to MCF7 cells, possibly because there is a smaller proportion of cells with active proliferation capabilities in the Caco-2 population. This interesting observation would otherwise not be detectable had the culture been started using many cells, instead of individual cells (indeed a high proportion of cells in G0- or out of the cell cycle, might be present in cancers[61] until a specific stimulus 'wakes them up'). In that regard, colorectal cancer cells appear to be sensitive to mechanotransduction (which is in part linked to ECM stiffness) for their quiescence/proliferation switch[62]. Future studies should explore the impact of matrix stiffness and composition on tumor development depending on the phenotype of the seeded cell since ECM composition is an important variable of colorectal cancer behavior[63]. Surprisingly, none of the MDA-MB-231 individual cells formed a tumor mass. Instead, they expressed their aggressive nature via a migratory phenotype. It needs to be emphasized that it has not been possible until now to study which specific cell phenotype among the MDA-MB-231 population is driving this aggressive behavior. Hence, it would be interesting to address this difference in behavior from a cell heterogeneity standpoint in future deterministic 3D culturing studies.

We have focused part of the analysis on intertumor heterogeneity that manifested in the form of variations in tumor morphometry, which is likely a reflection of the phenotypic heterogeneity in

the initial population of cancer cells. Most interestingly, the fact that heterogeneity increased over time, as shown for tumor size, might be not only linked to the disparity in the phenotype of the seeding cells but also acquired intratumor heterogeneity. The latter was measured via nuclear morphometry, a resilient feature of changes in phenotypes[64]. Although the sample size was small, the fact that there was statistical significance when comparing tumor and nuclear morphometric parameters suggests a strong correlation between tumor architectural (size, shape) and nuclear structural features. The average nuclear area was observed to be higher in luminal A breast tumors of large size. An increase in nuclear area and larger tumors have both been considered signs of cancer aggressiveness. Moreover, tumors of large size had increased intratumor heterogeneity based on nuclear size. Intratumor heterogeneity has been considered a driver of cancer progression[60].

We demonstrated that intratumor heterogeneity could develop from one single cell, as measured by heterogeneity in nucleus area and, also in tumor size and shape following second-generation deterministic 3D culturing, although there was no intentional selective pressure. How heterogeneity is established starting from a single cell might be linked to heterogeneity in the microenvironment (with different concentrations of signaling factors for instance). We cannot rule out such microenvironmental heterogeneity coming from neighboring matrix islands in the culture dish; however, the distance between islands (5 mm, center to center) is likely too high to produce heterogeneity linked to paracrine stimulation. Acquired heterogeneity might be the result of the intrinsic instability of cancer cells with the introduction of DNA damage and the uneven distribution of genetic material during cell division[65]. An additional possibility that the deterministic 3D culturing might help address is epigenetic heterogeneity (e.g., based on the type and quantity of epigenetic marks present at each given gene) since similarly to stem cells, many cancer cells possess marks of unstable local epigenetic make-up[66]. Upon cell division, the unstable epigenetic make-up might be driven towards changes in gene expression that differ between the two daughter cells, possibly due to changes in mechanical stimuli that might depend on the distance of the cell compared to the matrix contact. We determined that nuclear area was a source of intratumor heterogeneity. However, how the size of the nucleus or its roundness may be linked to the epigenetic expression of heterogeneity remains to be identified. This result calls for further analysis of the involvement of proteins that might regulate nuclear size via a possible impact on chromatin compaction, hence influencing both nuclear morphometry and gene expression profiles.

Our approach is cost-efficient, utilizes standard laboratory equipment, and consumes a low quantity of reagents. Due to the discrete, island-like nature of the collagen support, a cell culture dish of 35 mm uses less than 250 µl collagen matrix and 2 ml of culture medium. This condition eliminates the need to frequently change the medium due to extremely low consumption of nutrients by the tumors. The method is highly amenable for future automation for higher speed, throughput, and repeatability both for deposition of collagen islands and for choosing and seeding individual cells. Analyses such as immunomarker based assays, imaging assays, genetic sequencing assays can potentially be performed on the tumors cultured using this method.

5. FUTURE WORK

5.1 Future applications of the protocol

The single-cell culturing protocol that can selectively pick and place single cells onto 3D collagen islands, can be used to study a variety of cells including rare cells due to its precise and deterministic nature of cell transfer. Similarly, the ability to transfer the cultured tumors to a desired location makes it easy to perform a variety of analyses. Figure 5.1 summarizes the range of possible applications of the protocol.

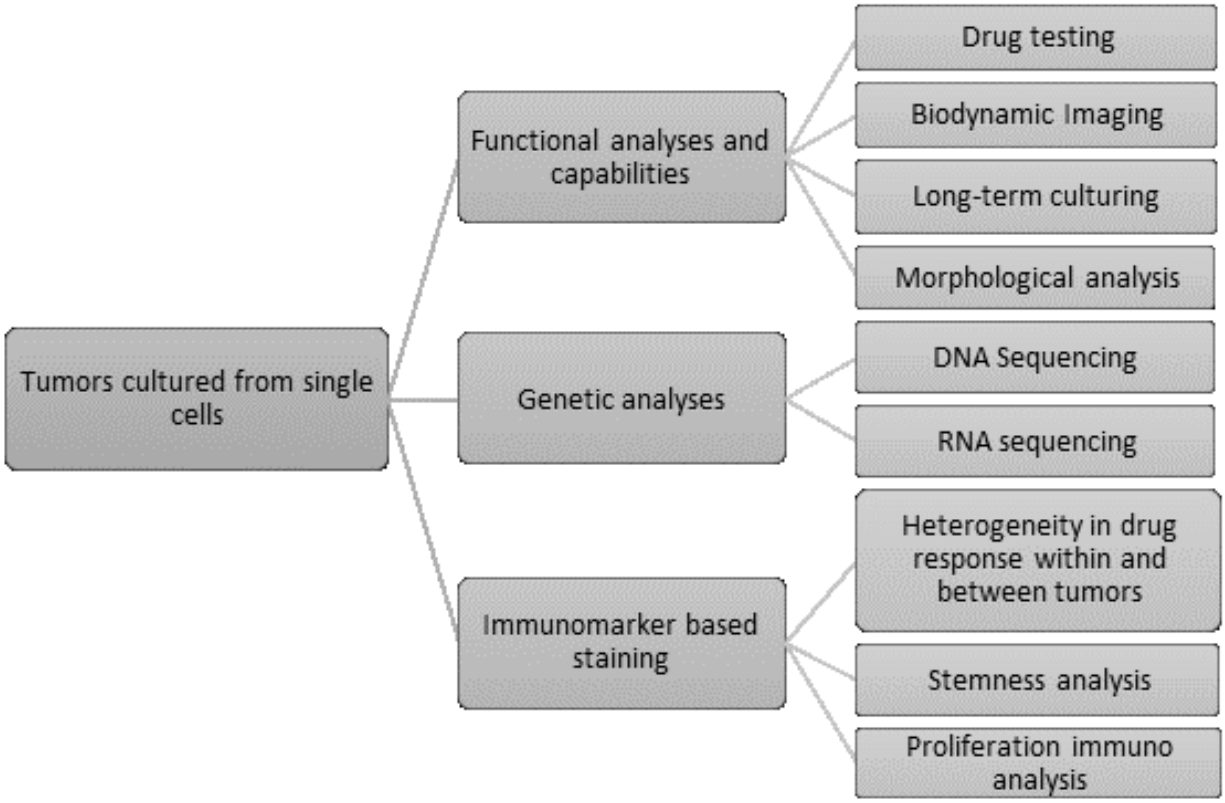

Figure 5.1. Possible future applications of the single-cell culturing protocol

As is evident from the Figure, the protocol can transfer rare cell types such as Circulating Tumor Cells (CTCs) and Circulating Fetal Cells (CFCs) that have been first captured using rare cell capture technologies. It is also possible to culture cells from cell lines, stem cell lines, or cells from animal models by simply making them accessible on top of any flat surface. The cultured tumors are available for pick up and transfer to other analysis platforms such as 96 well plate, RNA free

tubes, or another Petri dish. Many analyses can also be performed without separating from the original location. Some of the possible analyses are listed in Figure 5.1 which could be performed in the original Petri dish like immunomarker-based staining which may include markers for stemness, proliferation potential, morphological studies based on bright-field images, or nuclear staining and analysis. When transferred to a 96 well plate, a few possible analyses include drug sensitivity testing, bio-dynamic activity-based imaging, and long-term culture assays. Finally, when transferred to an RNA free tube, the spheroids can be studied for specific DNA or RNA patterns using gene sequencing or western blot analysis. The tumor can be transferred to the tube and supplied with Trypsin to break it down into individual cells which can be re-cultured using the single-cell culturing protocol as described before in the methods section.

5.2 Automation for future high-throughput assay

The micro-manipulating pipette setup consists of a syringe, microfluidic connections, a micro-pipetting needle, a 3D translation stage to move the tip, and a screw gauge for the syringe plunger. The syringe is connected to the micro-pipetting needle via airtight microfluidic tubes. The considerations for the selection of syringe and the tubing were based on the responsiveness and rigidity expected from the setup for smooth operation. Higher rigidity also leads to higher responsiveness but also higher oscillations in the fluid system which is undesirable. Thus, there is a need for optimization of the rigidity of the setup for this application. To minimize the oscillations while maintaining high responsiveness especially for manual control, we chose a glass syringe with a polytetrafluoroethylene (PTFE) coated plunger for smooth movement inside the barrel. We also experimentally tested both a PTFE tubing and a silicone tubing where PTFE tubing was stiff and more responsive while silicone tubing was softer with fewer oscillations but also less responsiveness. It was then experimentally observed that the PTFE tubing works better for picking cells from a flat surface and was chosen to connect the syringe to the pipette tip.

A simulation model would enable setting the desired pressure and fluid velocity conditions for picking setup for various applications such as cell aspiration, cell seeding, tumor aspiration, and tumor release. These conditions can be implemented using a syringe pump. This will an important advancement as it will give the assay a higher throughput. The second important aspect that can

be automated will be spotting of the collagen islands, and finally automation of the cell transfer process. This scheme of future automation is summarized in Figure 5.2 shown below.

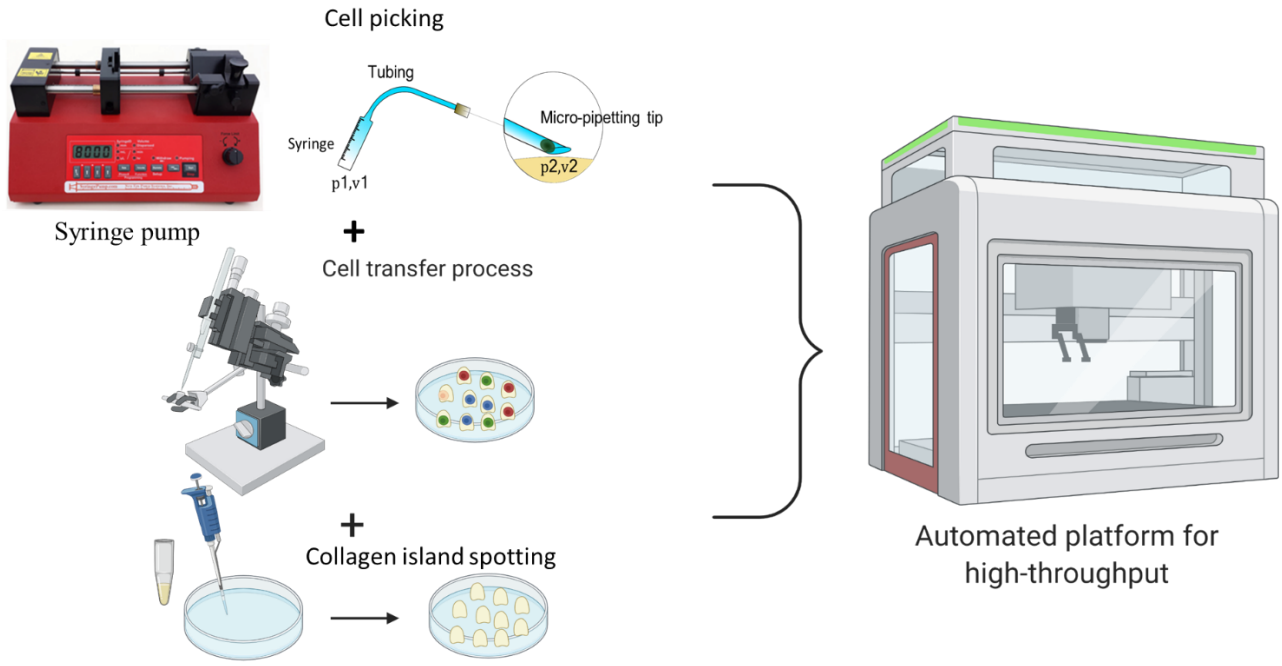

Figure 5.2. Schematic for automation of the different aspects of the protocol.

5.3 Co-culture with other cell types

In vivo tumors have different cell types that interact with each other and lead to sustained malignancy of the tissue. The presence of other cell types such as fibroblasts and immune cells has distinct effects on tumors such as facilitating tumor growth, extracellular matrix re-modeling, promoting angiogenesis, and mediation of tumor-promoting inflammation[67]. Together, these different types of cells may even lead to differences in response to drug treatments. They may even be a potential target for drugs. For these reasons, it would be important to incorporate these different cell types into the single-cell derived tumor model as shown in the schematic Figure 5.3.

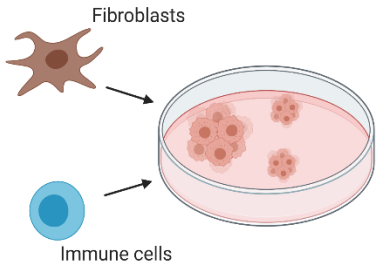

Figure 5.3. Co-culture with other cell types

Chemotherapy drugs used for breast cancer treatment are of a very wide variety. Some of the common types of chemotherapy agents are alkylating agents, anti-metabolites, anti-tumor antibiotics, topoisomerase inhibitors, mitotic inhibitors, and corticosteroids. These drugs have different mechanisms of action and may lead to different levels of heterogeneous outcomes. Using these drugs on the single-cell generated models that are co-cultured with fibroblasts or immune cells may help in understanding the heterogeneous responses. While a single cell generated model does not capture the complete *in vivo* response, it may provide the reductionist reasoning of an observed phenomenon and help understand the cell-to-cell variability in cellular responses to different conditions. Such reductionist insights may help model individual cellular responses in multi-cellular systems.

5.4 Other types of cell lines, stem cells, and rare cells

Breast cancer consists of a very heterogeneous population of cells. The most frequently used cell lines for generating models *in vitro* are very homogeneous when compared to the *in vivo* tumors, and no single cell line can capture all the heterogeneity found in breast cancer. MCF 7, for example, is one of the oldest cell lines used for studying breast cancer and is relatively easy to culture. But it has very little heterogeneity and aggressiveness when compared to some other cell lines such as MDA-MB-231. To understand varying levels of heterogeneity in cell populations, it may be necessary to culture other types of breast cancer cell lines. Some cell types may not proliferate actively starting from single cells. Special culturing conditions may need to be adopted for such cells, which can be the addition of particular growth factors, or the addition of other cell types.

Heterogeneity in cell populations is a feature that may be important to understand for many types of diseases. Thus, this protocol can be used with other types of cells such as cells from other cancer

types, stem cells, or primary cells. Since all cell types may not lead to multicellular entities starting from single cells, it may be necessary to look for markers such as a proliferation marker, or invasiveness marker, etc., and then choose cells based on the expression pattern. An interesting study in the future would be to use a high-throughput automatic version of the protocol to culture cells minced from primary tumors. This is depicted in figure 5.4 below. This can be followed by doing multivariate analysis such as those described in figure 5.1 above.

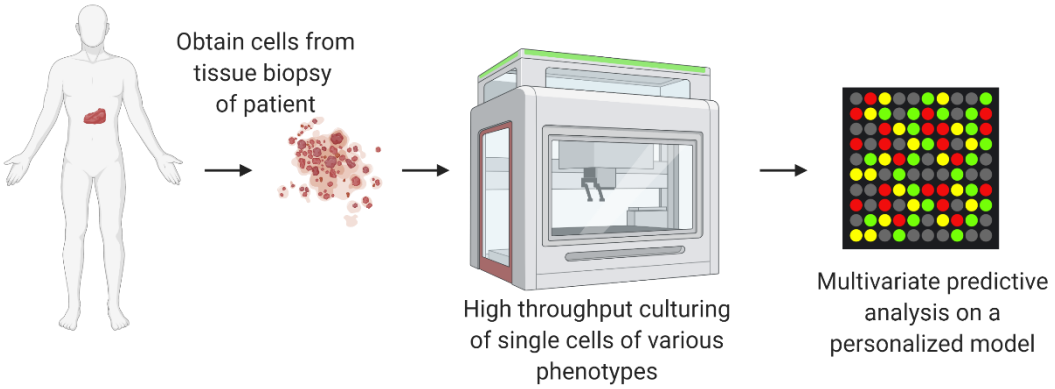

Figure 5.4. An example of a future application involving an automated high-throughput machine to study heterogeneity in primary cells from patient biopsy.

Yet another interesting application would be to culture rare cells obtained from patient blood, such as by using positive selection using microfluidic devices. This usually involves a first, separation using positive selection such as by attachment to antibody bead conjugates, followed by further enrichment. In a protocol that is used regularly as Savran lab, rare cells such as CTCs and fetal cells are first attached to magnetic beads by using targeted antibody mixtures. The whole blood sample is run through a microfluidic chip that enriches the sample with CTCs[68,69]. In the second step, the filtrate is distributed over microwells. These microwells catch roughly one cell per well. Thus, the CTCs are almost 100% enriched. These CTCs can be picked up from the microwells using the same picking setup that is used to seed cells in the single-cell culturing protocol[70]. Thus, the CTCs can be individually picked and placed on top of individual islands. This would allow culturing them individually in conditions that are best suitable for CTCs. This approach can be used repeatably with many patients, and personalized drugs can be tested on personalized models for each patient, created using only blood samples from patients. This scheme is summarized in

figure 5.5 and demonstrates the full extent of the power of this protocol in developing a personalized model of cancer as well as testing of personalized drugs.

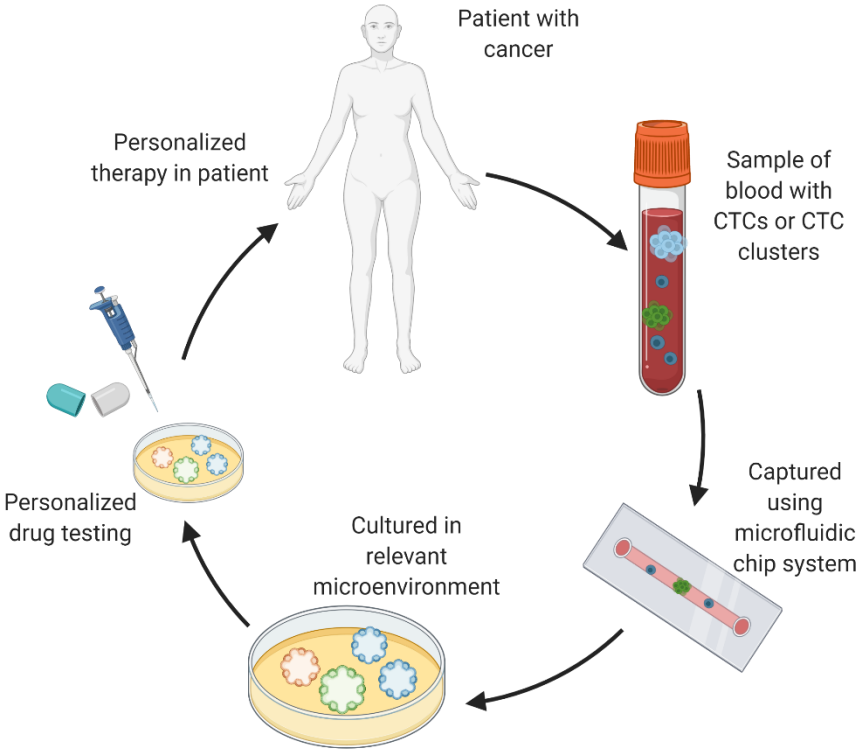

Figure 5.5. Schematic showing a proposed approach for personalized modeling and drug testing for cancer patients using liquid biopsies followed by deterministic single cell culturing in 3D.

LIST OF REFERENCES

1. Cancer Statistics - National Cancer Institute. https://www.cancer.gov/about-cancer/understanding/statistics.
2. Cancer. https://www.who.int/health-topics/cancer#tab=tab_1.
3. Prasad, V. & Mailankody, S. Research and development spending to bring a single cancer drug to market and revenues after approval. *JAMA Internal Medicine* **177**, 1569–1575 (2017).
4. Edmondson, R., Broglie, J. J., Adcock, A. F. & Yang, L. Three-dimensional cell culture systems and their applications in drug discovery and cell-based biosensors. *Assay and drug development technologies* **12**, 207–18 (2014).
5. Fang, Y. & Eglen, R. M. Three-Dimensional Cell Cultures in Drug Discovery and Development. *SLAS discovery : advancing life sciences R & D* **22**, 456–472 (2017).
6. Weiswald, L.-B., Bellet, D. & Dangles-Marie, V. Spherical cancer models in tumor biology. *Neoplasia (New York, N.Y.)* **17**, 1–15 (2015).
7. Kelm, J. M., Timmins, N. E., Brown, C. J., Fussenegger, M. & Nielsen, L. K. Method for generation of homogeneous multicellular tumor spheroids applicable to a wide variety of cell types. *Biotechnology and Bioengineering* **83**, 173–180 (2003).
8. Zhau, H. E., Goodwin, T. J., Chang, S.-M., Baker, T. L. & Chung, L. W. K. Establishment of a three-dimensional human prostate organoid coculture under microgravity-simulated conditions: Evaluation of androgen-induced growth and psa expression. *In Vitro Cellular & Developmental Biology - Animal* **33**, 375–380 (1997).
9. Ingram, M. *et al.* Three-dimensional growth patterns of various human tumor cell lines in simulated microgravity of a NASA bioreactor. *In Vitro Cellular & Developmental Biology - Animal* **33**, 459–466 (1997).
10. Souza, G. R. *et al.* Three-dimensional tissue culture based on magnetic cell levitation. *Nature nanotechnology* **5**, 291–6 (2010).
11. Hsiao, A. Y. *et al.* Microfluidic system for formation of PC-3 prostate cancer co-culture spheroids. *Biomaterials* **30**, 3020–3027 (2009).

12. Liu, W., Wang, J.-C. & Wang, J. Controllable organization and high throughput production of recoverable 3D tumors using pneumatic microfluidics. *Lab on a Chip* **15**, 1195–1204 (2015).
13. Foty, R. A simple hanging drop cell culture protocol for generation of 3D spheroids. *Journal of Visualized Experiments* **51**, (2011).
14. Varley, M. C., Markaki, A. E. & Brooks, R. A. Effect of Rotation on Scaffold Motion and Cell Growth in Rotating Bioreactors. *Tissue Engineering - Part A* **23**, 522–534 (2017).
15. Gupta, N. *et al.* Microfluidics-based 3D cell culture models: Utility in novel drug discovery and delivery research. *Bioengineering & translational medicine* **1**, 63–81 (2016).
16. Chen, S.-Y. C., Hung, P. J. & Lee, P. J. Microfluidic array for three-dimensional perfusion culture of human mammary epithelial cells. *Biomedical Microdevices* **13**, 753–758 (2011).
17. Aref, A. R. *et al.* 3D microfluidic *ex vivo* culture of organotypic tumor spheroids to model immune checkpoint blockade. *Lab on a Chip* **18**, 3129–3143 (2018).
18. Tibbitt, M. W. & Anseth, K. S. Hydrogels as extracellular matrix mimics for 3D cell culture. *Biotechnology and Bioengineering* **103**, 655–663 (2009).
19. Edmondson, R., Broglie, J. J., Adcock, A. F. & Yang, L. Three-dimensional cell culture systems and their applications in drug discovery and cell-based biosensors. *Assay and Drug Development Technologies* vol. 12 207–218 (2014).
20. Dagogo-Jack, I. & Shaw, A. T. Tumour heterogeneity and resistance to cancer therapies. *Nature Reviews Clinical Oncology* **15**, 81–94 (2017).
21. Meacham, C. E. & Morrison, S. J. Tumour heterogeneity and cancer cell plasticity. *Nature* **501**, 328–337 (2013).
22. Marusyk, A., Almendro, V. & Polyak, K. Intra-tumour heterogeneity: a looking glass for cancer? *Nature Reviews Cancer* **12**, 323–334 (2012).
23. Deng, G. *et al.* Single cell mutational analysis of PIK3CA in circulating tumor cells and metastases in breast cancer reveals heterogeneity, discordance, and mutation persistence in cultured disseminated tumor cells from bone marrow. doi:10.1186/1471-2407-14-456.
24. Scher, H. I. *et al.* Phenotypic Heterogeneity of Circulating Tumor Cells Informs Clinical Decisions between AR Signaling Inhibitors and Taxanes in Metastatic Prostate Cancer. *Cancer Res* **77**, 5687–98.

25. Gerlinger, M. *et al.* Intratumor Heterogeneity and Branched Evolution Revealed by Multiregion Sequencing. *New England Journal of Medicine* **366**, 883–892 (2012).
26. Smart, C. E. *et al.* In Vitro Analysis of Breast Cancer Cell Line Tumourspheres and Primary Human Breast Epithelia Mammospheres Demonstrates Inter- and Intrasphere Heterogeneity. *PLoS ONE* **8**, e64388 (2013).
27. Ivanov, D. P. & Grabowska, A. M. Spheroid arrays for high-throughput single-cell analysis of spatial patterns and biomarker expression in 3D. *Scientific Reports* **7**, 41160 (2017).
28. Stuart, T. & Satija, R. Integrative single-cell analysis. *Nature Reviews Genetics* vol. 20 257–272 (2019).
29. Krzyszczyk, P. *et al.* The growing role of precision and personalized medicine for cancer treatment. *TECHNOLOGY* **06**, 79–100 (2018).
30. Lindström, S. & Andersson-Svahn, H. Single-cell culture in microwells. *Methods in molecular biology (Clifton, N.J.)* **853**, 41 (2012).
31. Tirier, S. M. *et al.* Pheno-seq – linking visual features and gene expression in 3D cell culture systems. *Scientific Reports* **9**, (2019).
32. Qureshi-Baig, K. *et al.* What do we learn from spheroid culture systems? Insights from tumorspheres derived from primary colon cancer tissue. *PLoS ONE* **11**, (2016).
33. Lee, J. W., Sung, J. S., Park, Y. S., Chung, S. & Kim, Y. H. Isolation of spheroid-forming single cells from gastric cancer cell lines: enrichment of cancer stem-like cells. *BioTechniques* **65**, 197–203 (2018).
34. Cheng, Y. H., Chen, Y. C., Brien, R. & Yoon, E. Scaling and automation of a high-throughput single-cell-derived tumor sphere assay chip. *Lab on a Chip* **16**, 3708–3717 (2016).
35. Chen, Y. C. *et al.* Single cell dual adherent-suspension co-culture micro-environment for studying tumor-stromal interactions with functionally selected cancer stem-like cells. *Lab on a Chip* **16**, 2935–2945 (2016).
36. Lin, C. H., Chang, H. C. & Hsu, C. H. A microfluidic platform for high-throughput single-cell isolation and culture. *Journal of Visualized Experiments* **2016**, (2016).
37. Gracz, A. D. *et al.* A high-throughput platform for stem cell niche co-cultures and downstream gene expression analysis. doi:10.1038/ncb3104.

38. Zhang, Z., Chen, Y.-C., Cheng, Y.-H., Luan, Y. & Yoon, E. Microfluidics 3D gel-island chip for single cell isolation and lineage-dependent drug responses study. **16**, (2014).
39. Wang, Y.-K. & Chen, C. S. Cell adhesion and mechanical stimulation in the regulation of mesenchymal stem cell differentiation. doi:10.1111/jcmm.12061.
40. Ishihara, S., Inman, D. R., Li, W.-J., Ponik, S. M. & Keely, P. J. Mechano-Signal Transduction in Mesenchymal Stem Cells Induces Prosaposin Secretion to Drive the Proliferation of Breast Cancer Cells. *Cancer research* **77**, 6179–6189 (2017).
41. Chen, Y. *et al.* Rare cell isolation and analysis in microfluidics. *Lab on a chip* **14**, 626–45 (2014).
42. Yu, M. *et al.* Ex vivo culture of circulating breast tumor cells for individualized testing of drug susceptibility. *Science* **345**, 216–220 (2014).
43. Wang, R. *et al.* Cultured circulating tumor cells and their derived xenografts for personalized oncology. *Asian Journal of Urology* **3**, 240–253 (2016).
44. Maheswaran, S. & Haber, D. A. Ex vivo culture of CTCs: An emerging resource to guide cancer therapy. *Cancer Research* **75**, 2411–2415 (2015).
45. Celià-Terrassa, T. & Kang, Y. Distinctive properties of metastasis-initiating cells. *Genes & development* **30**, 892–908 (2016).
46. Pascual, G. *et al.* Targeting metastasis-initiating cells through the fatty acid receptor CD36. *Nature* **541**, 41–45 (2017).
47. Baccelli, I. *et al.* Identification of a population of blood circulating tumor cells from breast cancer patients that initiates metastasis in a xenograft assay. *Nature Biotechnology* **31**, 539–544 (2013).
48. Fiddler, M. Fetal Cell Based Prenatal Diagnosis: Perspectives on the Present and Future. *Journal of clinical medicine* **3**, 972–85 (2014).
49. Bianchi, D. W. Fetal cells in the maternal circulation: feasibility for prenatal diagnosis. *British Journal of Haematology* **105**, 574–583 (1999).
50. Acerbi, I. *et al.* Human breast cancer invasion and aggression correlates with ECM stiffening and immune cell infiltration. *Integrative Biology* **7**, 1120–1134 (2015).
51. Mehta, G., Hsiao, A. Y., Ingram, M., Luker, G. D. & Takayama, S. Opportunities and challenges for use of tumor spheroids as models to test drug delivery and efficacy. (2012) doi:10.1016/j.jconrel.2012.04.045.

52. Paszek, M. J. *et al.* Tensional homeostasis and the malignant phenotype. *Cancer Cell* **8**, 241–254 (2005).

53. Albini, A. *et al. A Rapid i/i Vitro Assay for Quantitating the Invasive Potential of Tumor Cells*. *CANCER RESEARCH* vol. 47 http://cancerres.aacrjournals.org/content/47/12/3239.full-text.pdf (1987).

54. Fleming, M., Ravula, S., Tatishchev, S. F. & Wang, H. L. Colorectal carcinoma: Pathologic aspects. *Journal of Gastrointestinal Oncology* vol. 3 153–173 (2012).

55. Schneider, C. A., Rasband, W. S. & Eliceiri, K. W. *NIH Image to ImageJ: 25 years of image analysis*. (2012) doi:10.1038/nmeth.2089.

56. Zhang, B. *et al.* Micro RNA 100 sensitizes luminal A breast cancer cells to paclitaxel treatment in part by targeting mTOR. *Oncotarget* **7**, 5702–5714 (2016).

57. Crowley, L. C., Marfell, B. J. & Waterhouse, N. J. Analyzing Cell Death by Nuclear Staining with Hoechst 33342. *Cold Spring Harbor protocols* **2016**, pdb.prot087205 (2016).

58. Chittiboyina, S. *et al.* Gradient-on-a-Chip with Reactive Oxygen Species Reveals Thresholds in the Nucleus Response of Cancer Cells Depending on the Matrix Environment. *ACS Biomaterials Science and Engineering* **4**, 432–445.

59. Schindelin, J. *et al.* Fiji: An open-source platform for biological-image analysis. *Nature Methods* vol. 9 676–682 (2012).

60. Janiszewska, M. The microcosmos of intratumor heterogeneity: the space-time of cancer evolution. *Oncogene* **39**, 2031–2039 (2020).

61. Davis, J., Kirk, J., Ji, Y. & Tang, D. Tumor Dormancy and Slow-Cycling Cancer Cells. *Human Cell Transformation: Advances In Cell Models For The Study Of Cancer* **1164**, 199–206 (2019).

62. Corvaisier, M. *et al.* Regulation of cellular quiescence by YAP/TAZ and Cyclin E1 in colon cancer cells: Implication in chemoresistance and cancer relapse. *Oncotarget* **7**, 56699–56712 (2016).

63. Brauchle, E. *et al.* Biomechanical and biomolecular characterization of extracellular matrix structures in human colon carcinomas. *Matrix Biology* **68–69**, 180–193 (2018).

64. Lelièvre, S. A. & Chittiboyina, S. Microphysiological systems to study microenvironment-cell nucleus interaction: importance of tissue geometry and heterogeneity. *Microphysiological Systems* **2**, 12–12 (2018).

65. Beca, F. & Polyak, K. Intratumor heterogeneity in breast cancer. in *Advances in Experimental Medicine and Biology* vol. 882 169–189 (Springer New York LLC, 2016).

66. Comet, I., Riising, E. M., Leblanc, B. & Helin, K. *Maintaining cell identity: PRC2-mediated regulation of transcription and cancer*. *Nature Publishing Group* www.nature.com/nrc (2016) doi:10.1038/nrc.2016.83.

67. Monteran, L. & Erez, N. The dark side of fibroblasts: Cancer-associated fibroblasts as mediators of immunosuppression in the tumor microenvironment. *Frontiers in Immunology* vol. 10 1835 (2019).

68. Chang, C. L. *et al.* Circulating tumor cell detection using a parallel flow micro-aperture chip system. *Lab on a Chip* **15**, 1677–1688 (2015).

69. Radovich, M. *et al.* Association of Circulating Tumor DNA and Circulating Tumor Cells after Neoadjuvant Chemotherapy with Disease Recurrence in Patients with Triple-Negative Breast Cancer: Preplanned Secondary Analysis of the BRE12-158 Randomized Clinical Trial. in *JAMA Oncology* vol. 6 1410–1415 (American Medical Association, 2020).

70. Gur, O., Chang, C.-L., Jain, R., Zhong, Y. & Savran, C. A. High-purity isolation of rare single cells from blood using a tiered microchip system. *PLoS ONE* **15**, (2020).

Following publications were studied but not necessarily referenced in the text:

1. Whitfield, M. J., Lee, W. C. J. & Van Vliet, K. J. Onset of heterogeneity in culture-expanded bone marrow stromal cells. *Stem Cell Res.* **11**, 1365–1377 (2013).

2. High-throughput particle capture and analysis. (2017).

3. Paclitaxel-induced apoptosis in MCF-7 breast-cancer cells - Saunders - 1997 - International Journal of Cancer - Wiley Online Library. Available at: https://onlinelibrary.wiley.com/doi/epdf/10.1002/(SICI)1097-0215(19970117)70:2%3C214::AID-IJC13%3E3.0.CO;2-I. (Accessed: 31st January 2020)

4. Micro-and Nanotechnologies for Quantitative Biology and Medicine. (2016). doi:10.1177/2211068216652846

5. Zhai, J. *et al.* A digital microfluidic system with 3D microstructures for single-cell culture. *Microsystems Nanoeng.* **6**, 1–10 (2020).

6. Acerbi, I. *et al.* Human breast cancer invasion and aggression correlates with ECM stiffening and immune cell infiltration. *Integr. Biol.* **7**, 1120–1134 (2015).

7. Akrap, N. *et al.* Stem Cell Reports Identification of Distinct Breast Cancer Stem Cell Populations Based on Single-Cell Analyses of Functionally Enriched Stem and Progenitor Pools. *Stem Cell Reports* **6**, 121–136 (2016).

8. Albini, A. *et al. A Rapid i/i Vitro Assay for Quantitating the Invasive Potential of Tumor Cells*. *CANCER RESEARCH* **47**, (1987).

9. Alizadeh, A. A. *et al.* Toward understanding and exploiting tumor heterogeneity. *Nat. Med.* **21**, 846–53 (2015).

10. Altschuler, S. J. & Wu, L. F. Cellular Heterogeneity: Do Differences Make a Difference? *Cell* **141**, 559–563 (2010).

11. Aref, A. R. *et al.* 3D microfluidic *ex vivo* culture of organotypic tumor spheroids to model immune checkpoint blockade. *Lab Chip* **18**, 3129–3143 (2018).

12. Assal, R. El *et al.* 3-D Microwell Array System for Culturing Virus Infected Tumor Cells. *Nat. Publ. Gr.* (2016). doi:10.1038/srep39144

13. Atefi, E., Lemmo, S., Fyffe, D., Luker, G. D. & Tavana, H. High Throughput, Polymeric Aqueous Two-Phase Printing of Tumor Spheroids. *Adv. Funct. Mater.* **24**, 6509–6515 (2014).

14. Baccelli, I. *et al.* Identification of a population of blood circulating tumor cells from breast cancer patients that initiates metastasis in a xenograft assay. *Nat. Biotechnol.* **31**, 539–544 (2013).

15. Baker, E. L., Lu, J., Yu, D., Bonnecaze, R. T. & Zaman, M. H. Cancer Cell Stiffness: Integrated Roles of Three-Dimensional Matrix Stiffness and Transforming Potential. *Biophys. J.* **99**, 2048–2057 (2010).

16. Beaver, C. M., Ahmed, A. & Masters, J. R. Clonogenicity: Holoclones and Meroclones Contain Stem Cells. *PLoS One* **9**, e89834 (2014).

17. Beca, F. & Polyak, K. Intratumor heterogeneity in breast cancer. in *Advances in Experimental Medicine and Biology* **882**, 169–189 (Springer New York LLC, 2016).

18. Bianchi, D. W. Fetal cells in the maternal circulation: feasibility for prenatal diagnosis. *Br. J. Haematol.* **105**, 574–583 (1999).

19. Bianchini, G., Balko, J. M., Mayer, I. A., Sanders, M. E. & Gianni, L. Triple-negative breast cancer: challenges and opportunities of a heterogeneous disease. *Nat. Rev. Clin. Oncol.* **13**, 674–690 (2016).

20. Bjerkvig, R. *Revival: Spheroid Culture in Cancer Research (1991)*.

21. Bobek, V., Kacprzak, G., Rzechonek, A. & Kolostova, K. Detection and cultivation of circulating tumor cells in malignant pleural mesothelioma. *Anticancer Res.* **34**, 2565–9 (2014).

22. Bobek, V., Kolostova, K., Gurlich, R. & Eliasova, P. OBSERVATIONAL STUDY Circulating tumor cells in pancreatic cancer patients: Enrichment and cultivation. *World J Gastroenterol* **20**, 17163–17170 (2014).

23. Bobek, V. *et al.* Cultivation of circulating tumor cells in esophageal cancer. *Folia Histochem. Cytobiol.* **52**, 171–177 (2014).

24. Boral, D. *et al.* Molecular characterization of breast cancer CTCs associated with brain metastasis. *Nat. Commun.* **8**, 196 (2017).

25. Boutin, M. E. *et al.* A high-throughput imaging and nuclear segmentation analysis protocol for cleared 3D culture models. *Sci. Rep.* **8**, 1–14 (2018).

26. Boyd, N. F. *et al.* Evidence That Breast Tissue Stiffness Is Associated with Risk of Breast Cancer. *PLoS One* **9**, e100937 (2014).

27. Brauchle, E. *et al.* Biomechanical and biomolecular characterization of extracellular matrix structures in human colon carcinomas. *Matrix Biol.* **68–69**, 180–193 (2018).

28. Brauchle, E. *et al.* Biomechanical and biomolecular characterization of extracellular matrix structures in human colon carcinomas. *Matrix Biol.* **68**–**69**, 180–193 (2018).

29. Breslin, S. & O'Driscoll, L. Three-dimensional cell culture: the missing link in drug discovery. *Drug Discov. Today* **18**, 240–249 (2013).

30. Bulfoni, M. *et al.* Dissecting the Heterogeneity of Circulating Tumor Cells in Metastatic Breast Cancer: Going Far Beyond the Needle in the Haystack. *Int. J. Mol. Sci.* doi:10.3390/ijms17101775

31. Cayrefourcq, L. *et al.* Establishment and Characterization of a Cell Line from Human Circulating Colon Cancer Cells. *Cancer Res.* **75**, 892–901 (2015).

32. Cegan, M. *et al.* In vitro culturing of viable circulating tumor cells of urinary bladder cancer. *Int J Clin Exp Pathol* **7**, 7164–7171 (2014).

33. Celià-Terrassa, T. & Kang, Y. Distinctive properties of metastasis-initiating cells. *Genes Dev.* **30**, 892–908 (2016).

34. Chen, J.-Y. *et al.* Sensitive and Specific Biomimetic Lipid Coated Microfluidics to Isolate Viable Circulating Tumor Cells and Microemboli for Cancer Detection. *PLoS One* (2016). doi:10.1371/journal.pone.0149633

35. Chen, S.-Y. C., Hung, P. J. & Lee, P. J. Microfluidic array for three-dimensional perfusion culture of human mammary epithelial cells. *Biomed. Microdevices* **13**, 753–758 (2011).

36. Chen, W., Hoffmann, A. D., Liu, H. & Liu, X. Organotropism: new insights into molecular mechanisms of breast cancer metastasis. *npj Precis. Oncol.* **2**, 1–12 (2018).

37. Chen, Y. C. *et al.* Single cell dual adherent-suspension co-culture micro-environment for studying tumor-stromal interactions with functionally selected cancer stem-like cells. *Lab Chip* **16**, 2935–2945 (2016).

38. Chen, Y. C. *et al.* Single cell dual adherent-suspension co-culture micro-environment for studying tumor-stromal interactions with functionally selected cancer stem-like cells. *Lab Chip* **16**, 2935–2945 (2016).

39. Chen, Y. *et al.* Rare cell isolation and analysis in microfluidics. *Lab Chip* **14**, 626–45 (2014).

40. Chen, Y.-C. *et al.* High-Throughput Single-Cell Derived Sphere Formation for Cancer Stem-Like Cell Identification and Analysis. *Sci. Rep.* **6**, 27301 (2016).

41. Chen, Y.-C., Lou, X., Zhang, Z., Ingram, P. & Yoon, E. High-Throughput Cancer Cell Sphere Formation for Characterizing the Efficacy of Photo Dynamic Therapy in 3D Cell Cultures. *Sci. Rep.* **5**, 12175 (2015).

42. Chen, Y.-C. *et al.* Single cell dual adherent-suspension co-culture micro-environment for studying tumor–stromal interactions with functionally selected cancer stem-like cells. *Lab Chip* **16**, 2935–2945 (2016).

43. Cheng, Y. H., Chen, Y. C., Brien, R. & Yoon, E. Scaling and automation of a high-throughput single-cell-derived tumor sphere assay chip. *Lab Chip* **16**, 3708–3717 (2016).

44. Choi, Y. H. & Yoo, Y. H. Taxol-induced growth arrest and apoptosis is associated with the upregulation of the Cdk inhibitor, p21WAF1/CIP1, in human breast cancer cells. in *Oncology Reports* **28**, 2163–2169 (2012).

45. Comet, I., Riising, E. M., Leblanc, B. & Helin, K. *Maintaining cell identity: PRC2-mediated regulation of transcription and cancer*. *Nature Publishing Group* (2016). doi:10.1038/nrc.2016.83

46. Corvaisier, M. *et al.* Regulation of cellular quiescence by YAP/TAZ and Cyclin E1 in colon cancer cells: Implication in chemoresistance and cancer relapse. *Oncotarget* **7**, 56699–56712 (2016).

47. Cyll, K. *et al.* Tumour heterogeneity poses a significant challenge to cancer biomarker research. *Br. J. Cancer* **117**, 367–375 (2017).

48. Dagogo-Jack, I. & Shaw, A. T. Tumour heterogeneity and resistance to cancer therapies. *Nat. Publ. Gr.* **15**, (2017).

49. Dagogo-Jack, I. & Shaw, A. T. Tumour heterogeneity and resistance to cancer therapies. *Nat. Rev. Clin. Oncol.* **15**, 81–94 (2017).

50. Dai, X., Cheng, H., Bai, Z. & Li, J. Breast Cancer Cell Line Classification and Its Relevance with Breast Tumor Subtyping. *J. Cancer* **8**, 3131–3141 (2017).

51. De Luca, F. *et al.* Mutational analysis of single circulating tumor cells by next generation sequencing in metastatic breast cancer. *Oncotarget* **7**, (2016).

52. Deng, G. *et al.* Single cell mutational analysis of PIK3CA in circulating tumor cells and metastases in breast cancer reveals heterogeneity, discordance, and mutation persistence in cultured disseminated tumor cells from bone marrow. doi:10.1186/1471-2407-14-456

53. Dusseiller, M. R., Schlaepfer, D., Ferrari, A., Kroschewski, R. & Textor, M. Micro-3D cell culture devices for single cell analysis. in *2005 3rd IEEE/EMBS Special Topic Conference on Microtechnology in Medicine and Biology* 365–367 (IEEE). doi:10.1109/MMB.2005.1548476

54. Ellsworth, R. E., Blackburn, H. L., Shriver, C. D., Soon-Shiong, P. & Ellsworth, D. L. Molecular heterogeneity in breast cancer: State of the science and implications for patient care. *Semin. Cell Dev. Biol.* **64**, 65–72 (2017).

55. Eramo, A. *et al.* Identification and expansion of the tumorigenic lung cancer stem cell population. *Cell Death Differ.* **15**, 504–514 (2008).

56. Fang, Y. & Eglen, R. M. Three-Dimensional Cell Cultures in Drug Discovery and Development. *SLAS Discov. Adv. life Sci. R D* **22**, 456–472 (2017).

57. Fennema, E., Rivron, N., Rouwkema, J., Van Blitterswijk, C. & De Boer, J. Spheroid culture as a tool for creating 3D complex tissues. *Trends Biotechnol.* **31**, 108–115 (2013).

58. Fiddler, M. Fetal Cell Based Prenatal Diagnosis: Perspectives on the Present and Future. *J. Clin. Med.* **3**, 972–85 (2014).

59. Fillmore, C. M. & Kuperwasser, C. Human breast cancer cell lines contain stem-like cells that self-renew, give rise to phenotypically diverse progeny and survive chemotherapy. *Breast Cancer Res.* **10**, R25 (2008).

60. Fleming, M., Ravula, S., Tatishchev, S. F. & Wang, H. L. Colorectal carcinoma: Pathologic aspects. *Journal of Gastrointestinal Oncology* **3**, 153–173 (2012).

61. Folkman, J. & Hochberg, M. Self-regulation of growth in three dimensions. *J. Exp. Med.* **138**, 745–753 (1973).

62. Franken, N. A. P., Rodermond, H. M., Stap, J., Haveman, J. & van Bree, C. Clonogenic assay of cells in vitro. *Nat. Protoc.* **1**, 2315–2319 (2006).

63. Frey, O., Misun, P. M., Fluri, D. A., Hengstler, J. G. & Hierlemann, A. Reconfigurable microfluidic hanging drop network for multi-tissue interaction and analysis. *Nat. Commun.* **5**, 4250 (2014).

64. Frimat, J. P. *et al.* A microfluidic array with cellular valving for single cell co-culture. *Lab Chip* **11**, 231–237 (2011).

65. Gao, D. *et al.* Organoid Cultures Derived from Patients with Advanced Prostate Cancer. *Cell* **159**, 176–187 (2014).

66. Gerlinger, M. *et al.* Intratumor Heterogeneity and Branched Evolution Revealed by Multiregion Sequencing. *N. Engl. J. Med.* **366**, 883–892 (2012).

67. Gong, X. *et al.* Generation of Multicellular Tumor Spheroids with Microwell-Based Agarose Scaffolds for Drug Testing. doi:10.1371/journal.pone.0130348

68. Goodspeed, A., Heiser, L. M., Gray, J. W. & Costello, J. C. Tumor-Derived Cell Lines as Molecular Models of Cancer Pharmacogenomics. *Mol. Cancer Res.* **14**, 3–13 (2016).

69. Gracz, A. D. *et al.* A high-throughput platform for stem cell niche co-cultures and downstream gene expression analysis. doi:10.1038/ncb3104

70. Greaves, M. & Maley, C. C. Clonal evolution in cancer. *Nature* **481**, 306–313 (2012).

71. Gupta, N. *et al.* Microfluidics-based 3D cell culture models: Utility in novel drug discovery and delivery research. *Bioeng. Transl. Med.* **1**, 63–81 (2016).

72. Ham, S. L., Joshi, R., Thakuri, P. S. & Tavana, H. Liquid-based three-dimensional tumor models for cancer research and drug discovery. *Exp. Biol. Med.* **241**, 939–954 (2016).

73. Hamilton, G., Burghuber, O. & Zeillinger, R. Circulating Tumor Cells in Small Cell Lung Cancer: Ex Vivo Expansion. *Lung* **193**, 451–452 (2015).

74. Han, Y. L. *et al.* Cell contraction induces long-ranged stress stiffening in the extracellular matrix. *Proc. Natl. Acad. Sci. U. S. A.* **115**, 4075–4080 (2018).

75. Hassanzadeh-Barforoushi, A. *et al.* Static droplet array for culturing single live adherent cells in an isolated chemical microenvironment. **18**, 2156 (2018).

76. He, C. K., Chen, Y. W., Wang, S. H. & Hsu, C. H. Hydrodynamic shuttling for deterministic high-efficiency multiple single-cell capture in a microfluidic chip. *Lab Chip* **19**, 1370–1377 (2019).

77. Holliday, D. L. & Speirs, V. Choosing the right cell line for breast cancer research. *Breast Cancer Res.* **13**, 215 (2011).

78. Hong, S., Pan, Q. & Lee, L. P. Single-cell level co-culture platform for intercellular communication. *Integr. Biol.* **4**, 374–380 (2012).

79. Hsiao, A. Y. *et al.* Microfluidic system for formation of PC-3 prostate cancer co-culture spheroids. *Biomaterials* **30**, 3020–3027 (2009).

80. Hsiao, A. Y. *et al.* Microfluidic system for formation of PC-3 prostate cancer co-culture spheroids. *Biomaterials* **30**, 3020–3027 (2009).

81. Hsiao, A. Y. *et al.* Micro-ring structures stabilize microdroplets to enable long term spheroid culture in 384 hanging drop array plates. *Biomed. Microdevices* **14**, 313–323 (2012).

82. Huang, S. Non-genetic heterogeneity of cells in development: More than just noise. *Development* **136**, 3853–3862 (2009).

83. Huang, W. *et al.* Lab on a Chip Separation and dual detection of prostate cancer cells and protein biomarkers using a microchip device. **17**, (2017).

84. Huang, Y. *et al.* Optical Coherence Tomography Detects Necrotic Regions and Volumetrically Quantifies Multicellular Tumor Spheroids. *Cancer Res* **77**, (2017).

85. Ingram, M. *et al.* Three-dimensional growth patterns of various human tumor cell lines in simulated microgravity of a NASA bioreactor. *Vitr. Cell. Dev. Biol. - Anim.* **33**, 459–466 (1997).

86. Ishiguro, T. *et al.* Tumor-derived spheroids: Relevance to cancer stem cells and clinical applications. *Cancer Sci.* **108**, 283–289 (2017).

87. Ishihara, S., Inman, D. R., Li, W.-J., Ponik, S. M. & Keely, P. J. Mechano-Signal Transduction in Mesenchymal Stem Cells Induces Prosaposin Secretion to Drive the Proliferation of Breast Cancer Cells. *Cancer Res.* **77**, 6179–6189 (2017).

88. Ishii, S., Tago, K. & Senoo, K. Single-cell analysis and isolation for microbiology and biotechnology: methods and applications. *Appl. Microbiol. Biotechnol.* **86**, 1281–1292 (2010).

89. Ivanov, D. P. & Grabowska, A. M. Spheroid arrays for high-throughput single-cell analysis of spatial patterns and biomarker expression in 3D. *Sci. Rep.* **7**, 41160 (2017).

90. Ivanov, D. P. & Grabowska, A. M. Spheroid arrays for high-throughput single-cell analysis of spatial patterns and biomarker expression in 3D. *Sci. Rep.* **7**, 41160 (2017).

91. Jaffe, A. B., Kaji, N., Durgan, J. & Hall, A. Cdc42 controls spindle orientation to position the apical surface during epithelial morphogenesis. *J. Cell Biol.* **183**, 625–633 (2008).

92. Jaffe, A. B., Kaji, N., Durgan, J. & Hall, A. Cdc42 controls spindle orientation to position the apical surface during epithelial morphogenesis. *J. Cell Biol.* **183**, 625–633 (2008).

93. Janiszewska, M. The microcosmos of intratumor heterogeneity: the space-time of cancer evolution. *Oncogene* **39**, 2031–2039 (2020).

94. Kagawa, S. *et al.* Deficiency of caspase-3 in MCF7 cells blocks Bax-mediated nuclear fragmentation but not cell death. *Clin. Cancer Res.* **7**, 1474–80 (2001).

95. Kelm, J. M., Timmins, N. E., Brown, C. J., Fussenegger, M. & Nielsen, L. K. Method for generation of homogeneous multicellular tumor spheroids applicable to a wide variety of cell types. *Biotechnol. Bioeng.* **83**, 173–180 (2003).

96. Kessel, S. *et al.* High-Throughput 3D Tumor Spheroid Screening Method for Cancer Drug Discovery Using Celigo Image Cytometry. *SLAS Technol.* **22**, 454–465 (2017).

97. Kolostova Rafal Matkowski Robert Gü rlich Krzysztof Grabowski Katarzyna Soter Robert Lischke Jan Schü tzner Vladimir Bobek, K. *et al.* Detection and cultivation of circulating tumor cells in gastric cancer. *Cytotechnology* **68**, 1095–1102 (2016).

98. Kolostova, K. *et al.* Circulating tumor cells in localized prostate cancer: isolation, cultivation in vitro and relationship to T-stage and Gleason score. *Anticancer Res.* **34**, 3641–6 (2014).

99. Kolostova, K., Cegan, M. & Bobek, V. Circulating tumor cells in patients with urothelial tumours: Enrichment and in vitro culture. *Can Urol Assoc J* **88**, 9–10 (2014).

100. Kolostova, K., Spicka, J., Matkowski, R. & Bobek, V. Isolation, primary culture, morphological and molecular characterization of circulating tumor cells in gynecological cancers. *Am J Transl Res* **7**, 1203–1213 (2015).

101. Kolostova, K., Zhang, Y., Hoffman, R. M. & Bobek, V. In Vitro Culture and Characterization of Human Lung Cancer Circulating Tumor Cells Isolated by Size Exclusion from an Orthotopic Nude-Mouse Model Expressing Fluorescent Protein. (2014). doi:10.1007/s10895-014-1439-3

102. Kondo, J. *et al.* Retaining cell-cell contact enables preparation and culture of spheroids composed of pure primary cancer cells from colorectal cancer. *Proc. Natl. Acad. Sci. U. S. A.* **108**, 6235–40 (2011).

103. Kramer, N. *et al.* In vitro cell migration and invasion assays. *Mutat. Res. Mutat. Res.* **752**, 10–24 (2013).

104. Langhans, S. A. Three-Dimensional in Vitro Cell Culture Models in Drug Discovery and Drug Repositioning. *Front. Pharmacol.* **9**, 6 (2018).

105. Lea, T. Caco-2 cell line. in *The Impact of Food Bioactives on Health: In Vitro and Ex Vivo Models* 103–111 (Springer International Publishing, 2015). doi:10.1007/978-3-319-16104-4_10

106. Lee, J. W., Sung, J. S., Park, Y. S., Chung, S. & Kim, Y. H. Isolation of spheroid-forming single cells from gastric cancer cell lines: enrichment of cancer stem-like cells. *Biotechniques* **65**, 197–203 (2018).

107. Lelièvre, S. A. & Chittiboyina, S. Microphysiological systems to study microenvironment-cell nucleus interaction: importance of tissue geometry and heterogeneity. *Microphysiological Syst.* **2**, 12–12 (2018).

108. Liebmann, J. E. *et al.* Cytotoxic studies of pacfitaxel (Taxol®) in human tumour cell lines. *Br. J. Cancer* **68**, 1104–1109 (1993).

109. Lindström, S. & Andersson-Svahn, H. Single-Cell Culture in Microwells. *Methods Mol. Biol.* **853**,

110. Liu, J., Dang, H. & Wang, X. W. The significance of intertumor and intratumor heterogeneity in liver cancer. *Exp. Mol. Med.* **50**, e416 (2018).

111. Liu, W., Wang, J.-C. & Wang, J. Controllable organization and high throughput production of recoverable 3D tumors using pneumatic microfluidics. *Lab Chip* **15**, 1195–1204 (2015).

112. Liu, Y. & Walther-Antonio, M. Microfluidics: A new tool for microbial single cell analyses in human microbiome studies. *Cit. Biomicrofluidics* **11**, (2017).

113. Lu, L.-C., Hsu, C.-H., Hsu, C. & Cheng, A.-L. Tumor Heterogeneity in Hepatocellular Carcinoma: Facing the Challenges. *Liver cancer* **5**, 128–38 (2016).

114. Lv, D., Hu, Z., Lu, L., Lu, H. & Xu, X. Three-dimensional cell culture: A powerful tool in tumor research and drug discovery. *Oncol. Lett.* **14**, 6999–7010 (2017).

115. Ma, X.-J., Dahiya, S., Richardson, E., Erlander, M. & Sgroi, D. C. Gene expression profiling of the tumor microenvironment during breast cancer progression. *Breast Cancer Res.* **11**, R7 (2009).

116. Maheswaran, S. & Haber, D. A. Ex vivo culture of CTCs: An emerging resource to guide cancer therapy. *Cancer Res.* **75**, 2411–2415 (2015).

117. Malara, N. *et al.* Ex-vivo characterization of circulating colon cancer cells distinguished in stem and differentiated subset provides useful biomarker for personalized metastatic risk assessment. *J. Transl. Med.* **14**, (2016).

118. Marusyk, A., Almendro, V. & Polyak, K. Intra-tumour heterogeneity: a looking glass for cancer? *Nat. Rev. Cancer* **12**, 323–334 (2012).

119. Meacham, C. E. & Morrison, S. J. Tumour heterogeneity and cancer cell plasticity. *Nature* **501**, 328–337 (2013).

120. Mehta, G., Hsiao, A. Y., Ingram, M., Luker, G. D. & Takayama, S. Opportunities and challenges for use of tumor spheroids as models to test drug delivery and efficacy. (2012). doi:10.1016/j.jconrel.2012.04.045

121. Miyamoto, D. T., Ting, D. T., Toner, M., Maheswaran, S. & Haber, D. A. Single-Cell Analysis of Circulating Tumor Cells as a Window into Tumor Heterogeneity. doi:10.1101/sqb.2016.81.031120

122. Munshi, A., Hobbs, M. & Meyn, R. E. Clonogenic Cell Survival Assay.

123. Nicholson, K. M., Bibby, M. C. & Phillips, R. M. Influence of drug exposure parameters on the activity of paclitaxel in multicellular spheroids. *Eur. J. Cancer Part A* **33**, 1291–1298 (1997).

124. Owens, T. W. & Naylor, M. J. Breast cancer stem cells. *Front. Physiol.* **4**, 225 (2013).

125. Pajouhi, H. *et al.* Flexible complementary metal oxide semiconductor microelectrode arrays with applications in single cell characterization. *Appl. Phys. Lett.* **107**, 203103 (2015).

126. Pang, M.-F. *et al.* Tissue Stiffness and Hypoxia Modulate the Integrin-Linked Kinase ILK to Control Breast Cancer Stem-like Cells. *Cancer Res.* **76**, 5277–87 (2016).

127. Paris, P. L. *et al.* Functional phenotyping and genotyping of circulating tumor cells from patients with castration resistant prostate cancer. *Cancer Lett.* **277**, 164–173 (2009).

128. Pascual, G. *et al.* Targeting metastasis-initiating cells through the fatty acid receptor CD36. *Nature* **541**, 41–45 (2017).

129. Paszek, M. J. *et al.* Tensional homeostasis and the malignant phenotype. *Cancer Cell* **8**, 241–254 (2005).

130. Pelham, R. J. *et al.* Cell locomotion and focal adhesions are regulated by substrate flexibility. *Proc. Natl. Acad. Sci. U. S. A.* **94**, 13661–5 (1997).

131. Powers, M. J. *et al.* A microfabricated array bioreactor for perfused 3D liver culture. *Biotechnol. Bioeng.* **78**, 257–269 (2002).

132. Prasetyanti, P. R. & Medema, J. P. Intra-tumor heterogeneity from a cancer stem cell perspective. doi:10.1186/s12943-017-0600-4

133. Qureshi-Baig, K. *et al.* What do we learn from spheroid culture systems? Insights from tumorspheres derived from primary colon cancer tissue. *PLoS One* **11**, (2016).

134. Rajcevic, U. *et al.* Colorectal cancer derived organotypic spheroids maintain essential tissue characteristics but adapt their metabolism in culture. *Proteome Sci.* **12**, 39 (2014).

135. Ratner, B. The correlation coefficient: Its values range between 1/1, or do they. *J. Targeting, Meas. Anal. Mark.* **17**, 139–142 (2009).

136. Reynolds, D. S. *et al.* Breast Cancer Spheroids Reveal a Differential Cancer Stem Cell Response to Chemotherapeutic Treatment. *Sci. Rep.* **7**, 10382 (2017).

137. Reynolds, D. S. *et al.* Breast Cancer Spheroids Reveal a Differential Cancer Stem Cell Response to Chemotherapeutic Treatment. *Sci. Rep.* **7**, (2017).

138. Ruppen, J. *et al.* A microfluidic platform for chemoresistive testing of multicellular pleural cancer spheroids. *Lab Chip* **14**, 1198–1205 (2014).

139. Sart, S., F-X Tomasi, R., Amselem, G. & Baroud, C. N. Multiscale cytometry and regulation of 3D cell cultures on a chip. doi:10.1038/s41467-017-00475-x

140. Sasaki, T., Yamamoto, M., Yamaguchi, T. & Sugiyama, S. Development of multicellular spheroids of HeLa cells cocultured with fibroblasts and their response to X-irradiation. *Cancer Res.* **44**, 345–51 (1984).

141. Saunders, D. E. *et al.* Paclitaxel-induced apoptosis in MCF-7 breast-cancer cells. *Int. J. Cancer* **70**, 214–220 (1997).

142. Scher, H. I. *et al.* Phenotypic Heterogeneity of Circulating Tumor Cells Informs Clinical Decisions between AR Signaling Inhibitors and Taxanes in Metastatic Prostate Cancer. *Cancer Res* **77**, 5687–98

143. Schindelin, J. *et al.* Fiji: An open-source platform for biological-image analysis. *Nature Methods* **9**, 676–682 (2012).

144. Schneider, C. A., Rasband, W. S. & Eliceiri, K. W. NIH Image to ImageJ: 25 years of image analysis. *Nature Methods* **9**, 671–675 (2012).

145. Schneider, C. A., Rasband, W. S. & Eliceiri, K. W. *NIH Image to ImageJ: 25 years of image analysis*. (2012). doi:10.1038/nmeth.2089

146. Seoane, J. & De Mattos-Arruda, L. The challenge of intratumour heterogeneity in precision medicine. *J. Intern. Med.* **276**, 41–51 (2014).

147. Sheng, W. *et al.* Lab on a Chip Capture, release and culture of circulating tumor cells from pancreatic cancer patients using an enhanced mixing chip. **14**, (2014).

148. Shi, W. *et al.* Facile Tumor Spheroids Formation in Large Quantity with Controllable Size and High Uniformity. *Sci. Rep.* **8**, 6837 (2018).

149. Shoag, J. & Barbieri, C. E. Clinical variability and molecular heterogeneity in prostate cancer. *Asian J. Androl.* **18**, 543–8 (2016).

150. Singh, S. K. *et al.* Identification of a cancer stem cell in human brain tumors. *Cancer Res.* **63**, 5821–8 (2003).

151. Smart, C. E. *et al.* In Vitro Analysis of Breast Cancer Cell Line Tumourspheres and Primary Human Breast Epithelia Mammospheres Demonstrates Inter- and Intrasphere Heterogeneity. *PLoS One* **8**, e64388 (2013).

152. Souza, G. R. *et al.* Three-dimensional tissue culture based on magnetic cell levitation. *Nat. Nanotechnol.* **5**, 291–6 (2010).

153. Stott, S. L. *et al.* Isolation and Characterization of Circulating Tumor Cells from Patients with Localized and Metastatic Prostate Cancer.

154. Stuart, T. & Satija, R. Integrative single-cell analysis. *Nature Reviews Genetics* **20**, 257–272 (2019).

155. Tamura, M. *et al.* Morphology-based optical separation of subpopulations from a heterogeneous murine breast cancer cell line. *PLoS One* **12**, e0179372 (2017).

156. Thomadaki, H., Talieri, M. & Scorilas, A. Treatment of MCF-7 cells with taxol and etoposide induces distinct alterations in the expression of apoptosis-related genes BCL2, BCL2L12, BAX, CASPASE-9 and FAS. *Biol. Chem.* **387**, 1081–1086 (2006).

157. Tibbitt, M. W. & Anseth, K. S. Hydrogels as extracellular matrix mimics for 3D cell culture. *Biotechnol. Bioeng.* **103**, 655–663 (2009).

158. Tibbitt, M. W. & Anseth, K. S. Hydrogels as extracellular matrix mimics for 3D cell culture. *Biotechnol. Bioeng.* **103**, 655–663 (2009).

159. Tirier, S. M. *et al.* Pheno-seq – linking visual features and gene expression in 3D cell culture systems. *Sci. Rep.* **9**, (2019).

160. Todaro, M. *et al.* Colon Cancer Stem Cells Dictate Tumor Growth and Resist Cell Death by Production of Interleukin-4. *Cell Stem Cell* **1**, 389–402 (2007).

161. Tummala, P., Junaidi, O. & Agarwal, B. Imaging of pancreatic cancer: An overview. *J. Gastrointest. Oncol.* **2**, 168–74 (2011).

162. Turashvili, G. & Brogi, E. Tumor Heterogeneity in Breast Cancer. *Front. Med.* **4**, 227 (2017).

163. Veelken, C., Bakker, G.-J., Drell, D. & Friedl, P. Single cell-based automated quantification of therapy responses of invasive cancer spheroids in organotypic 3D culture. *Methods* **128**, 139–149 (2017).

164. Wang, B. L. *et al.* Microfluidic high-throughput culturing of single cells for selection based on extracellular metabolite production or consumption. *Nat. Biotechnol.* (2014). doi:10.1038/nbt.2857

165. Wang, R. *et al.* Cultured circulating tumor cells and their derived xenografts for personalized oncology. *Asian J. Urol.* **3**, 240–253 (2016).

166. Wang, Y.-K. & Chen, C. S. Cell adhesion and mechanical stimulation in the regulation of mesenchymal stem cell differentiation. doi:10.1111/jcmm.12061

167. Weiswald, L.-B. *et al.* Newly characterised ex vivo colospheres as a three-dimensional colon cancer cell model of tumour aggressiveness. *Br. J. Cancer* **101**, 473–482 (2009).

168. Weiswald, L.-B., Bellet, D. & Dangles-Marie, V. Spherical cancer models in tumor biology. *Neoplasia* **17**, 1–15 (2015).

169. Wong, S. F. *et al.* Concave microwell based size-controllable hepatosphere as a three-dimensional liver tissue model. *Biomaterials* **32**, 8087–8096 (2011).

170. Wullkopf, L. *et al.* Cancer cells' ability to mechanically adjust to extracellular matrix stiffness correlates with their invasive potential. *Mol. Biol. Cell* **29**, 2378–2385 (2018).

171. Yeh, C.-F. & Hsu, C.-H. Microfluidic Techniques for Single-Cell Culture 7.1 ADVANTAGES OF MICROFLUIDIC TECHNIQUES FOR SINGLE-CELL CULTURE. (2019). doi:10.1016/B978-0-12-814919-5.00007-5

172. Yu, M. *et al.* Ex vivo culture of circulating breast tumor cells for individualized testing of drug susceptibility. *Science (80-.).* **345**, 216–220 (2014).

173. Yuhas, J. M., Tarleton, A. E. & Molzen, K. B. Multicellular Tumor Spheroid Formation by Breast Cancer Cells Isolated from Different Sites. *Cancer Res.* **38**, 2486–2491 (1978).

174. Zaman, M. H. *et al.* Migration of tumor cells in 3D matrices is governed by matrix stiffness along with cell-matrix adhesion and proteolysis. *Proc. Natl. Acad. Sci.* **103**, 10889–10894 (2006).

175. Zhang, B. *et al.* Micro RNA 100 sensitizes luminal A breast cancer cells to paclitaxel treatment in part by targeting mTOR. *Oncotarget* **7**, 5702–5714 (2016).

176. Zhang, L. *et al.* The Identification and Characterization of Breast Cancer CTCs Competent for Brain Metastasis. (2013).

177. Zhang, S. *et al.* Identification and characterization of ovarian cancer-initiating cells from primary human tumors. *Cancer Res.* **68**, 4311–20 (2008).

178. Zhang, Z., Chen, Y.-C., Cheng, Y.-H., Luan, Y. & Yoon, E. Microfluidics 3D gel-island chip for single cell isolation and lineage-dependent drug responses study. **16**, (2014).

179. Zhang, Z. *et al.* Expansion of CTCs from early stage lung cancer patients using a microfluidic co-culture model. *Oncotarget* **5**, (2014).

180. Zhau, H. E., Goodwin, T. J., Chang, S.-M., Baker, T. L. & Chung, L. W. K. Establishment of a three-dimensional human prostate organoid coculture under microgravity-simulated conditions: Evaluation of androgen-induced growth and psa expression. *Vitr. Cell. Dev. Biol. - Anim.* **33**, 375–380 (1997).

181. Copyright_2019_Microfluidic-Cell-Culture-Systems.

182. Contributors_2019_Microfluidic-Cell-Culture-Systems.

183. Borenstein, J. T., Tandon, V., Tao, S. L. & Charest, J. L. *Microfluidic Cell Culture Systems Second Edition*.

184. Chen, L.-J., Raut, B. & Kaji, H. On-chip disease models of the human retina. in *Microfluidic Cell Culture Systems* 351–372 (Elsevier, 2019). doi:10.1016/b978-0-12-813671-3.00012-8

185. Cooper, M., Charest, J. L. & Coppeta, J. Design principles for dynamic microphysiological systems. in *Microfluidic Cell Culture Systems* 1–29 (Elsevier, 2019). doi:10.1016/b978-0-12-813671-3.00001-3

186. Dash, A. & Proctor, W. R. Hepatic microphysiological systems: Current and future applications in drug discovery and development. in *Microfluidic Cell Culture Systems* 159–186 (Elsevier, 2019). doi:10.1016/b978-0-12-813671-3.00006-2

187. Esch, M. B. & Mahler, G. J. Body-on-a-chip systems: Design, fabrication, and applications. in *Microfluidic Cell Culture Systems* 323–350 (Elsevier, 2019). doi:10.1016/b978-0-12-813671-3.00011-6

188. Jeong, C. G., Dal Negro, G., Getsios, S. & Ekert, J. E. Application of complex in vitro models (CIVMs) in drug discovery for safety testing and disease modeling. in *Microfluidic Cell Culture Systems* 121–158 (Elsevier, 2019). doi:10.1016/b978-0-12-813671-3.00005-0

189. Mack, P. *et al.* A high-throughput system to probe and direct biological functions driven by complex hemodynamic environments. in *Microfluidic Cell Culture Systems* 297–322 (Elsevier, 2019). doi:10.1016/b978-0-12-813671-3.00010-4

190. Mishra, A. *et al.* Ultrahigh-throughput magnetic sorting of large blood volumes for epitope-agnostic isolation of circulating tumor cells. doi:10.1073/pnas.2006388117/-/DCSupplemental

191. Mungenast, A. E., Aron, R., White, J. D., Tardiff, D. F. & Raja, W. K. Neural tissue microphysiological systems in the era of patient-derived pluripotent stem cells. in *Microfluidic Cell Culture Systems* 249–296 (Elsevier, 2019). doi:10.1016/b978-0-12-813671-3.00009-8

192. Selimović, Š., Kaji, H., Bae, H. & Khademhosseini, A. Microfluidic systems for controlling stem cell microenvironments. in *Microfluidic Cell Culture Systems* 31–63 (Elsevier, 2019). doi:10.1016/b978-0-12-813671-3.00002-5

193. Seo, J. & Huh, D. Microphysiological models of human organs: A case study on microengineered lung-on-a-chip systems. in *Microfluidic Cell Culture Systems* 187–208 (Elsevier, 2019). doi:10.1016/b978-0-12-813671-3.00007-4

194. Vedula, E. M. & Charest, J. L. Microfabricated kidney tissue models. in *Microfluidic Cell Culture Systems* 91–120 (Elsevier, 2019). doi:10.1016/b978-0-12-813671-3.00004-9

195. Yang, Y. & Leong, K. W. Microfluidic platforms with nanoscale features. in *Microfluidic Cell Culture Systems* 65–90 (Elsevier, 2019). doi:10.1016/b978-0-12-813671-3.00003-7

196. Yeh, C.-F. & Hsu, C.-H. Microfluidic Techniques for Single-Cell Culture 7.1 ADVANTAGES OF MICROFLUIDIC TECHNIQUES FOR SINGLE-CELL CULTURE. (2019). doi:10.1016/B978-0-12-814919-5.00007-5

197. Yip, J. K. & McCain, M. L. Cardiac tissue models. in *Microfluidic Cell Culture Systems* 209–248 (Elsevier, 2019). doi:10.1016/b978-0-12-813671-3.00008-6

198. Bidhendi, A. J. & Korhonen, R. K. A finite element study of micropipette aspiration of single cells: effect of compressibility. *Comput. Math. Methods Med.* **2012**, 192618 (2012).

199. Hochmuth, R. M. Review: Micropipette aspiration of living cells. *Journal of Biomechanics* 15–22 (2000). Available at: http://ac.els-cdn.com.ezproxy.lib.purdue.edu/S002192909900175X/1-s2.0-S002192909900175X-main.pdf?_tid=89547458-6e9c-11e4-9234-00000aacb35f&acdnat=1416258112_3850f75b36f277dc001e82a73a523403. (Accessed: 17th November 2014)

200. Yun, H., Kim, K. & Lee, W. gu. Cell manipulation in microfluidics. *Biofabrication* **5**, (2013).

201. Cancer Statistics - National Cancer Institute. Available at: https://www.cancer.gov/about-cancer/understanding/statistics. (Accessed: 5th January 2021)

202. Altschuler, S. J. & Wu, L. F. Cellular Heterogeneity: Do Differences Make a Difference? *Cell* **141**, 559–563 (2010).

203. Burrell, R. A., McGranahan, N., Bartek, J. & Swanton, C. The causes and consequences of genetic heterogeneity in cancer evolution. *Nature* **501**, 338–345 (2013).

204. Hassanzadeh-Barforoushi, A. *et al.* Static droplet array for culturing single live adherent cells in an isolated chemical microenvironment. **18**, 2156 (2018).

205. Hrdlickova, R., Toloue, M. & Tian, B. RNA-Seq methods for transcriptome analysis. doi:10.1002/wrna.1364

206. Huang, S. Non-genetic heterogeneity of cells in development: More than just noise. *Development* **136**, 3853–3862 (2009).

207. Inde, Z. & Dixon, S. J. The impact of non-genetic heterogeneity on cancer cell death. *Critical Reviews in Biochemistry and Molecular Biology* **53**, 99–114 (2018).

208. Mao, A. S. *et al.* Deterministic encapsulation of single cells in thin tunable microgels for niche modelling and therapeutic delivery. *Nat. Mater.* **16**, 236–243 (2017).

209. McGranahan, N. & Swanton, C. Clonal Heterogeneity and Tumor Evolution: Past, Present, and the Future. *Cell* **168**, 613–628 (2017).

210. Mertz, D. R., Ahmed, T. & Takayama, S. Engineering cell heterogeneity into organs-on-a-chip. *Lab Chip* **18**, 2378–2395 (2018).

211. Prasetyanti, P. R. & Medema, J. P. Intra-tumor heterogeneity from a cancer stem cell perspective. *Molecular Cancer* **16**, 41 (2017).

212. Ranjan, V. D., Zeng, P., Li, B. & Zhang, Y. In vitro cell culture in hollow microfibers with porous structures. *Biomater. Sci.* **8**, 2175–2188 (2020).

213. Seoane, J. & De Mattos-Arruda, L. The challenge of intratumour heterogeneity in precision medicine. *J. Intern. Med.* **276**, 41–51 (2014).

214. Stewart, C. A. *et al.* Single-cell analyses reveal increased intratumoral heterogeneity after the onset of therapy resistance in small-cell lung cancer. *Nat. Cancer* **1**, 423–436 (2020).

215. Stuart, T. & Satija, R. Integrative single-cell analysis. *Nature Reviews Genetics* **20**, 257–272 (2019).

216. Wang, B. L. *et al.* Microfluidic high-throughput culturing of single cells for selection based on extracellular metabolite production or consumption. *Nat. Biotechnol.* (2014). doi:10.1038/nbt.2857

217. Weaver, W. M. *et al.* Advances in high-throughput single-cell microtechnologies. *Current Opinion in Biotechnology* **25**, 114–123 (2014).